ROLES OF STING IN A LUPUS MOUSE MODEL OF *FCGR2B*-DEFICIENT MICE

Mr. Arthid Thim-uam

จุฬาลงกรณ์มหาวิทยาลัย
CHULALONGKORN UNIVERSITY

A Dissertation Submitted in Partial Fulfillment of the Requirements

for the Degree of Doctor of Philosophy in Biomedical Sciences

Inter-Department of Biomedical Sciences

Graduate School

Chulalongkorn University

Academic Year 2018

การศึกษาบทบาทของ Sting ในหนูลูปัสที่ขาดยีน *Fcgr2b*

นายอาทิตย์ ทิมอ่วม

วิทยานิพนธ์นี้เป็นส่วนหนึ่งของการศึกษาตามหลักสูตรปริญญาวิทยาศาสตรดุษฎีบัณฑิต
สาขาวิชาชีวเวชศาสตร์ สหสาขาวิชาชีวเวชศาสตร์
บัณฑิตวิทยาลัย จุฬาลงกรณ์มหาวิทยาลัย
ปีการศึกษา 2561

Thesis Title	ROLES OF STING
	IN A LUPUS MOUSE MODEL OF *FCGR2B*-DEFICIENT MICE
By	Mr. Arthid Thim-uam
Field of Study	Biomedical Sciences
Thesis Advisor	TRAIRAK PISITKUN, M.D.
Thesis Co Advisor	Prapaporn Pisitkun, M.D.

Accepted by the Graduate School, Chulalongkorn University in Partial Fulfillment of the Requirement for the Doctor of Philosophy

.... Dean of the Graduate School

(Associate Professor THUMNOON NHUJAK, Ph.D.)

DISSERTATION COMMITTEE

.... Chairman

(Assistant Professor AMORNPUN SEREEMASPUN, M.D., Ph.D.)

.... Thesis Advisor

(TRAIRAK PISITKUN, M.D.)

.... Thesis Co-Advisor

(Prapaporn Pisitkun, M.D.)

.... Examiner

(Professor NATTIYA HIRANKARN, M.D., Ph.D.)

.... Examiner

(Professor TANAPAT PALAGA, Ph.D.)

.... External Examiner

(Professor Watchara Kasinrerk, Ph.D.)

อาทิตย์ ทิมอ่วม : การศึกษาบทบาทของ Sting ในหนูลูปัสที่ขาดยีน *Fcgr2b*. (ROLES OF STING IN A LUPUS MOUSE MODEL OF *FCGR2B*-DEFICIENT MICE) อ.ที่ปรึกษาหลัก : อ. นพ.ไตรรักษ์ พิสิษฐ์กุล, อ.ที่ปรึกษาร่วม : อ. พญ.ประภาพร พิสิษฐ์กุล

เอสแอลอีเป็นโรคที่เกิดจากภูมิต้านทานผิดปกติเรื้อรัง เกิดขึ้นเมื่อเซลล์ภูมิคุ้มกันตอบสนองต่อแอนติเจนของตัวเองผิดปกติซึ่งจะทำให้เกิดการสร้างแอนติบอดี้ต่อต้านเนื้อเยื่อตนเองและทำให้เกิดอิมมูนคอมเพล็กซ์และสารไซโตไคน์ซึ่งจะนำไปสู่การอักเสบในเนื้อเยื่อต่างๆ สารไซโตไคน์ที่ทำให้เกิดโรคเอสแอลอีที่สำคัญคือ อินเตอร์เฟอร์รอนชนิดที่หนึ่ง การส่งสัญญาณผ่านเซ็นเซอร์กรดนิวคลีอิคสามารถกระตุ้นการผลิตอินเตอร์เฟอร์รอนชนิดที่หนึ่งจากเดนไดรติกเซลล์และส่งเสริมความรุนแรงของโรคเอสแอลอี Stimulator of interferon genes หรือ Sting เป็นตัวรับดีเอ็นเอและส่งสัญญาณต่อเพื่อให้เกิดการสร้างอินเตอร์เฟอร์รอนชนิดที่หนึ่ง จากการศึกษาเร็วๆนี้พบความผิดปกติของ Sting ที่ส่งผลทำให้มีการสร้างอินเตอร์เฟอร์รอนมากกว่าปกติสามารถก่อให้เกิดโรคหลอดเลือดอักเสบในเด็กซึ่งมีอาการคล้ายโรคเอสแอลอี อย่างไรก็ตามการศึกษาการทำงานของ Sting ในสัตว์ทดลองของโรคแพ้ภูมิตนเองในหลายโมเดลยังมีความขัดแย้งกันอยู่ เพื่อที่จะค้นหาว่า Sting มีส่วนร่วมในการเกิดโรคลูปัส ดังนั้นหนูลูปัส *Fcgr2b*-deficient จะถูกทำการผสมพันธุ์กับหนู *Sting*-deficient และหนูที่ได้จากการผสมนี้จะถูกติดตามอาการของโรคลูปัส จากผลการศึกษานี้พบว่า หนูลูปัส *Fcgr2b*-deficient ที่ไม่มี Sting สามารถมีชีวิตอยู่ได้นานขึ้น มีการสร้างแอนติบอดี้ต่อเนื้อเยื่อตนเองลดลงรวมถึงเกิดไตอักเสบลดลง และยังพบว่าการกระตุ้นเซลล์ผ่านวิถีของ Sting ส่งเสริมให้เดนไดรติกเซลล์ทำงานได้ดี อีกทั้งยังมีการเปลี่ยนแปลงไปเป็น plasmacytoid dendritic เซลล์ โดยการกระตุ้นนี้ยังทำให้เกิดการฟอสโฟรีเลชั่นอีกทั้งยังพบโปรตีน Lyn มีปฏิสัมพันธ์กับ Sting อีกด้วยและจากการให้เดนไดรติกเซลล์ที่ถูกกระตุ้นผ่านวิถี Sting ในหนูลูปัส *Fcgr2b*-deficient ที่ไม่มี Sting นั้นส่งผลให้หนูกลุ่มดังกล่าวมีความรุนแรงของโรคลูปัสมากขึ้นอีกด้วย ความรู้จากการศึกษานี้เป็นหลักฐานยืนยันแนวคิดสำหรับการวางแผนที่จะยับยั้ง Sting ในการรักษาโรคแพ้ภูมิตนเองในอนาคต

จุฬาลงกรณ์มหาวิทยาลัย
CHULALONGKORN UNIVERSITY

สาขาวิชา   ชีวเวชศาสตร์   ลายมือชื่อนิสิต ....
ปีการศึกษา   2561   ลายมือชื่อ อ.ที่ปรึกษาหลัก ....
                                                      ลายมือชื่อ อ.ที่ปรึกษาร่วม ....

5787830020 : MAJOR BIOMEDICAL SCIENCES

KEYWORD: Systemic lupus Erythematosus Fc gamma receptor IIb (Fcgr2b) Stimulator of
interferon genes (Sting) Lyn kinase, Interferon type I, Dendritic cells

Arthid Thim-uam : ROLES OF STING IN A LUPUS MOUSE MODEL OF *FCGR2B*-DEFICIENT MICE. Advisor: TRAIRAK PISITKUN, M.D. Co-advisor: Prapaporn Pisitkun, M.D.

Systemic Lupus Erythematosus (SLE) is a chronic autoimmune disease causing the immunological abnormalities leads to the production of autoantibodies, immune complex deposition and inflammatory cytokines that affect multiple organs. Type I interferon has been shown as one of the most crucial cytokines involving in the pathogenesis of autoimmune diseases such as SLE. Activation via nucleic acid sensors can induce the production of type I interferon from dendritic cells and promote SLE severity. Stimulator of interferon genes (Sting) is a cytoplasmic DNA sensor that signals downstream to enhance type I interferon production after its activation. Recently, it was shown that a gain mutation in the STING gene resulting in over-activity of the IFN pathway can cause familial inflammatory syndrome with lupus-like manifestations in humans. However, the functional studies of Sting in different autoimmune mouse models suggest the conflicting roles of Sting in the pathogenesis of autoimmune diseases. In order to determine if Sting participates in lupus pathogenesis, the *Fcgr2b*-deficienct mice (lupus mouse model) were bred with *Sting*-deficient mice to create the double-deficient mice. All mice were determined the disease phenotypes. The results show that in the absence of Sting, the *Fcgr2b*-deficient mice do not develop fatal glomerulonephritis and autoantibodies. Sting signaling promoted the dendritic cell maturation and the plasmacytoid dendritic cell differentiation. After Sting activation, Sting was phosphorylated, and Lyn was recruited to interact with Sting. The adoptive transfer of Sting-activated bone marrow-derived dendritic cells (BMDC) into the double-deficient mice restored the lupus phenotypes. The original knowledge from this study is a proof of concept for targeting Sting as a future promising treatment in autoimmune diseases.

Field of Study:	Biomedical Sciences	Student's Signature	
Academic Year:	2018	Advisor's Signature	
		Co-advisor's Signature	

ACKNOWLEDGEMENTS

This dissertation would not be completed without the support and kindness of my advisor, co-advisor, my family and my colleagues. I would first like to express my gratitude and appreciation to my thesis advisor, Dr. Prapaporn Pisitkun, M.D. and Dr. Trairak Pisitkun, M.D. for their help, support, supervisions, suggestion and encouragement during my Ph.D. study.

I would foremost like to thank my partner laboratory, Miss Mookmanee Tansakul, D.V.M., for her helpful advice during my research.

I sincerely thank to all the staffs of Center of Excellence in Systems Biology, Faculty of Medicine, Chulalongkorn University, for their friendship, help and support in the laboratory during my research.

I would also like to thank Miss Benjawan Wongprom and the staffs of animal center from the Faculty of Medicine of Chulalongkorn University for their help and care the animals during my research.

Additionally, I would also like to thank Thaneas Prabakaran, Ph.D. and Prof. Søren Paludan, Ph.D., Department of Biomedicine, Aarhus University, Aarhus, Denmark for their suggestion and help the essential laboratory.

This study was supported by National Research Council of Thailand, Thailand research fund and Chulalongkorn Academic Advancement into Its 2nd Century (CUAASC) Project, Thailand Research Fund, and the International Network for lupus research for their grants.

Moreover, I am very grateful to the members of my thesis committee of their helpful advice, constructive criticism and correction for the completeness for this thesis.

Finally, I must express my very deep appreciation to my family for their love, understanding and providing me with unfailing support and continuous encouragement throughout my years of study and through the process of researching and writing this thesis. This achievement would not have been probable without them.

Arthid Thim-uam

TABLE OF CONTENTS

จุฬาลงกรณ์มหาวิทยาลัย

CHULALONGKORN UNIVERSITY

LIST OF TABLES

จุฬาลงกรณ์มหาวิทยาลัย
CHULALONGKORN UNIVERSITY

LIST OF FIGURES

LIST OF ABBREVIATIONS

ANA	Antinuclear antibody
BCA	Bicinchoninic acid assay
bp	Base pair
BSA	Bovine serum albumin
cDNA	Complementary DNA
CFSE	Carboxyfluorescein succinimidyl ester
cGAMP	Cyclic guanosine monophosphate–adenosine monophosphate
cGAS	Cyclic GMP-AMP synthase
ddCt	Delta delta cycle threshold
DTT	Dithiothreitol
ELISA	Enzyme-linked immunosorbent assay
FA	Formic acid
Fcgr2b	Fc fragment of IgG receptor IIb
IA	Iodoacetamide
Ifi	interferon-inducible Ifi200 family
IFNR	Interferon receptor
Ifn-γ	Interferon-gamma
Ifn-α	Interferon-alpha
Ifn-β	Interferon-beta
Irf3	Interferon regulatory factor 3
Irf5	Interferon regulatory factor 5
Irf7	Interferon regulatory factor 7
IL	Interleukin
IP	Immunoprecipitation
ISG	Interferon-stimulated gene
LC	Liquid chromatography
M	Molar

MHC	Major histocompatibility complex
MS/MS	Tandem mass spectrometry
pDC	Plasmacytoid dendritic cell
qPCR	Quantitative polymerase chain reaction
RT-PCR	Reverse-transcription polymerase chain reaction
SD	Standard deviation
SDS-PAGE	Sodium dodecyl sulfate-polyacrylamide gel electrophoresis
SEM	Standard error of the mean
SLE	Systemic lupus erythematosus
Sting	Stimulator of interferon gene
TEAB	Triethylammonium bicarbonate
TEMED	N,N,N',N'-tetramethylethylenediamine
TFA	Trifluoroacetic acid
Tlrs	Toll-like-receptor
Tmem173	Transmembrane 173
WB	Western blotting assay

จุฬาลงกรณ์มหาวิทยาลัย

CHULALONGKORN UNIVERSITY

CHAPTER I

INTRODUCTION

Systemic lupus erythematosus (SLE) is an autoimmune disease with characteristics of autoantibody production and immune complex deposition that lead to severe inflammation in the multi-organ and fatal glomerulonephritis. The heterogeneity of lupus disease has been shown through several mouse models of lupus disease, suggesting the different pathways participating in the pathogenesis. Type I interferon (IFN-I) significantly involves in SLE pathogenesis (1). SLE patients show the increased expression of interferon-inducible genes in peripheral blood mononuclear cells (2). This cytokine can break tolerance by inducing monocytes to differentiate into activated dendritic cells capable of presenting self-antigen (3, 4). Nucleic acid sensing pathways are the main contributors to IFN-I production (5). Several studies suggest that inappropriate recognition of self-nucleic acid can induce the production of IFN-I and promote SLE pathogenesis (1).

The nucleic acid derived from extracellular organisms such as bacteria and viruses is sensed via endosomal Toll-like-receptor (TLRs), whereas cytosolic nucleic acids are independent of TLRs (5). The activation of the endosomal nucleic acid sensors, such as toll-like receptor 7 (TLR7) and 9 (TLR9), lead to type I interferon production (6). Spontaneous duplication of *Tlr7* in *Yaa*-carrying BXSB mice develops autoimmune lupus phenotypes (7). Overexpression of Tlr7 promotes autoimmunity through dendritic cell proliferation while deletion of *Tlr7* in lupus-prone MRL/*lpr* mice diminishes the autoantibody and immune activation (8, 9). However, blocking TLR-mediated signaling by the anti-malarial drug can effectively treat SLE with mild disease activity (10). Thus, there is still needed to discover the other pathways that involve the main mechanisms of lupus development. Several cytosolic DNA sensors can induce IFN-I production (5). Cytosolic DNA sensing is also essential for innate immune signaling, and breaking this process can cause autoimmune and inflammatory diseases (11). TREX1, a DNA-specific exonuclease, functions as a DNA-digesting enzyme. The *TREX1* mutation leads to Aicardi-Goutieres syndrome (AGS) and chilblain lupus in

human (12, 13). *Trek1*-deficient mice show fatal inflammation and autoimmunity (14, 15). The mice with deficiency of DNase II show the embryonic lethality with the production of several inflammatory cytokines, including type I IFN (16).

The stimulator of interferon genes (Sting), also known as Transmembrane Protein 173 (Tmem173), is a cytoplasmic DNA sensor that signals downstream to enhance IFN-I production (17). After cytosolic nucleic acids activate Sting, TBK1 is recruited to phosphorylate IRF3, which subsequently induces the translocation of IRF3 into the nucleus along with NF-kB to make IFN-I and other cytokines production (18). Recent studies show that cGAMP synthase (cGAS) mediated cGAMP (cyclic GMP-AMP) synthesis lead to the stimulation of Sting-induced IFN-I production (19, 20). The inhibition of Sting pathway in the *Trex1*$^{-/-}$ mice improves the survival and decreases the inflammatory process (21). Also, in the absence of Sting, the *DNase II*$^{-/-}$ mice are rescued and do not develop arthritis (16).

The spontaneous lupus mouse models that commonly used to study SLE pathogenesis are MRL/*lpr*, NZBxNZW.F1, and BxSB (22). These models similarly show autoantibody production, circulating immune complex, and glomerulonephritis but the differences are the genetic defects that could contribute to the diverse mechanisms of pathogenesis (7, 22, 23). Autoimmune phenotypes in the MRL/*lpr* mice are TLRs dependent (24). The absence of Sting in the MRL/*lpr* mice promotes the inflammation and hyperresponsive to TLR ligands (25). The IFN-RI deficient MRL/*lpr* mice show the worsened lymphoproliferation, autoantibody production, and end-organ disease (24, 26). These data suggested that the pathogenesis of the MRL/*lpr* mice not mainly initiate by IFN-I production.

The genetic deletion of *Fcgr2b* in mice causes autoimmune disease in a specific genetic background. The *Fcgr2b*$^{-/-}$ created in embryonic stem (ES) cells of 129 strain with subsequently backcrossed into C57BL/6 develop overt lupus disease, but the one generated directly in ES cells of C57BL/6 strain shows mild autoimmune phenotypes (27, 28). The autoimmune diseases developed in the 129/B6.*Fcgr2b*$^{-/-}$ mice suggest the epistatic interaction of *Fcgr2b* and other autoimmune susceptibility genes neighboring region. The 129-derived *Sle16* locus (the locus covers the Nba2 interval genes containing *Fcgr2b*) locates on chromosome 1 and includes the *Slam* family and

interferon-inducible *Ifi200* family genes (28-30). Among the Ifi200 family, the Ifi202 shows the highest expression in the splenocytes from Nba2 carrying mice (31). Ifi202 or Ifi16 (human homolog) signals through Sting to initiate IFN-I production and create an inflammatory response (32).

The defect of this inhibitory Fc gamma receptor is also identified as one of the SLE susceptibility genes in human SLE (33). Interestingly, the association with FcGRIIb polymorphisms in SLE patients around the Asia Pacific region is also common (34). In addition, polymorphisms of the FCGR2B associated with susceptibility to SLE in Asians, including Thai, Chinese, and Japanese (35). Therefore, this study selected *Fcgr2b$^{-/-}$* lupus mouse model to study in depth pathogenesis as a representative of human SLE.

Although publications show the various results of Sting function in the different lupus mouse models, the reason for this controversy could derive from the heterogeneity of lupus pathogenesis among the models (11, 25). Deficiency of interferon regulatory factor 5 (*Irf5*) in the 129/ B6. *Fcgr2b$^{-/-}$* mice reduce the development of autoantibody and glomerulonephritis. The data suggest the important role of IFN-I signaling, at least in part that mediated through *Irf5*, in the pathogenesis of this lupus model (36). Based on the genetic data, Sting may be a key molecule in the pathogenesis of lupus in the 129/B6.*Fcgr2b$^{-/-}$* mice.

This study aims to determine if Sting participates in lupus pathogenesis using the *Fcgr2b*-deficient lupus mouse model. The original knowledge from this study is a proof of concept for targeting Sting as a promising future treatment in autoimmune disease.

CHAPTER II

OBJECTIVES

Research question

Does the activation of Sting/Tmem173 pathway involve in the pathogenesis of SLE and, if yes, what are the mechanisms?

Hypothesis

1. The activation of Sting pathway involved in the pathogenesis of SLE

2. The activation of Sting pathway leads to SLE via DNA sensor-mediated signaling in antigen presenting cells.

Objectives

1. To determine the role of Sting pathway involving in the pathogenesis of SLE in a lupus mouse model of *Fcgr2b*-deficient mice.

2. To identify mechanisms of the Sting signaling that contributes to SLE development.

จุฬาลงกรณ์มหาวิทยาลัย

CHULALONGKORN UNIVERSITY

Conceptual framework

> *Fcgr2b*^{-/-} lupus mice increase the expression of type I interferon cytokines, IFN signature genes, and Sting mediated signaling.

$\downarrow$

> *Fcgr2b*^{-/-} mice at the age of 6 months developed inflammation in the tissues and autoantibody production.

$\downarrow$

> The immune-phenotypes of *Fcgr2b*^{-/-} lupus mice are improved in the absence of Sting.

$\downarrow$

> Sting might be a new targeted therapy in SLE patients.

จุฬาลงกรณ์มหาวิทยาลัย

CHULALONGKORN UNIVERSITY

Research Design: Objective 1 in *Vivo*

Wild-type, *FcgR2b$^{-/-}$* and *Fcgr2b$^{-/-}$, Sting$^{gt/gt}$*
mice at the age of 6 months

Investigate the survival rate at the age of 6 months up to 12 months

Determine disease activity (sacrifice)

Serum

Spleen

Kidneys

- Measure anti-dsDNA levels and
  Anti-nuclear antibody (ANA)
- Measure total IgG by ELISA
- Measure the inflammatory cytokines by Flow cytometry

- Determination of immune cells by flow cytometer
- Determination of IFN-signature by real-time PCR
- Sting expression by western
  Blot.

- To determine IFN signature by real-time PCR
- To determine infiltrated cells in kidney by immunohistochemistry

Research Design: Objective 2 in *Vitro*

Wild-type, *FcgR2b*$^{-/-}$ and *Fcgr2b*$^{-/-}$, *Sting*$^{gt/gt}$ mice at the age of 6 months

↓

Isolation of bone marrow derive dendritic cell → Stimulate cells by IL-4/GM-CSF

↓

DMXAA (Sting ligand)-induced mouse bone marrow-derived dendritic cell (mature BMDCs)

↓ ↓

To investigate DC maturation | To investigate DC function

Isolate CD4 and naiive T cells in lymph nodes and spleen.

- To determine the DC maturation

Method: collect the BMDC cells after stimulation 24 h. and staining with anti-IAb, anti-PDCA, anti-CD80 and anti-CD11c

- To determine the cytokines production

Method: collect the culture media after stimulation 24 h. and detect the cytokines by Flow

Co-culture: DC and T cells (T cells labeled with CFSE)

1. To determine cytokine production from T cells

Method: collect the cells after co-culture 72 h. and surface staining with anti-CD3 and anti-CD4 follow intracellular staining for IFNg, IL-2, IL17A and IL21

2. To determine T cells proliferation

Method: collect the cells after co-culture 72 h. and measure the dilution of CFSE by Flow

3. Adoptive transfer of activated BMDC to recipient mice.

CHAPTER III

LITERATURE REVIEWS

Systemic Lupus Erythematosus (SLE)

Systemic lupus erythematosus (SLE), also called lupus, is a complex, chronic systemic autoimmune disease occur when the immune cells react against self-antigens and subsequently lead to inflammation in the various organ (37). The exact etiologies of lupus are widely unknown. However, many studies have hypothesized that the progression of SLE disease depends on a combination of genetic and environmental factors including hormones, diet, toxins, drugs, and infection (38, 39). The SLE severity varies among individuals ranging from mild symptoms, including cutaneous rashes, oral ulcers, fatigue, arthritis, and anemia to life-threatening manifestations such as glomerulonephritis and neurological disorders (40) (Figure 1).
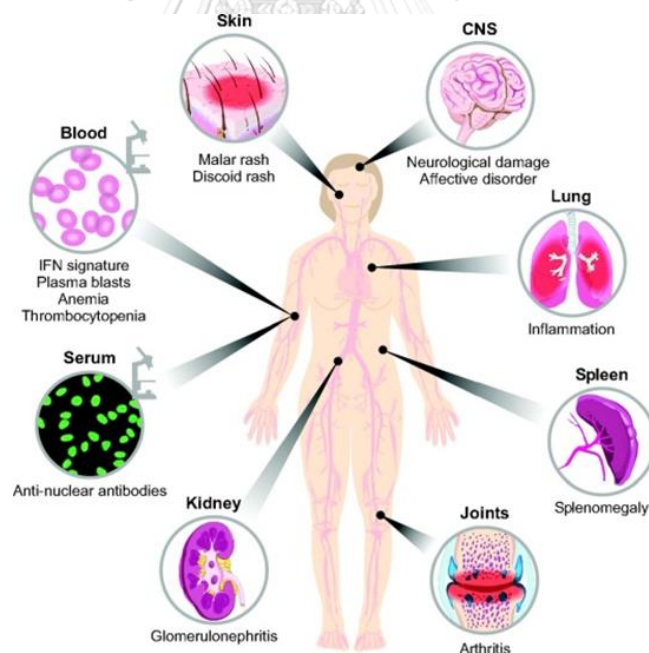
Figure 1 Multi-organ involvement in systemic lupus erythematosus

Crampton SP and et al., Disease Models & Mechanisms. 2014

Moreover, SLE showed a higher prevalence in Asia in comparison with other regions of the world (41, 42) and predominantly in the female. These data suggest that hormones play a significant role in susceptibility (43). In addition, dysregulation of inflammatory cytokine production, including type I interferon, interleukin-6 (IL-6), IL-1, tumor necrosis factor-alpha (TNF-α), IL-10 and TGF-β, have been identified as important players in SLE pathogenesis (44).

Pathogenesis of lupus disease by immunological abnormalities

Mostly any cell of the immune system has been reported to be abnormal in lupus disease. It is unclear which of the many immunological defects has a significant association with lupus process. This disease identified by immune abnormalities such as dysfunction of DC, T cell, and B cell resulting in releasing the autoantibodies. From several studies, the major pathogenesis of SLE can summarize, as shown in Figure 2 (40).

1. After sensing of unknown antigens or apoptotic cells by MHC molecules in antigen presenting cells such as dendritic cells leads to activate naïve T cells to become activated   T cells.

2. These activated T cells stimulate B cells in autoreactive germinal centers resulting in undergo class switching, maturation, and differentiation into plasma cells that can secrete the soluble autoantibodies.

3. Next, the soluble autoantibodies from plasma B cells form immune complexes with the antigens, and then activate the complement or engage Fcγ receptors on different cell types. These processes recruit the inflammatory cells and release the inflammatory cytokines that can support inflammation and tissue destruction.

4. Also, apoptotic cells from damaged tissues can be present a novel autoantigens by antigen presenting cells, which supporting further activates T cell.

5. Moreover, engagements of TLRs, including TLR7 or TLR9 (45) by environmental triggers such as viral infection or DNA damage, induce the secretion of IFN-I and other cytokines, leading to the tissue destruction.
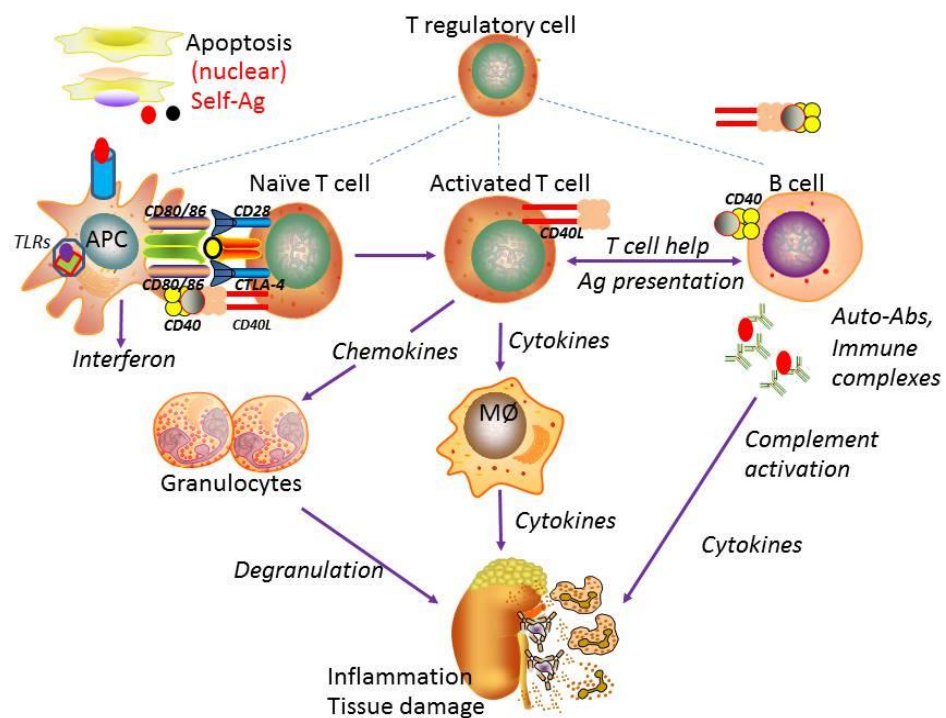
Figure 2 Overview of major pathogenesis pathways in SLE

In addition to immune cells, cytokines, especially interferon alpha (IFN-α), play an important role in SLE pathogenesis (46). It is found that SLE patients have high levels of serum IFN-α and expression of IFN signature in peripheral blood mononuclear cells (PBMC). IFN-α induces the monocytes differentiation into activated dendritic which capable to stimulated the IgG and IgA secretion (47). Moreover, polymorphisms in gene involving in IFN pathway signaling and production associated with SLE susceptibility (48). The previous studies in vitro showed that the lupus mice lacking IFN-α receptor 1 (IFNAR1) improved disease activity by reducing IFN signature, proteinuria, and autoantibodies production (49, 50). All these findings confirmed that IFN-α is crucial in SLE pathogenesis, and it may be a target for SLE therapeutic interventions.

Type I Interferons and plasmacytoid dendritic cells

Type I interferons (IFN-I) are cytokines, which response to the pathogenic infection and compose of IFN-α, IFN-β, IFN-ϵ, IFN-κ, and IFN-ω. Although IFNs-I can be produced by all leukocytes, the major IFN-I producing cells are plasmacytoid dendritic cells (pDCs) (44). Plasmacytoid dendritic cells are found only 0.2–0.8% in peripheral mononuclear cells (PBMCs), but their capacity to produce IFN-I is 100–200 times higher than other cell types (48). After secretion, IFN binds to type I IFN-α receptor (IFNAR), which is a heterodimeric receptor composed of IFNAR1 and IFNAR2 on target cells, and then signals transduction via JAK/STAT pathways, and initiates gene transcription of IFN-stimulated genes (ISGs) as shown in Figure 3 (45). Several pieces of evidence suggest that high production of IFN-I in SLE patients resulting in the overexpression of IFN stimulated genes (ISGs) in PBMCs such as ISG15 and Mx1. This interferon signature is clinically important and correlating with disease activity such as renal pathology, and the presence of autoantibodies against dsDNA (51).

Figure 3 The role of plasmacytoid dendritic cells and type I interferon.

Kim J-M and et al., International Journal of Molecular Sciences. 2015

Role of Type I interferon in immune-pathogenesis of SLE

After sensing of self-nucleic acids containing immune complexes activated pDCs produce IFN-I, which effect on many types of immunologic cells (Figure 3). Presentation of the immune complex by dendritic cells via MHC molecules leads to priming of CD4$^+$ T cells resulting in Th1 or Th17 cell differentiation and cytokines production (52). These activated T cells help B cells to become maturation and differentiation into plasma cells that secrete the soluble autoantibodies of the IgG isotypes. The inflammatory cytokines and autoantibody production will promote tissue damage (53). Also IFN-I activates myeloid DCs (mDCs) to produce various stimulators including B lymphocyte stimulator (BLyS), a proliferation-inducing ligand (APRIL), interleukin-6 (IL-6), IL-23, and tumor necrosis factor-α (TNF-α). The BLys and IL-6 demonstrated the significant roles in SLE pathogenesis (44).

Moreover, cytotoxic T lymphocyte (CTL) induction by IFN-I leads to the overload of antigen (Ag) and stimulate the immune complex formation as well as autoantibody production in SLE (40, 51). According to several actions of IFN-I in the regulation of innate and adaptive immunity in SLE, the biologic drugs targeted this pathway has been designed and implicated in the SLE clinical trials. However, not all of the patients respond to the treatment (54).

Animal models of Systemic lupus erythematosus

The animal models of SLE characterized an attempt to explain the cellular mechanism and genetic requirements for SLE induction. There are various murine models because studying a variety of mouse models of disease provides a more understanding of the genetics and pathological mechanisms in autoimmunity. The animal models generally used lupus-prone strains compose of:

Spontaneous lupus mouse models

The three spontaneous lupus mouse models that commonly used to study SLE pathogenesis are MRL/lpr, NZBxNZW.F1, and BxSB (55). These three models similarly showed autoantibody production, circulating immune complex, and glomerulonephritis. The difference between models is the genetic defect and background that could contribute to the onset and severity of lupus phenotypes.

For example, female mice of MRL/lpr, and NZBxNZW.F1 showed higher severity than male mice, while BxSB mice have the predominant effect on the male mice (22, 23). NZBxNZW.F1 mice do not strongly show the increase of IFN-I, while BxSB mice have high expression of IFN-I mediated signaling.

The genetic abnormality in the lupus mice may not always represent the same disease in human. This phenomenon was shown in the MRL/lpr, which has the mutation of the *Fas* gene, and the patient with FAS mutation develops the autoimmune lymphoproliferative disorder, not SLE. It is better to choose the model that has a similar genetic defect with human SLE so we can apply the knowledge from the study of SLE pathogenesis for the patients.

Table 1 Susceptible genes of spontaneous lupus mouse models

Gene Name	Chromosome	Locus	Susceptible strain(background)
SLAM family	1	Sle1b	NZM2410/NZW (B6)
CR1/2, CD35/CD21	1	Sle1c	NZM2410/NZW (B6)
Ifi202	1	Nba2	NZB (B6), MRL
FcγRIIb	1	Nba2, Lbw7	NZB, BXSB, MRL, SB/Le
CD72	4	Arvm1	MRL
C1q	4	Nba1	NZB
P2X7 receptor	5	Lbw3	NZW
Cd22	7	Sle5	NZM2410/NZW (B6), NZB
H2 (MHC complex)	17	H2	BXSB, NZB
Tnf	17	H2	NZW (BWF1)
Fas	19	lpr	MRL
Tlr7	Y	Yaa	BXSB, SB/Le

Modified from Park H and et al., J Rheum Dis. 2012 (56)

Gene manipulation-derived models

The modified genes by knock out or transgene in the mouse model were studied to understand the single gene that can promote, resist, and lupus susceptibility. The commonly use to study such as $C1q^{-/-}$, $Fc\gamma r2b^{-/-}$, $DNaseI^{-/-}$, $Tlr7^{-/-}$, $Baff^{-/-}$, and several these models have studied that shown in Table 2. However, the genetic background affects the autoimmune progression of SLE in gene-targeted mice (57). The data show that $Fc\gamma r2b^{-/-}$ in Yaa/B6 background significantly enhanced the lupus phenotypes. In contrast, the $Fc\gamma r2b^{-/-}$ in B6 background do not develop the significant disease (55).

Table 2 List of gene manipulation-derived lupus mouse models

Mechanisms	Gene Name	Mouse phenotype
Enhanced B cell activation	Ptprc	Lymphoproliferation, dsDNA, splenomegaly, GN
	FcgRIIb	Exacerbation of lupus, germinal center formation, ANA, GN
	Lyn	Splenomegaly, hyperIgM, autoAb, GN
	CD22	AutoAb
	CD19	Increase B1 cell, hyperIgG, autoAb
	Aiolos	HyperIgG, autoAb
	Tlr7	Splenomegaly, germinal center formation, autoAb, GN
Maintain B cell homeostasis	TACI	Fatal lymphoproliferation, autoAb, GN
	BAFF	AutoAb, GN
Increased Ag Presentation	CD40L	Late-onset autoAb, GN
Reduced clearance of apoptosis material and immune complex	Trex1	Type-I IFN-dependent generalized autoimmunity
	DNaseI	ANA, immune complex GN
	C1q	ANA, GN

Increased T cell activation	CTLA-4	multiorgan lymphoid infiltrates, myocarditis, pancreatitis
	PD-1	Proliferative arthritis, GN, glomerular IgG3 deposits
	TGFb1	Multiorgan lymphocytic and monocytic inflitrates
Proautoimmune cytokine environment	IL-17	Decrease disease severity in FcγRIIb - KO mice
	IL-10	Increase disease severity in MRL/lpr mice
	IFNg	AutoAb, GN, female predominate

Abbreviations: ANA, anti-nuclear antibodies; GN, glomerulonephritis; IFN, interferon; Ab, antibodies; Ig, immunoglobulin (56)

Fcgr2b receptor and systemic lupus erythematosus

FcgRs is the receptors for the Fc region of IgG) and expressed in many immune cells (58). Immune complexes can bind the Fc gamma receptors (FcgRs), which subsequently activate inflammatory cells (59). In all mammalian species, FcGRs are classified into three activation receptors (Fcgr1, Fcgr3, Fcgr4) and only one inhibitory receptor (Fcgr2b). The inhibitory Fc gamma receptor 2b (Fcgr2b) are well studies in B cells and plays a critical role in maintaining B cells activation and inhibition as shown in Figure 4 (60).
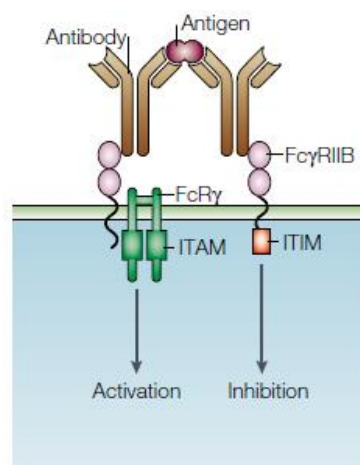
Figure 4 Structure of Fc gamma receptor 2b

Toshiyuki Takai. Nature Reviews Immunology 2, 580–592 (2002)

The activation mechanism through this receptor results in cellular activation leads to the production and release of inflammatory cytokines. By contrast, the main function of Fcgr2b is to inhibit activating signals (61). This signal leads to phosphorylation of the cytoplasmic domain ITIM by the Src-family kinase, LYN (62). This phosphorylation event is thought to require access of Fcgr2b to sphingolipid rafts in which activating FcgRs and the BCR reside following cross-linking. After that, subsequent binding of SH2-domain-containing inositol phosphatases (SHIPs) results in the de-phosphorylation of downstream molecules and inhibition of the activating signaling pathway (58).

The previous study shows the *Fcgr2b*-deficient mice develop lupus phenotypes including glomerulonephritis, immune complex deposition, and autoantibody production (55). The *Fcgr2b*-deficient lupus mice have strong expression of IFN signature, Anti-dsDNA, ANA, LN, and anemia like SLE patients (55).

Induced model of lupus

The pristane-induced lupus model

A single intraperitoneal injection of 2, 6, 10, and 14 Tetramethylpentadecane (TMPD, or commonly known as pristine), a hydrocarbon substance found in mineral oil or petroleum, is a standard method causes chronic peritoneal inflammation and induces lupus phenotypes (63). The evidence shows the mechanism of pristane-induced lupus by increasing the production of IFN-I. Also, these data found that the production of interferon is mediated by signaling through TLR7 and the adapter protein MyD88 (64).

Table 3 The mouse model of SLE

Animal model	IFN signature	Anti-DNA	Anti-Sm/RNP	Clinical	SLE criteria
NZB/W, NZM2410	Weak	Yes	No	ANAs, severe LN	3
MRL/lpr	Absent	Yes	Yes	ANAs, severe LN, arthritis, skin rash	6
MRL+/+	Absent	Low (late)	Yes(late)	ANAs	2
B6/lpr	Absent	No	No	ANAs	1
BXSB male	N/A	Yes	No	ANAs, severe LN	3
BAFF Tg	N/A	Yes	No	ANAs, LN	3
Pristane	Strong	Yes	Yes	ANAs, LN, arthritis, DAH, anemia, serositis	8

Tg, transgenic, N/A, not available.

ANAs, antinuclear antibodies; LN, lupus nephritis; DAH, diffuse alveolar hemorrhage.

Number of the SLICC criteria for the classification of SLE that are met (65)

Induction of Type I interferon of lupus mouse models

Nucleic acid sensing pathways are major contributors to IFN-I production. The breakthrough that identified a significant role of nucleic acid sensing pathway in SLE pathogenesis is the discovery of genetic abnormalities in BxSB mice which carry Yaa (Y-linked autoimmune accelerator) locus (9). The genetic abnormality of Yaa locus is the translocation of X-chromosome genes onto the Y chromosome of Yaa. The responsible gene for lupus phenotypes in BxSB is toll-like receptor 7 (TLR7) (7, 9). Also, MRL/lpr mice deficient in TLR7 experienced reduced autoantibody levels and lymphocyte activation (8). However, the Tlr7 inhibitors did not show the dramatic effect in treating SLE patients (54). This result suggested that the Tlr7-independent pathway may also influence IFN-I signaling.

Stimulator of interferon genes (Sting)

Several pieces of evidence suggest that inappropriate recognition of self-nucleic acid can induce the production of type I interferon and then promote SLE severity. Also, the nucleic acid derived from extracellular organisms such as bacteria and viruses is sensed via endosomal Toll-like-receptor (TLRs), whereas cytosolic nucleic acids are independent of TLRs. Recent studies have shown that Stimulator of interferon genes (Sting), a.k.a. Transmembrane Protein 173 (Tmem173), is a cytoplasmic DNA sensor that signals downstream to enhance type I interferon production after its activation, as shown in Figure 5 (66).
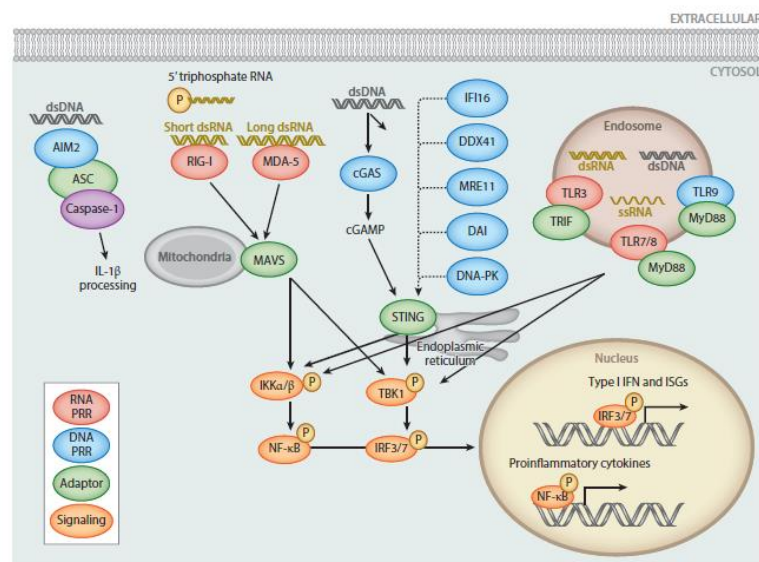
Figure 5 Overview of Sting signaling
Barrat, Elkon, and Fitzgerald. Ann. Rev. Med. 2016

After cytosolic nucleic acids and cyclic dinucleotides that synthesize by Cyclic GMP-AMP synthase (cGAS) binds and activates Sting, which resides in the ER membrane, through a structural change. Activated Sting recruits TBK1 to phosphorylate IRF3, which induces its dimerization and translocation to the nucleus along with NF-kB to produce type I IFNs and other cytokines production (18).

Sting and autoimmunity

The data reported that activation of Sting by infection of *L. monocytogenes* increase the type I IFN production and enhanced responses to the innate immune system by activating the expression of Toll-like receptors, Sting and their downstream signaling pathways including Ifnb1, Ifna4, Mx1 and Irf7 (67). Interestingly, mouse embryonic fibroblasts (MEFs) derived from Sting-knockout mice on a 129SvEv3 × C57BL/6J background decreased in the production of IL-6 and IFN-beta after transfected with a variety of DNA ligands (68).

Moreover, the cGAS-STING signaling by cyclic dinucleotides, including cGAMP, can activate human pDCs to produce IFN-I and knockdown of Sting using siRNA in CAL-1 cells can cause the reduction of IFN response (69). These data indicated that Sting was essential for inducing IFN-I and pDCs sense cytosolic nucleic acids and cyclic dinucleotides via this mechanism.

Recently, it was shown that a mutation at position V155R in the STING gene is constitutively active and result in over-activity of the IFN pathway that can cause a familial inflammatory syndrome with lupus-like manifestations in humans (70). Sting mutation also causes a newly described disease so call "Stimulator of Interferon Genes (STING)–Associated Vasculopathy with Onset in Infancy (SAVI)" (71). These reports suggest that Sting may play roles in human autoimmune diseases and represent a new therapeutic target molecule in this disease as well as other inflammatory autoimmune diseases which cause by cytosolic DNA stimulation resulting in dysregulated type I IFN production.

However, Sting has demonstrated its conflicting role in some of lupus mouse models. The DNase II-deficient mice were rescued by loss of STING function, and polyarthritis completely prevented (16). In contrast, the MRL/lpr mice developed more severe inflammation in the absence of Sting (25). To better understand the effects of Sting in lupus pathogenesis, the Sting- deficient mouse were breed together with Fcgr2b-deficient lupus mouse model and explain the mechanism if Sting participates in this mouse model.

CHAPTER IV

MATERIALS AND METHODS

Animals and animal model

The *Fcgr2b*-deficient mice on C57BL/6 background were obtained from Bolland S. (NIH, Maryland, USA). Sting-deficient mice were provided by Paludan (Aarhus University, Aarhus, Denmark). Wild type mice were purchased from the National Laboratory Animal Center, Nakornpathom, Thailand.

Generation of Double Knockout Mice

The *Fcgr2b*-deficient mice were crossed with Sting-deficient mice to generate the double deficient mice (*Fcgr2b$^{-/-}$.Sting$^{-/-}$*) and their littermate controls. The animal protocols were approved by the Animal Experimentation Ethics Committee of Chulalongkorn University Medical School.

Survival study

The double deficient mice were aged and observed the survival rates compared to their littermates up to 12 months. The mice were euthanized to collect the tissues (kidney, spleen, bone marrow, and sera) for phenotypes analysis.

Measurement the levels of murine anti-dsDNA Antibodies

All mice at the age of 6 months were sacrificed. Blood were collected by cardiac puncture and spun to keep serum for serological analyzes. The levels of autoantibodies (anti-dsDNA) were measured by Enzyme-linked immunosorbent assay (ELISA). Briefly, the ELISA plates were coated with 1 µg of calf thymus DNA (Invitrogen, CA, USA). After incubation at 4 °C for overnight, The plates were washed, dried, and added 100 µl of blocking solution containing 5% FBS, 3% BSA, and 0.1% Tween 20 in 1XPBS, then incubated at room temperature for 1 hour, and washed. Serum samples diluted 1:100 (100 µl) were added and incubated for 1 hour at 37 °C. Then, plates were incubated with 100 µl of HRP conjugated goat anti-mouse isotype specific antibody (1:4,000 in blocking solution) to the plates and incubate at 37°Cfor 1 hour then washed and developed with OPD Substrate Tablets (o-phenylenediamine dihydrochloride) (Sigma, Darmstadt, Germany) for 10 minutes in the dark. The stop solution (2N H_2SO_4)

was then added (100 ul), and the absorbance was measured by Varioskan Flash Microplate Reader at 492 nm. (Thermo Fisher Scientific, MA USA).

Cytokines measurements in Serum

Cytokine panels in serum including IL-1α, IL-1β, IL-6, IL-10, IL-12p70, IL-17A, IL-23, IL-27, MCP-1, IFN-β, IFN-γ, TNF-α, and GM-CSF were measured using LEGENDplex™ Mouse Inflammation Panel kit (Biolegend, San Diego, CA, USA) according to the manufacturer's instructions. In brief, serum samples were incubated with mixed beads and shake at approximate 500 rpm for 2 hours at room temperature. After incubation, the beads were washed and added the detection antibodies, and shake at approximately 500 rpm for 1 hour at room temperature. Then, the beads were added 25 µl of SA-PE for 30 minutes at room temperature. The beads were read on a flow cytometer using BD™ LSR-II (BD Biosciences, USA) and analyzed by LEGENDplex™ Data Analysis Software.

Antinuclear antibodies (ANA)

Anti-nuclear antibodies in serum were detected by indirect immunofluorescence using HEp-2 cells (EUROIMMUN, Luebeck, Germany). Serum samples diluted 1:800 (30 ul) were added to the reaction field and incubated for 30 minutes at room temperature. The slices were washed and added 1: 500 (25 ul) of FITC-conjugated goat anti-mouse IgG antibodies (Abcam, Cambridge, MA, USA), and incubated for 30 minutes at room temperature. Then, slides were mounted with ProLong™ diamond antifade mountant (Invitrogen, CA, USA). Samples were showed fluorescence intensity and blindly graded as 4 = Maximal fluorescence (brilliant yellow-green), 3 = less brilliant (yellow-green fluorescence), 2 = Definite (dull yellow-green), and 1 = very dim (subdued fluorescence).

Flow cytometry analysis

Splenic cells were isolated from all experiment group and littermate wild-type mice. Spleens were dispersed through a cell strainer to generate a single-cell suspension and eliminated red blood cells by osmotic shock (ACK buffer: NH_4Cl, $KHCO_3$ and EDTA). The splenocytes (1×10^6 cells) were stained with flow antibody including anti-CD4 (clone: GK1.5; cat.100423), CD8 (clone: 53-6.7; cat. 100708), CD62L (clone:

MEL-14; cat. 104417), CD44 (clone: IM7; cat.103035), CD3Ɛ (clone: 145-2C11; cat.100312), ICOS (clone: C398.4A; cat. 313517), CD11c (clone: N418; cat. 117312), B220 (clone: RA3-6B2; cat. 103222), CD11b (clone: M1/70; cat. 101228), I-Ab (clone: AF6-120.1; cat. 116406), PDCA-1 (clone: 129c1; cat. 127103), CD80 (clone: 16-10A1; cat. 104733), GL7 (clone: GL7; cat. 144604), CD138 (clone: 281-2; cat. 142506) (Biolegend, San Diego, CA, USA). The flow cytometry was performed using BD™ LSR-II (BD Biosciences, USA) and analysis by FlowJo software (version 10, USA).

Gene expression analysis

A total of RNA was extracted from the kidneys and spleen by Trizol reagent (Invitrogen, CA, USA) as per manufacturer's instructions followed by RNA purified using the RNeasy mini kit and treated with DNase I (Qiagen, MD, USA). Then, 1 µg of total RNA was used as a template for cDNA synthesis using iScript RT Supermix (Biorad, California, USA) The expression of interest genes were assessed by quantitative real-time PCR. The gene expression profiles were tested using SsoAdvanced Universal SYBR Green Supermix (Biorad, California, USA). The sequences of primers tested are followed:

Table 4 List of primer for determine the IFN-inducible genes by qPCR

Primer name	Sequence
CXCL10	F: 5'- ATGACGGGCCAGTGAGAATG-3'
	R: 5'- TCGTGGCAATGATCTCAACAC-3'
Mx1	F: 5'-GATCCGACTTCACTTCCAGATGG-3'
	R: 5'-CATCTCAGTGGTAGTCAACCC-3'
ISG15	F: 5'-TCTGACTGTGAGAGCAAGCAG-3'
	R: 5'-ACCTTTAGGTCCCAGGCCATT-3'
IRF3	F: 5'- GCTTGTGATGGTCAAGGTTGT-3'
	R: 5'- AGATGTGCAAGTCCACGGTT-3'
IRF5	F: 5'-TTTGAGATCTTCTTTTGCTTTGGA-3'
	R: 5'-GTACCACCTGTACAGTAATGAGCTTCTT-3'
IRF7	F: 5'-CCCAGACTGCCTGTGTAGACG-3'
	R: 5'-CCAGTCTCCAAACAGCACTCG-3'

IFN-β	F: 5'- GCTTGTGATGGTCAAGGTTGT-3'
	R: 5'- AGATGTGCAAGTCCACGGTT-3'
IFN-γ	F: 5'- ACT GAC TTG AAT GTC CAA CGC A-3'
	R: 5'- ATC TGA CTC CTT TTT CGC TTC C-3'
P202	F: 5'-AGC CTC TCC TGG ACC TAA CA-3'
	R: 5'- GCA GTG AGT ACC ATC ACT GTC A-3'
Sting	F: 5'-TCTGACTGTGAGAGCAAGCAG-3'
	R: 5'-ACCTTTAGGTCCCAGGCCATT-3'
β- actin	F: 5'-TAGCACCATGAAGATCAAGAT-3'
	R: 5'-CCGATCCACACAGAGTACTT-3'

The thermal cycling conditions are as follows: 1 cycle of 95°C for 5 minutes followed by 40 cycles of 95°C for 15 seconds and 60°C for 1 minute. The relative amounts of target mRNA will be normalized to β-actin mRNA as housekeeping gene and determined by the 2-ddCt method.

Microarray analysis from kidney

A total of RNA was extracted from the kidneys by Trizol reagent (Invitrogen, CA, USA) as per manufacturer's instructions followed by RNA purified using the RNeasy mini kit and treated with DNase I (Qiagen, MD, USA). RNA labeling and hybridization were performed by using the Agilent One-Color Microarray-Based Gene Expression analysis protocol (Agilent Technology, V 6.5, 2010). Microarray results were extracted using Agilent Feature Extraction software v11.0 (Agilent Technologies, Palo Alto, USA).

Immunofluorescence

Frozen renal sections were fixed in acetone and blocked with 1% BSA in PBS. After that, the sections were stained with FITC-conjugated goat anti-mouse IgG antibodies and PE-conjugated goat anti-mouse C45RB antibodies (Abcam, Cambridge, MA, USA). Then, samples were stained with DAPI (4',6-Diamidino-2-Phenylindole, Dihydrochloride) (Thermo Fisher Scientific, MA USA) for 5 minutes in the dark at room temperature. Slides were washed 3 times and mounted with ProLong^{TM} diamond antifade mountant (Invitrogen, CA, USA). The fluorescent signaling was visualized by ZEISS LSM 800 with Airyscan (Carl Zeiss, Germany).

Histopathology

The deparaffinized kidney sections were fixed with formalin subsequently stained with H&E. The pathology grading from kidney sections was blinded analysis by the experience nephrologist followed by Chan O et al., Ann N Y Acad Sci. 1997 (72). Disease was scored semi-quantitatively according to the system in the following table.

Table 5 Kidney pathology score

Score	Glomerular	Interstitial	vascular
0 to 1	focal, mild, or early proliferative	occasional, focal, or small pockets of MNC (10-15 cells)	occasional perivascular infiltrate
1 to 2	moderate or definite proliferative; increased matrix	focal infiltrates (15-30 cells)	several foci of perivascular infiltrate; no necrosis
2 to 3	diffuse and focal or diffuse proliferative	multifocal extensive infiltrates; with necrosis	multifocal perivascular; more extensive; +/- necrosis (3 +)
3 to 4	severe diffuse proliferative, with cres centslsclerosis	severe disease with extensive necrosis	multifocal or diffuse; extensive with necrosis

Bone marrow-derived dendritic cell (BMDC)

Dendritic cells were obtained from mice' femur bone (BMDC) that had been euthanized by cervical dislocation. Cells were cultured in RPMI 1640 supplement with 10 % FBS, 1 mM Na pyruvate, 10 mM Hepes buffer, 1X L-glutamine, 1X non-essential amino acid, 100 Units/ml of pen/strep (Gibco-Thermo Fisher Scientific, MA USA) and 50 µM of 2-Mercaptoethanol (Sigma-Aldrich, Darmstadt, Germany) and maintained at 37°C in a CO_2 incubator then stimulated with 20 ng/ml of IL4 and 20 ng/ml of GM-CSF (Miltenyi, Bergisch Gladbach, Germany) for 5 days followed by adding 10 ug/ml of DMXAA (5,6-Dimethylxanthenone-4-acetic acid or STING ligand) (Invivogen, San Diego, USA) for 24 hours. The mature BMDC were stained with the following antibodies: anti-

mPDCA, CD80, I-Ab, CD11b and CD11c (Biolegend, San Diego, CA, USA). The stained cells will be subjected to flow cytometer (BD Biosciences) and analyzed by FlowJo software (version 10, USA).

Determination of Cytokine in BMDCs

BMDC cells were cultured in 6-well plate and stimulated with IL4 and GM-CSF for 5 days and followed by 10 ug/ml of DMXAA (STING ligand) for 24 hours. The supernatants were collected, and the concentration of cytokines panel including: IL-1α, IL-1β, IL-6, IL-10, IL-12p70, IL-17A, IL-23, IL-27, MCP-1, IFN-β, IFN-γ, TNF-α, and GM-CSF were measured by LEGENDplex™ Mouse Inflammation Panel kit (Biolegend, San Diego, CA, USA) as describe above.

T cells isolation from lymph nodes and spleen

Lymph nodes and spleens were removed from sacrificed mice and littermate wild-type mice. Lymph nodes and spleens were dispersed through a cell strainer to generate a single-cell suspension as described above. T cells were isolated and purified using CD4$^+$ T Cells Isolation Kit (Miltenyi, Bergisch Gladbach, Germany) as per manufacturer's instructions. Briefly, splenocytes and total cells from lymph nodes were prepared (2 x 10^7) and incubated with 20 ul of Biotin-Antibody Cocktail for 5 minutes at 4°C. Then, the mixed cells were incubated with 40 ul of Anti-Biotin MicroBeads for 10 minutes at 4°C, and proceed to subsequent magnetic cell separation (Miltenyi, Bergisch Gladbach, Germany). The viability and purity of purified CD4$^+$T cells were stained with anti-CD3, CD4 (Biolegend, San Diego, CA, USA) and Fixable Viability Dye eFluor® 780 (Thermo Fisher Scientific, MA USA), then examined by flow cytometer.

Intracellular staining of T cells

2 x 10^5 cells of CD4$^+$ T cells were plated in 200 ul of complete medium supplemented with 25 ng/ml PMA, 1 ug/ml ionomycin (Sigma-Aldrich, Darmstadt, Germany) and 1X GolgiPlug (brefeldin A, Biolegend). After 4 h of incubation at 37°C and 5% CO$_2$, cells were collected and stained with anti-CD3, anti-CD4 and ICOS before following the cytokines intracellular staining. Briefly, after performed cell surface antigen staining, cells were fixed in 200 ul of fixation buffer (Biolegend) in the dark at 4 °C for overnight. Cells were washed 3 times with 1X permeabilization buffer (Biolegend) and resuspend fixed/permeabilized cells in 50 ul of 1X permeabilization

buffer, then added the fluorophore-conjugated antibody for anti-IFN-γ (clone: XMG1.2: cat. 505821) (Biolegend, San Diego, CA, USA). The flow cytometry was performed using BD^{TM} LSR-II (BD Biosciences, USA) and analysis by FlowJo software (version 10, USA).

CFSE (Carboxyfluorescein succinimidyl ester) Labeling

CD4$^+$ T cells and Naïve T cells were isolated from spleen using CD4 isolation kit and naïve CD4$^+$ T cell isolation kit (Miltenyi, Bergisch Gladbach, Germany) as per manufacturer's instructions. Then, 1x 10^6 cells of T cells in pre-warmed (37℃) 1x PBS were incubated cells with 0.5 uM CFSE (Biolegend, San Diego, CA, USA) at 37°C in a CO$_2$ incubator for 10 minutes. Cells were quench labeling reaction with 10 volumes of ice cold complete medium and centrifuged for 5 minutes at 1, 500 rpm, 4℃. Labeled cells were washed by re-suspending pellet in complete medium. CFSE-labeled cells are now ready for in vitro culture

In vitro co-cultures of DCs and T cells

BMDCs were cultured with T cells for 6 hours. Briefly, immature BMDCs were cultured and activated with DMXAA (STING ligand) for 24 hours at 37 ℃ and washed twice before co-culture. Activated BMDCs (4 x 10^4) were plated in 200 ul of complete medium with CD4$^+$ T cells (2 x 10^5) from lymph nodes (1:5, 4 x10^4 DC: 2 x 10^5 T cells) for 6 hr. at 37°C and 5% CO$_2$ followed by intracellular staining for anti-IFN-γ as describe above.

For proliferation assays, naïve T cells were labeled with CFSE as described above, according to the manufacturer's instruction (Biolegend, San Diego, CA, USA), before co-culture with activated BMDCs. In brief, activated BMDCs (4 x 10^4) were plated in 200 ul of complete medium with naïve T cells (2 x 10^5) from spleen (1:5, 4 x10^4 DC: 2 x 10^5 T cells) for 72 hours at 37°C and 5% CO$_2$. After co-culture, T cells were stained with intracellular cytokine for anti-IFN-γ and detect their proliferation by dilution of CFSE fluorescence by flow cytometer.

Colocalization of Sting and Lyn in BMDC cells

Immature BMDCs from WT and *Fcgr2b$^{-/-}$* were culture, then stimulated with DMXAA for 3 and 6 hr. Cells were fixed with 4% formalin (Sigma-Aldrich, Darmstadt, Germany) at room temperature for 15 minutes. Incubate the fixed cells for 10 min with

0.2 % Triton X-100 and block unspecific binding of the antibodies with 0.1% BSA for 1 hour. BMDCs were probed with Lyn antibody (1:200)(Cell Signaling, MA, USA) for overnight at 4°C. After incubation, secondary antibody Alexa fluor 488 rabbit IgG (Thermo Fisher Scientific, MA, USA) was added for 1 hour at room temperature. For Sting detection, Sting antibody (1 ug) was incubated with 5 ul (1 ug) of Zenon™ Alexa fluor™ 555 rabbit IgG labeling kit (Thermo Fisher Scientific, MA, USA)) as per manufacturer's instructions prior to probe with the BMDC cells. After that, cells were stained with 1 μM DAPI (Thermo Fisher Scientific, MA USA) for 5 minutes in the dark and the fluorescent signaling was visualized by ZEISS LSM 800 with Airyscan (Carl Zeiss, Germany).

Sample preparation for MS analysis

Quantitative proteomic analysis of mature BMDC was studied using a dimethyl labeling method (73). Briefly, BMDC were cultured, and then stimulated with 10 ug/ml of DMXAA (STING ligand) for 24 hours. Three hundred microgram proteins per group from BMDC were digested overnight at 37°C with trypsin [1:50 (w/w)]. Next, stimulated BMDC's peptides from WT mice, *Fcgr2b*$^{-/-}$ mice, and *Fcgr2b*$^{-/-}$.*Sting*$^{gt/gt}$ mice were labeled with light reagents [formaldehyde (Sigma) and sodium cyanoborohydride (Sigma)], medium reagents [formaldehyde-d2 (CIL) and sodium cyanoborohydride], and heavy reagents [deuterated and ^{13}C-labeled formaldehyde (Sigma) and cyanoborodeuteride (CIL)], respectively, for an hour at room temperature. The peptides were fractionated and subjected to LC-MS/MS (Thermo). Significantly differentially regulated proteins were determined by unpaired t-tests with p-value < 0.05 considered significant. The online resource Database for Annotation, Visualization and Integrated Discovery (DAVID, v 6.8, https://david.ncifcrf.gov/) was employed to classify the significant proteins into functional categories using all proteins identified by MS as background.

Western Blot Analysis

Splenocytes were lysed in 2 % SDS lysis buffer. Lysates were homogenized and centrifuged at 12,000×g for 15 min at 4°C. The supernatants were collected, and total protein was measured by BCA protein assay (Thermo Scientific, Illinois, USA). Cell lysates containing equal amounts of protein (20 μg) were boiled in SDS sample buffer

at 37°C for 15 min before separation on a 10 % SDS-polyacrylamide gel. Proteins were transferred to nitrocellulose membranes and Western blot analysis.

Determination of STING and co-IP by western blot

BMDCs from WT, $Fcgr2b^{-/-}$ and $Sting^{gt/gt}$ were culture and stimulated with DMXAA for 3 and 6 hr. as describe above. Protein lysates were prepared and run on 10 % SDS-polyacrylamide gel, then proteins were transferred to nitrocellulose membranes and probed with Sting antibody (1:2000) and Lyn antibody (clone:LYN-01;1:1000) (Biolegend, San Diego, CA, USA). After incubation at 4 °C for overnight, membrane were washed and probed with IRDye® 680RD Donkey anti-Rabbit IgG (H + L) and IRDye® 800CW Donkey anti-Mouse IgG (H + L) secondary antibody (1:10000) (LI-COR, Lincoln, Nebraska USA) for 1 hour at room temperature. Membrane were determined the signals by ODYSSEY CLx   (LI-COR, Lincoln, Nebraska USA).

Immunoprecipitation of STING in BMDC

BMDCs from WT, $Fcgr2b^{-/-}$ and $Sting^{gt/gt}$ were cultured, then stimulated with DMXAA for 3 and 6 hr. Cells were collected and lysed with 1 % IGEPAL CA-630, 0.5% TritonX-100, 150 mM NaCl, 50 mM Tris pH 7.4, 5% glycerol, 100 mM beta-Glycerophosphate, 2 mM Na3VO4 and 1X proteases inhibitor cocktail (Roche). First, antibody were mixed with the magnetic beads by adding 10 µg of STING antibody with 400 ug of SureBeads™ Protein A magnetic beads (Biorad, California, USA) and incubated for 1 hour at room temperature. Then, Protein lysates were added and incubated with antibody-conjugated beads for overnight at 4°C.   After incubation, the beads were washed 3 times with wash buffer (150 mM NaCl and 50 mM Tris-HCL pH 7.4). Samples were eluted by adding 5X laemmli buffer and, boiled 95^0C for 10 minutes. The eluted protein samples were separated by 10 % SDS-PAGE gel.   The STING interacting proteins from co-IP were analyzed by in-gel digestion followed by LC-MS/MS analysis as described above.

Adoptive transfer

BMDCs from WT, *Fcgr2b$^{-/-}$* and *Fcgr2b$^{-/-}$.Stin$^{ggt/gt}$* mice were cultured as described above. The recipient *Fcgr2b$^{-/-}$.Stin$^{ggt/gt}$* mice (at the age of 4 months) received approximately 10^6 cells of BMDC by tail vein every two weeks per injection time. Control *Fcgr2b$^{-/-}$.Stin$^{ggt/gt}$* mice received only sterile PBS (vehicle). Sera were collected and the levels of anti-dsDNA were measured by ELISA. Mice were euthanized 2 weeks after the final transfer (at the age of 6 months).

Statistical analysis

All statistical analyses employed the two-tailed Mann-Whitney test. Statistical analyses were performed using GraphPad Prism 4.0 (GraphPad Software, San Diego, CA).

CHAPTER V

RESULTS

Loss of the stimulator of type I interferon genes (Sting) increases survival rate of *Fcgr2b*^{-/-} lupus mice

First, to determine the expression of lupus-susceptibility gene and Sting in a lupus mouse model, the result confirmed that the 129/B6. *Fcgr2b*^{-/-} mice (or *Fcgr2b*^{-/-} in short) showed the increase of Ifi202 or p202 expression (Figure 6A). The mRNA and protein expressions of Sting in the spleen were also upregulated in the *Fcgr2b*^{-/-} mice (Figure 6B and 6C).
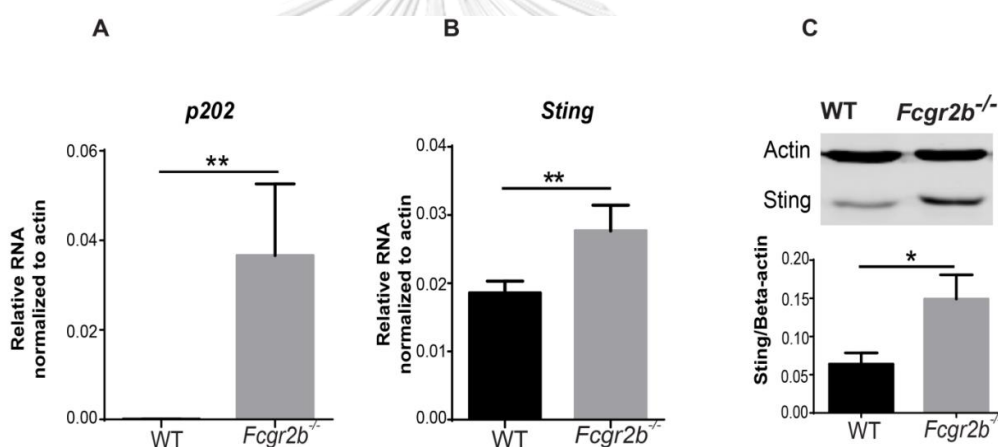

Figure 6 Increasing of susceptibility gene p202 and stimulator of type I interferon genes (STING) in *Fcgr2b*^{-/-} lupus mice.

Gene expression from spleens of wild-type and Fcgr2b^{-/-} mice at the age of 6-7 months were tested by real-time PCR (N=10-12 per group). The mRNA expressions of (A) p202 and (B) Sting were shown. (C) Isolated splenocytes were analyzed for STING protein expression by western blot. Data are representative of 3 mice per group. Quantification of the intensity was normalized by actin (N= 3 per group). Error bars indicate SEM, *p < 0.05 and **p<0.01.

Moreover, mRNA expression of Ifn-β, Ifn-γ, and interferon-inducible genes, including *Irf3, Irf7, Mx1,* and *Cxcl10* in the spleen were also increased in the *Fcgr2b^{-/-}* mice (Figure 7A-2F).
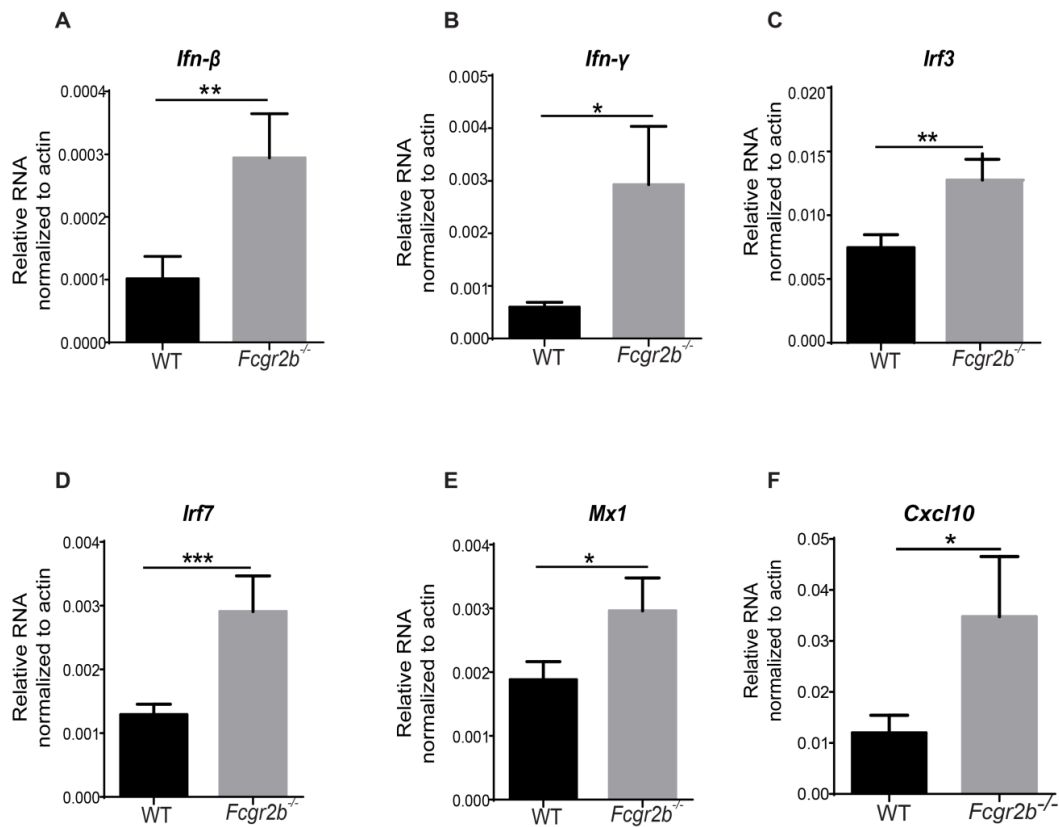

Figure 7 Increase of interferon-inducible genes *in Fcgr2b^{-/-} lupus mice.*

mRNA expression of (A) Ifn-β, (B) Ifn-γ, (C) Irf3, (D) Irf7, (E) Mx1, and (F) Cxcl10 were shown by real-time PCR. (N= 10-15 per group). Error bars indicate SEM, *p < 0.05, **p<0.01, and ***p<0.001.

To determine whether the Sting signaling is required for lupus development in the *Fcgr2b^{-/-}* mice, the double deficiency of *Fcgr2b* and Sting were generated together with control littermates. The *Fcgr2b^{-/-}* mice were crossed with the C57BL/6.*Sting* deficiency or Goldenticket mice (Sting[gt]) which behave as a functional knockout of Sting (74). The *Fcgr2b*-deficient mice start to die at the age of 6 months and the double-deficient mice (*Fcgr2b^{-/-}. Sting[gt/gt]*) showed the higher survival rate compared to the *Fcgr2b^{-/-}* mice (Figure 8) while the *Fcgr2b^{-/-}* with heterozygote of Sting (*Sting[wt/gt]*) did not show the difference from the one with wild-type Sting (*Sting[wt/wt]*).
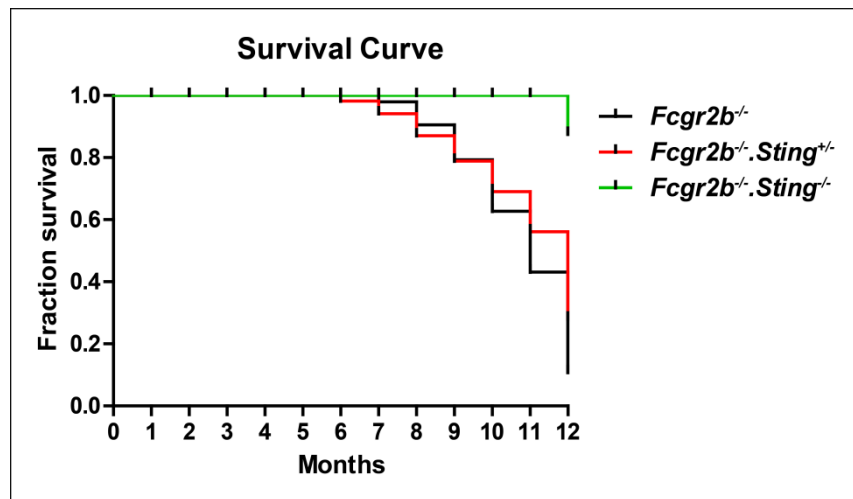
Figure 8 Increase in survival rates of the *Fcgr2b*-deficient mice in the absence of Sting.

The *Fcgr2b*-deficient mice were crossed with Sting-deficient mice (Sting$^{gt/gt}$) to generate the double-deficient mice (*Fcgr2b$^{-/-}$. Sting$^{gt/gt}$*) and littermate controls. The survival curve of the mice was observed up to 12 months (N= 14 per group).

Sting pathway promotes autoantibody production and glomerulonephritis in the *Fcgr2b$^{-/-}$* lupus mice

To examine the lupus phenotypes of the double-deficient mice compared with littermate controls, serum and kidney were collected at the age of 6-7 months. The level of anti-dsDNA antibody from the sera of the double-deficient mice (*Fcgr2b$^{-/-}$.Sting$^{gt/gt}$*) was determined by ELISA assay and showed significantly lower than the *Fcgr2b$^{-/-}$* mice (Figure 9A). It is likely that the anti-nuclear antibody (ANA), the fluorescence intensity grading showed a decrease in *Fcgr2b$^{-/-}$.Sting$^{gt/gt}$* mice (Figure 9B-9D).
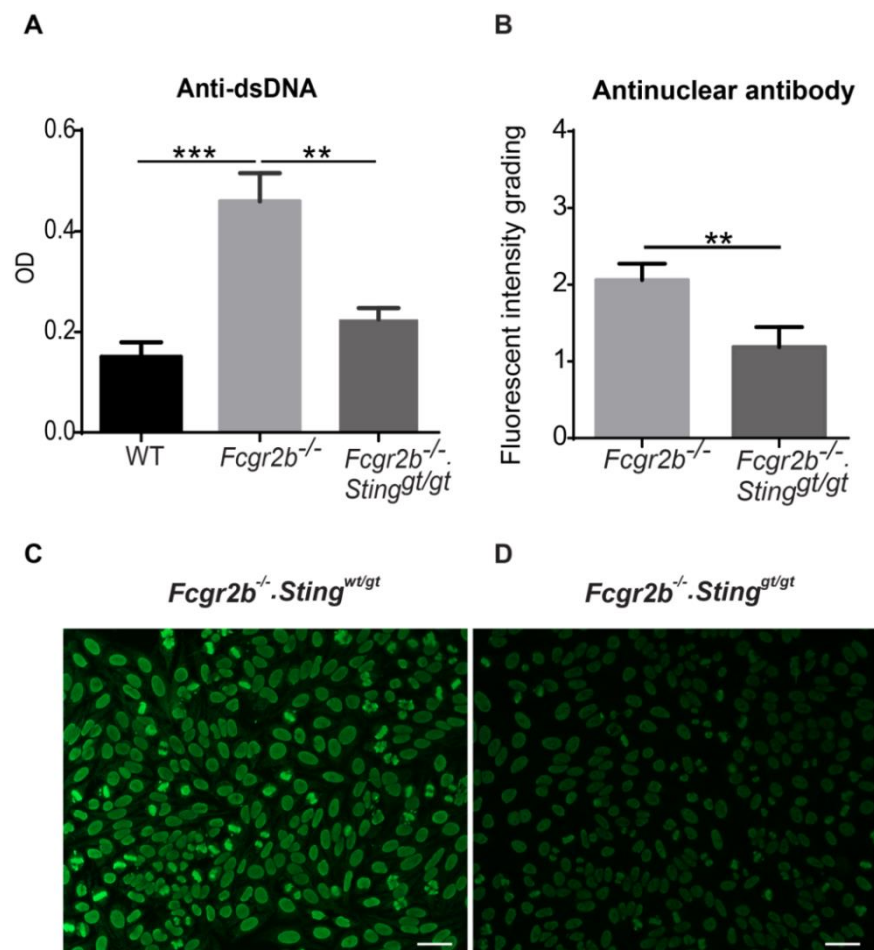
Figure 9 Decrease autoantibody productions in the double deficient mice.

(A) Anti-dsDNA from sera (dilution 1:100) of *Fcgr2b*$^{-/-}$ and *Fcgr2b*$^{-/-}$. *Sting*$^{gt/gt}$ was detected by ELISA (N=10-11 per group).The anti-nuclear antibodies (ANA) from the sera of *Fcgr2b*$^{-/-}$ and *Fcgr2b*$^{-/-}$. *Sting*$^{gt/gt}$ (dilution 1:800) shows by (C and D) the immunofluorescence staining. Data are representative of 8 mice per group (scale bar = 20 µm). (B) Semi-quantification of ANA was graded by fluorescence intensity (N=8 mice per group). Error bars indicate SEM, *p < 0.05, **p<0.01, and ***p<0.001.

Moreover, the kidneys of *Fcgr2b*$^{-/-}$ mice showed pathology of diffuse proliferative glomerulonephritis, enlarged glomeruli, and crescentic glomeruli, which did not present in the *Fcgr2b*$^{-/-}$. *Sting*$^{gt/gt}$ mice (Figure 10A-10B). The glomerular and

interstitial scores in the kidneys of $Fcgr2b^{-/-}$ mice were significantly higher than the double-deficient mice (Figure 10C-10D).
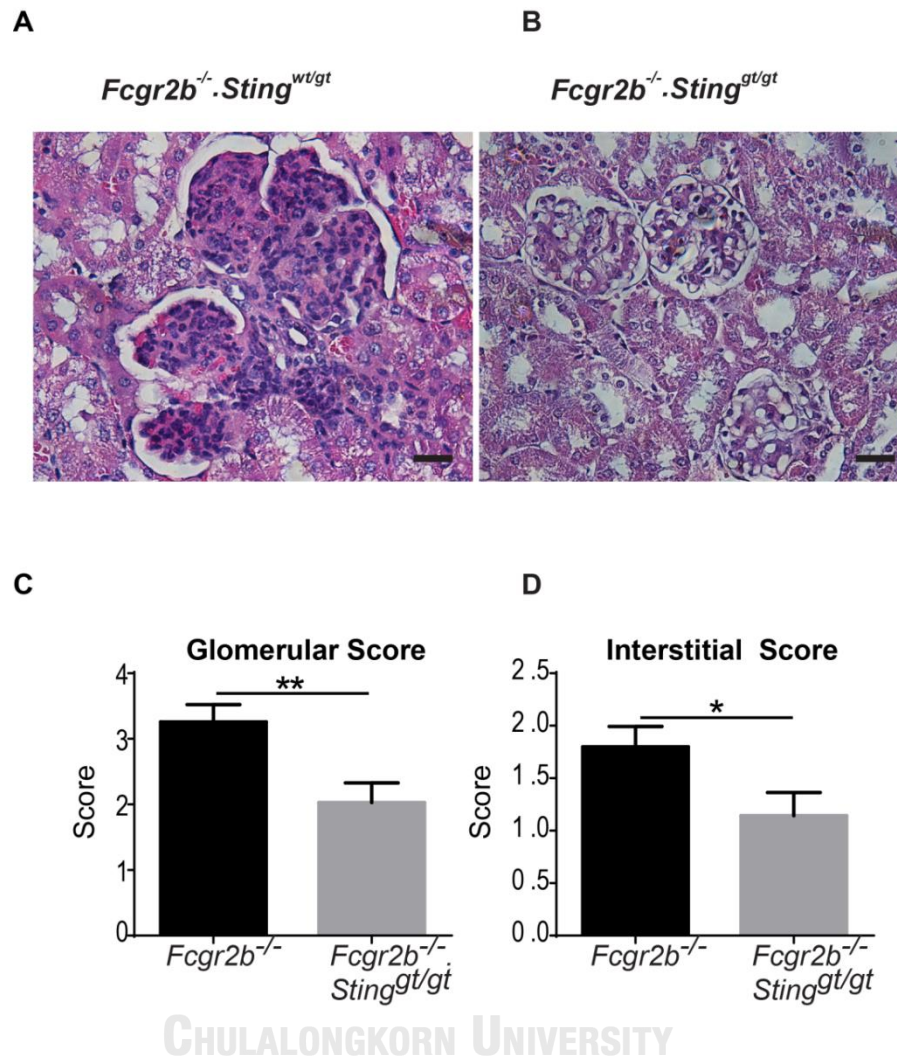

Figure 10 Sting deficiency diminishes fatal glomerulonephritis in the Fcgr2b-deficient mice.

(A-B) Kidney sections of $Fcgr2b^{-/-}$ and $Fcgr2b^{-/-}$. $Sting^{gt/gt}$ mice (6-8 months old) were stained with H&E. Data are representative of 7-10 mice per group (scale bar = 25 μm). (C-D) Glomerular scores and interstitial scores of kidney sections were blindly graded (N=7–10 per group). Data show as mean ± SEM (*p < 0.05, **p<0.01 and ***p<0.001).

Consistent with the pathology, the immunofluorescence staining showed fewer leukocyte infiltration cells (CD45$^+$ cells) and immune complex deposition (IgG) in the kidneys of *Fcgr2b$^{-/-}$.Sting$^{gt/gt}$* mice (Figure 11).
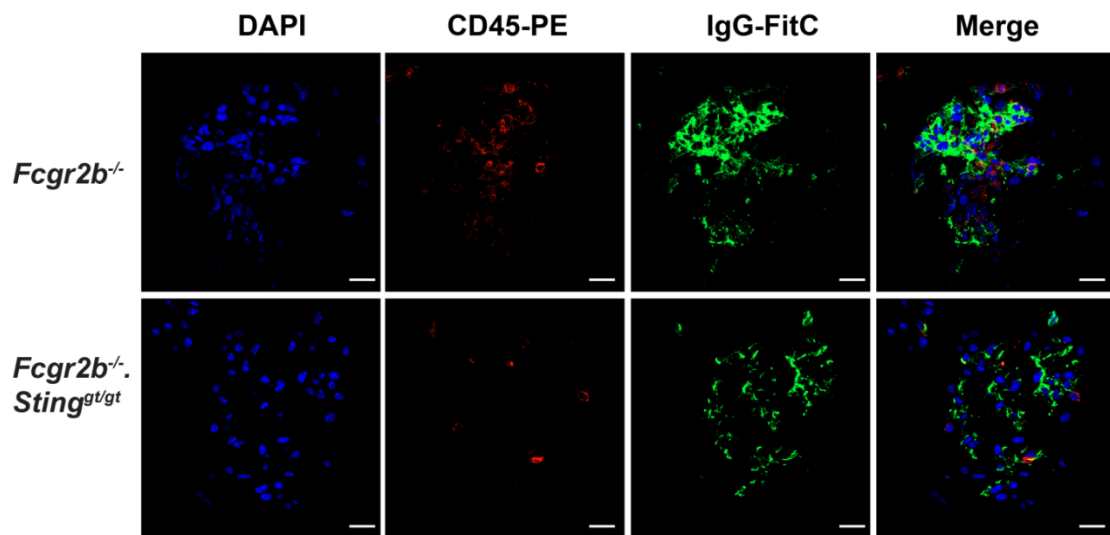

Figure 11 Decrease IgG deposition and leukocyte infiltration in the kidneys of the double-deficient mice.

Immunofluorescence staining in the kidney of *Fcgr2b$^{-/-}$* and double- deficient mice by confocal microscope show in green (IgG), red (CD45), and blue (DAPI). Data are representative of 3 mice per group (scale bar=10 μm).

Decrease interferon-inducible gene expression in the kidneys of the double-deficient mice

In order to determine the expression of interferon-inducible genes in the kidney of these mice, RNA was performed by microarray. The results found that the higher expression in the *Fcgr2b$^{-/-}$* mice, especially in the ones with greater severity (mouse number 003, 004) and a significant reduction of interferon-inducible genes in the kidneys of *Fcgr2b$^{-/-}$.Sting$^{gt/gt}$* mice (Figure 12). However, not all of these interferon-inducible genes decreased in the *Fcgr2b$^{-/-}$.Sting$^{gt/gt}$* mice (Figure 12).
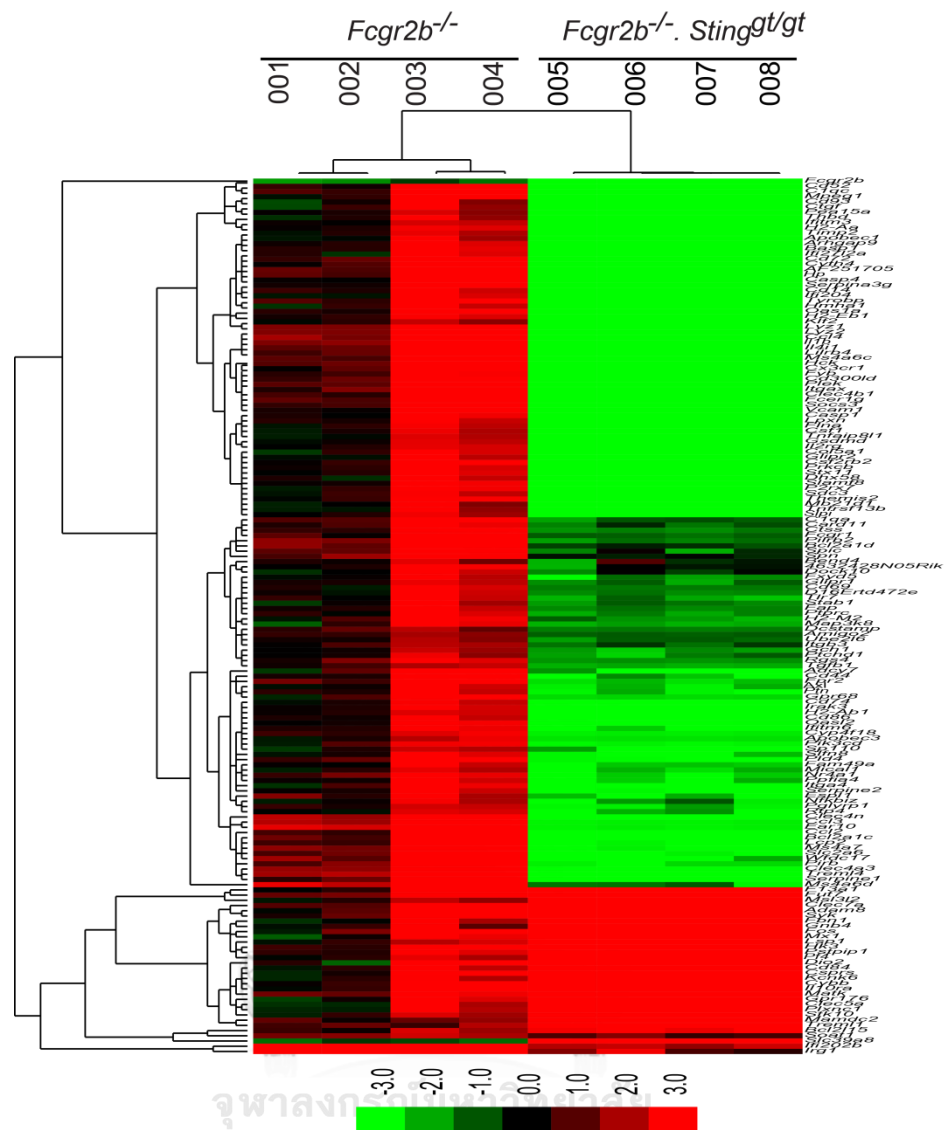
Figure 12 Gene expression profiles of kidneys in the Fcgr2b^-/- and Fcgr2b^-/-. Sting^gt/gt mice

A heat map shows that the interferon signature genes significantly changed in the *Fcgr2b^-/-* mice (N=4 mice per group). Data show in $\log_2$ (sample/wild-type).

Furthermore, the significantly 167 genes of interferon-inducible genes were identified and clustered using the online resource Database for Annotation (DAVID, v 6.8, https://david.ncifcrf.gov/) in the immune system majoring that shown in Table 6.

Table 6 Annotation Cluster of interferon-inducible genes of microarray data from the kidneys of *Fcgr2b*$^{-/-}$ and *Fcgr2b*$^{-/-}$. *Sting*$^{gt/gt}$ mice

Annotation Cluster	Count	P-Value
Immunity	38	4.20E-31
immune system process	36	5.30E-28
innate immune response	28	1.10E-19
Innate immunity	24	2.00E-19
Adaptive immunity	11	6.70E-10
adaptive immune response	12	7.40E-10
B cell activation	3	1.80E-02

Additionally, more observed show that the genes are not in the interferon-inducible genes that significantly changed in the *Fcgr2b*$^{-/-}$ and *Fcgr2b*$^{-/-}$. *Sting*$^{gt/gt}$ (Figure 13). Those genes were identified and determined to the pathway using the online resource Database for Annotation (DAVID, v 6.8, https://david.ncifcrf.gov/). The data suggested that those genes were clustered in the several pathways that show in Table 7.
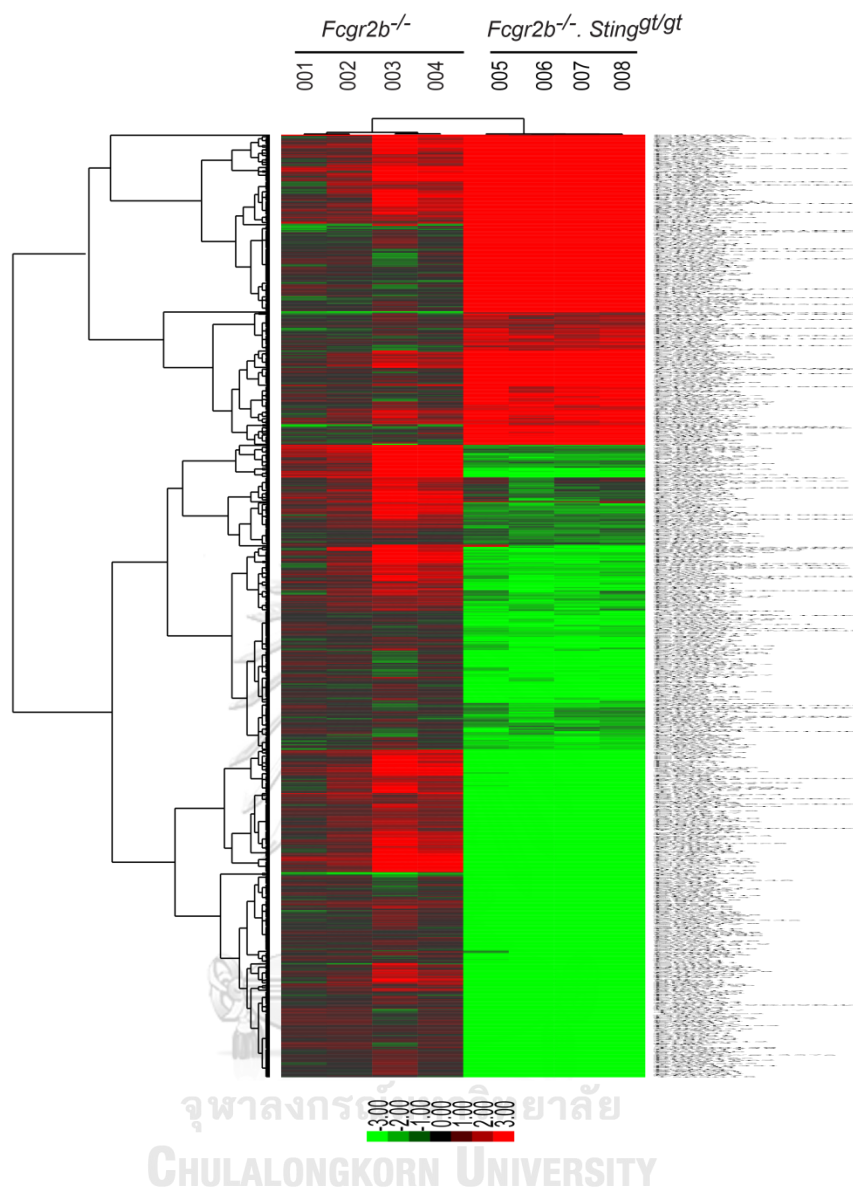
Figure 13 Non-interferon-inducible genes profiles of kidney in the *Fcgr2b*^{-/-} and

Fcgr2b^{-/-}*. Sting*[gt/gt] mice.

A heat map of microarray data show the genes that significantly changed up to 2 fold

compared between *Fcgr2b*^{-/-} and *Fcgr2b*^{-/-}*. Sting*[gt/gt] mice (N=4 mice per group; p<0.05).

Data show in log2 (sample/wild-type).

This data suggested that Sting-dependent pathology mediated by both
interferon and non-interferon signaling and not all of the interferon signaling in the
Fcgr2b^{-/-} mice contributed by Sting pathway.

Table 7 Pathway list of non-interferon inducible genes of microarray data from the kidneys of $Fcgr2b^{-/-}$ and $Fcgr2b^{-/-}$. $Sting^{gt/gt}$ mice

Pathways	p-value
Leukocyte trans-endothelial migration	0.0031
PI3K-Akt signaling pathway	0.0043
Jak-STAT signaling pathway	0.013
Chemokine signaling pathway	0.017
Focal adhesion	0.02
Staphylococcus aureus infection	0.023
Cytosolic DNA-sensing pathway	0.026
Osteoclast differentiation	0.032
RIG-I-like receptor signaling pathway	0.04
Leishmaniasis	0.04
Measles	0.045
B cell receptor signaling pathway	0.075
Natural killer cell mediated cytotoxicity	0.077

Next, to confirm the expression of interferon-inducible genes by real-time PCR in the kidneys of the $Fcgr2b^{-/-}$ mice, the results show that the expressions of $Isg15$, $Mx1$, $Irf3$, and $Irf7$ were upregulated in the $Fcgr2b^{-/-}$ mice and downregulated in the absence of Sting (Figure 14A-14E). Also, the expression of $Irf5$, the lupus susceptibility gene, that upregulated in the kidneys of the $Fcgr2b^{-/-}$ mice was Sting-dependent (Figure 14D).
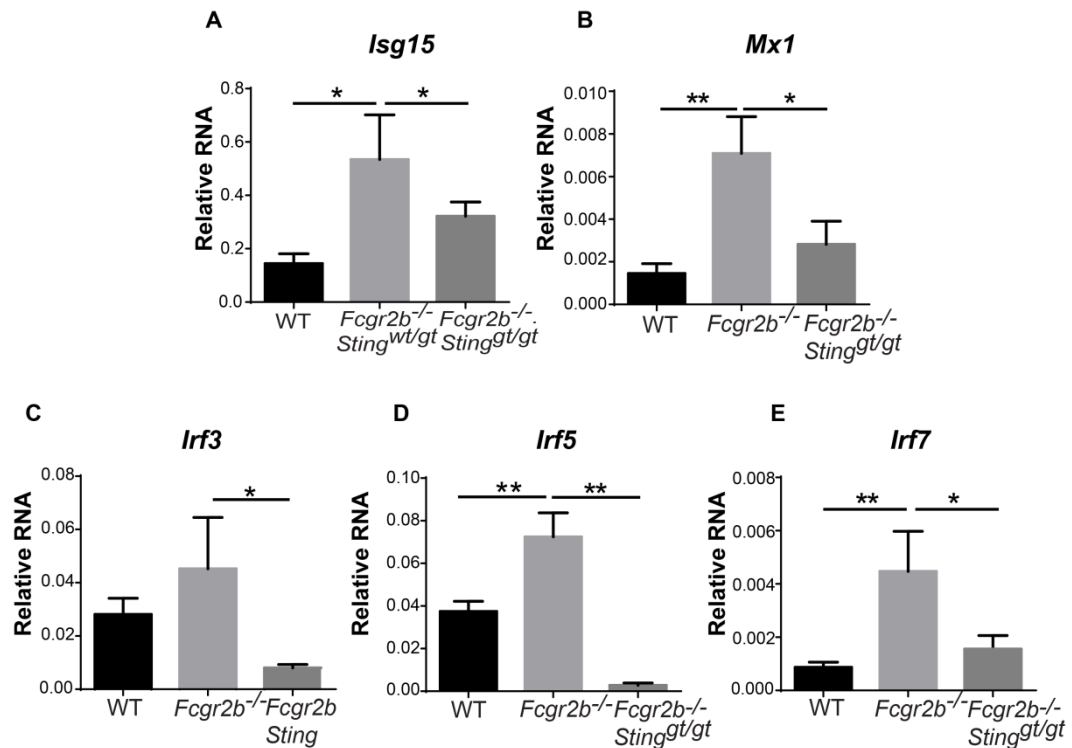
Figure 14 Decrease interferon-inducible gene expressions in the kidneys of the double-deficient mice.

(A-E) Gene expression profiles from the kidneys of wild-type, *Fcgr2b*$^{-/-}$ and *Fcgr2b*$^{-/-}$.*Sting*$^{gt/gt}$ mice at the age of 6-7 months were tested by real-time PCR (N=10-17 per group). The mRNA expressions of interferon-inducible genes shown in (A) *Isg15, (B) Mx1,(C) Irf3,(D) Irf5, and (E) Irf7*. Data show as mean ± SEM (*p < 0.05 and **p<0.01).

Sting signaling is essential for inflammatory phenotypes of the *Fcgr2b*$^{-/-}$ lupus mice

The splenocytes were analyzed from the mice at the age of 6-7 months to characterize the alteration of immune-phenotypes. The expansion of dendritic cells (CD11c$^+$) and plasmacytoid dendritic cells (CD11c$^+$PDCA$^+$) in the *Fcgr2b*$^{-/-}$ mice diminished in the *Fcgr2b*$^{-/-}$.*Sting*$^{gt/gt}$ mice (Figure 15A-15B). Also, these data found that the reduction of T effector memory cells (CD3$^+$CD4$^+$CD62L^{lo}CD44^{hi}), CD3$^+$CD4$^+$ICOS$^+$ cells, and germinal center B cells (B220$^+$GL7$^+$) in the double-deficient mice (Figure 15C-15E). Besides, the mean fluorescence intensity of MHC-II (IA-b) on B cells significantly reduced in the double-deficient mice (Figure 15F). However, the expansion of plasma

cells did not show the difference between single and double-deficient mice (Figure 15G). The representatives of flow cytometric analysis are shown in Figure 16.
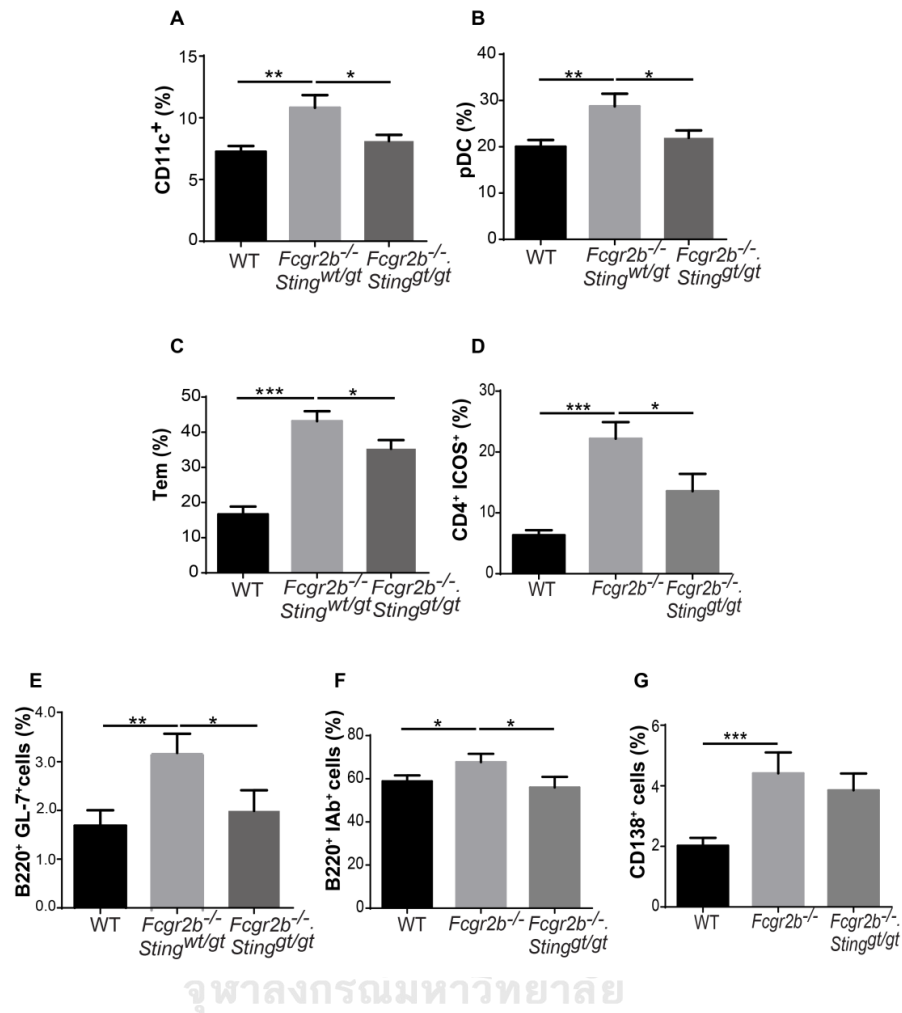
Figure 15 Decrease of dendritic cells, plasmacytoid dendritic cells, effector T cells, and germinal center in the double-deficient mice.

(A-G) Flow cytometry analysis of splenocytes isolated from wild-type, $Fcgr2b^{-/-}$, and $Fcgr2b^{-/-}$. $Sting^{gt/gt}$ mice at the age of 6-7 months (N= 13-14 per group). Data shown in the percentage of (A) CD11c$^+$, (B) plasmacytoid dendritic cells (pDC), (C) T effector memory (CD3$^+$CD4$^+$CD44^{hi}CD62L^{lo}), (D) CD3$^+$CD4$^+$ICOS$^+$ cells, (E) B220$^+$GL7$^+$ cells and (G) CD138$^+$ cells. Data show as mean ± SEM (*p < 0.05, **p<0.01 and ***p<0.001).

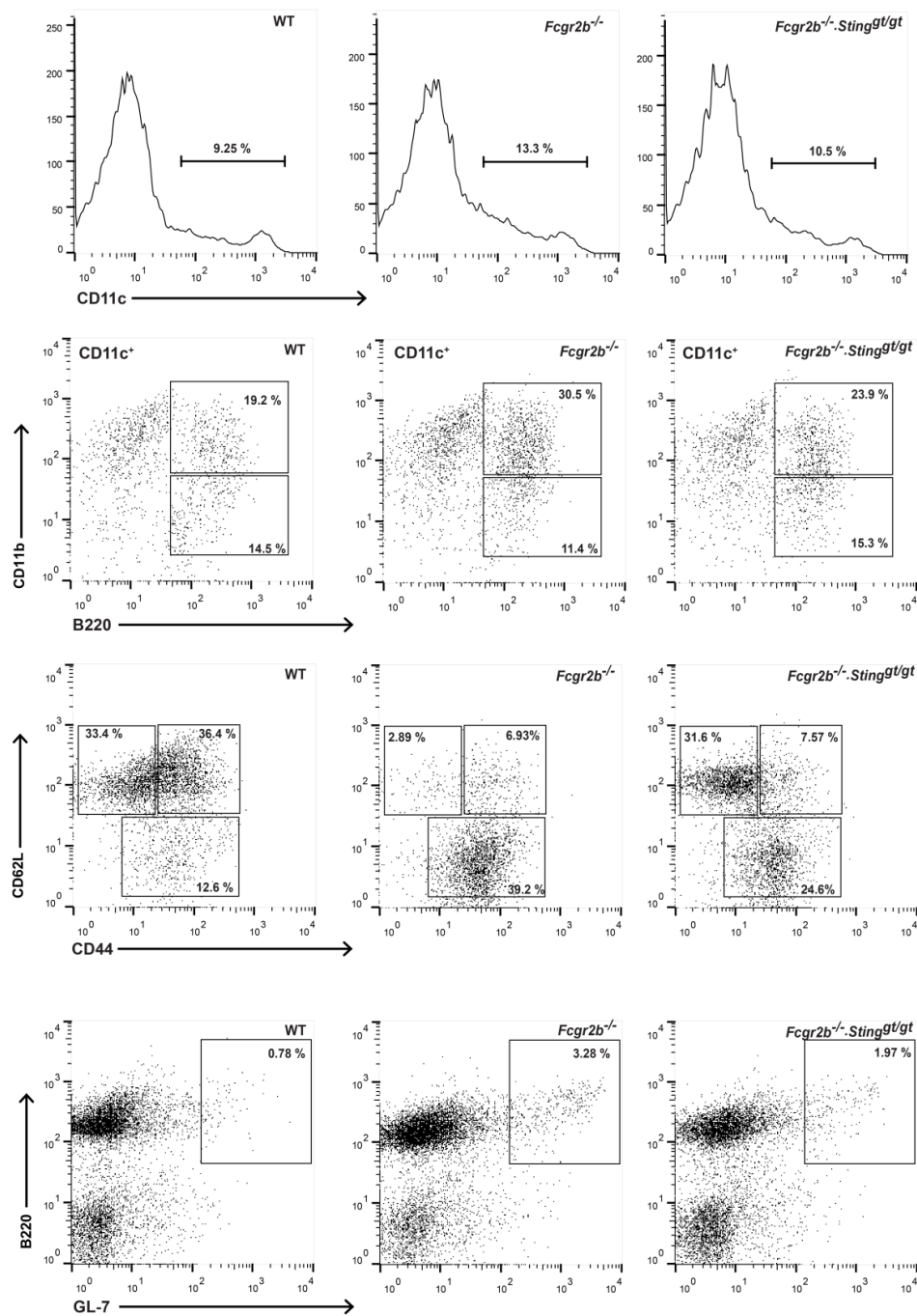Figure 16 Representative of flow cytometric analysis from the spleen of WT, *Fcgr2b*$^{-/-}$, and *Fcgr2b*$^{-/-}$.*Sting*$^{gt/gt}$ mice.

Data shows in the percentage of (A) CD11c$^+$, (B) plasmacytoid dendritic cells (pDC), (C) T effector memory (CD3$^+$CD4$^+$CD44^{hi}CD62L^{lo}) and (D) B220$^+$GL7$^+$ cells by Flowjo software version 10.

Furthermore, the sera levels of MCP-1 and TNF-α from the *Fcgr2b*^{-/-} mice were significantly increased compared to WT mice (Figure 17A-17B) whereas IL-1β and IL-23 did not show the significant changes (Figure 17C-17D). However, the levels of TNF-α, IL-1β, and IL-23 from the *Fcgr2b*^{-/-} mice were significantly decreased in the absence of Sting (Figure 17B-17D). These data suggested that Sting participates in the inflammatory mediated pathway in the *Fcgr2b*-deficient lupus mice.
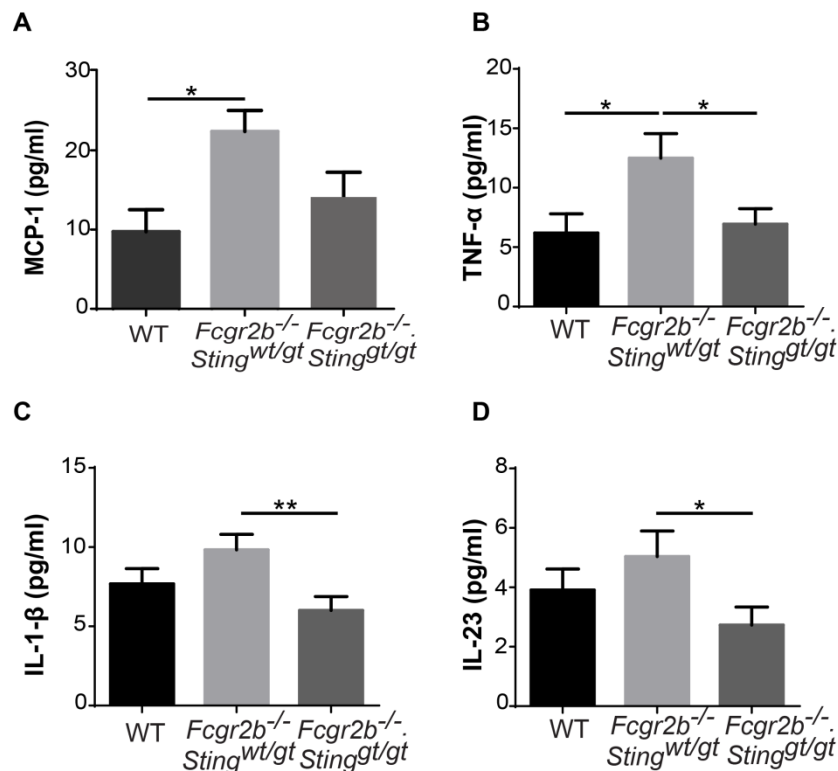
Figure 17 Sting mediated signaling decrease the production of inflammatory cytokines in double-deficient mice.

(A-D) The sera cytokines of wild-type, *Fcgr2b*^{-/-} and *Fcgr2b*^{-/-}. *Sting*[gt/gt] mice at the age of 6-7 months were analyzed by cytometric bead array. Serum cytokines of (A) MCP-1, (B) TNF-α, (C) IL-1β, and (D) IL-23 (N=10-15 per group). Data show as mean ± SEM (*p < 0.05 and **p<0.01).

Sting activated dendritic cells induce the proliferation of naïve CD4+ T cells

The splenocytes of *Fcgr2b*^{-/-} mice showed an increase of effector memory T cells (T$_{em}$) and *Ifn-γ* expression (Figure 15C and 6B). The hypothesis of this study is the high proportion of T$_{em}$ in the *Fcgr2b*^{-/-} mice might contribute to the increase of *Ifn-*

γ expression. To test if this assumption is correct, the intercellular staining of IFN-γ from lymph nodes of the affected mice were performed. The results show that the numbers and percentage of IFN-γ producing CD4$^+$ T cells from the *Fcgr2b$^{-/-}$* mice were higher than wild-type and double-deficient mice (Figure 18A-18C).
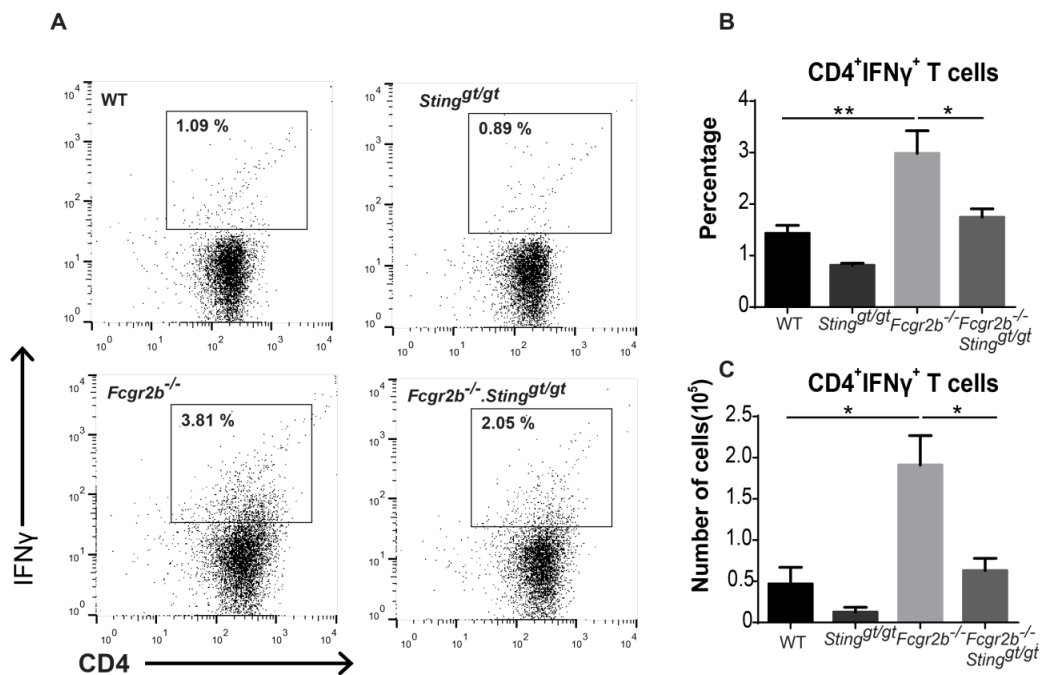

Figure 18 Sting mediated pathway induces IFN-γ producing CD4$^+$ T cells from the *Fcgr2b$^{-/-}$* mice.

(A-C) Flow cytometry analysis of (A-B) intracellular staining of IFN-γ -producing CD4$^+$ T cells isolated from lymph nodes of wild-type, *Sting$^{gt/gt}$*, *Fcgr2b$^{-/-}$*, and *Fcgr2b$^{-/-}$. Sting$^{gt/gt}$* mice at the age of 6-7 months. (A) Data are representative of 3-4 mice per group. (B) The percentage of IFN-γ^+ CD4$^+$ T cells and (C) the number of IFN-γ^+ CD4$^+$ T cells (N=3-4 per group). Data show as mean ± SEM (*p < 0.05, and **p<0.01).

To determine if the Sting-expressing DC could directly influence the T cell phenotypes, T cells were co-cultured with activated BMDC. The short-interval (6 hours) co-cultured between Sting-activated BMDC derived from *Fcgr2b$^{-/-}$* and double-deficient mice and CD4$^+$ T cells from lymph nodes showed comparable numbers of

IFN-**γ** producing CD4$^+$ T cells independent of Sting expression on BMDC (Figure 18A and 18B). However, the CD4$^+$ T cells derived from the *Fcgr2b*$^{-/-}$ mice expressed the intracellular staining of IFN-**γ** higher than the double-knockout mice when co-cultured with *Sting*-sufficient BMDC (Figure 19A and 19B).
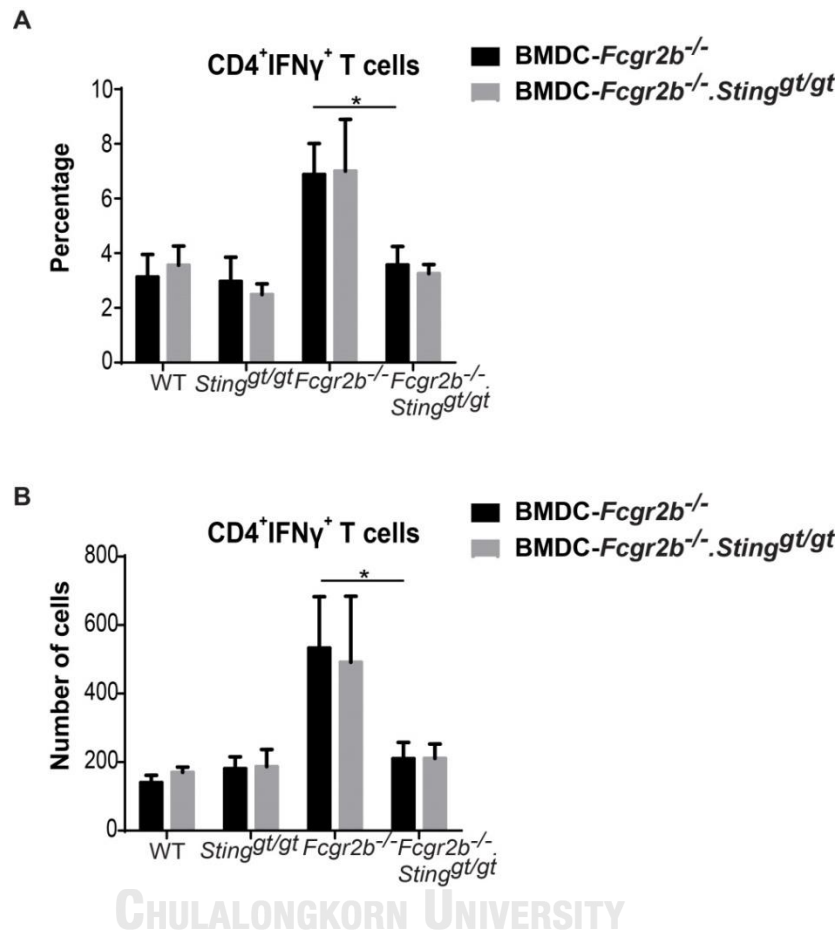

Figure 19 Sting express on BMDC independent IFN-**γ** producing CD4$^+$ T cells for a short time.

(A) The percentage and (B) the number of intracellular IFN-**γ** producing CD4$^+$ cells after co-cultured with DMXAA activated BMDC from *Fcgr2b*$^{-/-}$ and *Fcgr2b*$^{-/-}$. *Sting*$^{gt/gt}$ (6–7 months old) for six hours (N=3-4). Data show as mean ± SEM (*p < 0.05).

Next, to examine if Sting activated BMDC can promote T cell proliferation, purified naïve T cells from spleen were co-cultured with Sting-activated BMDC for 72 hours and assessed with CFSE dilution assay (Figure 20A and 20B). The proliferation ability of naïve T cells was independent on Sting expression on T cells but depended on Sting-expression on BMDC (Figure 20A and 20B). The naïve T cells that primed with Sting expressing BMDC became more proliferative, and these cells were capable of producing higher IFN-γ compared to the cells that were co-cultured with Sting deficient BMDC (Figure 20C). These data suggest that Sting activation promoted the DC differentiation, which subsequently the activated DC primed the naïve CD4$^+$ T cells to proliferate and become the IFN-γ producing T cells.
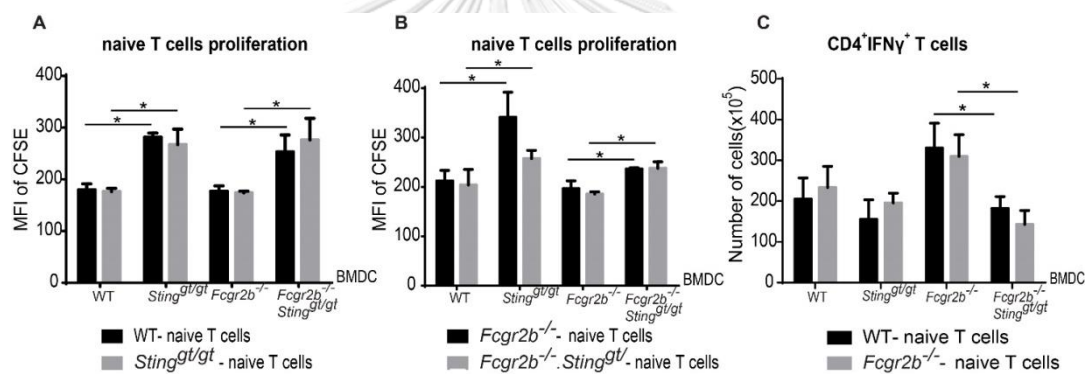
Figure 20 Sting activated dendritic cells induce the proliferation of naïve CD4$^+$ T cells. *(A-C) Co-culture of naïve T cells with DMXAA activated BMDC from wild-type, Sting$^{gt/gt}$, Fcgr2b$^{-/-}$ and Fcgr2b$^{-/-}$. Sting$^{gt/gt}$ mice (labeled at x-axis) for 72 hours. (A and B) CFSE dilution of isolated naïve T cells showed in mean fluorescence intensity (MFI), and (C) the total numbers of IFN-γ^+ CD4$^+$ T cells (N=4 per group). Data show as mean ± SEM (*p < 0.05).*

Sting activation increases the maturation of dendritic cells and cytokine production

In order to understand the immunological importance of Sting in lupus *Fcgr2b*-deficient mice, the flow cytometry was characterize the subsets of splenocytes from affected mice and their controls. The activated immune cells showed that the expansion of the DC in the spleen of the *Fcgr2b$^{-/-}$* mice was Sting-dependent (Figure 15A), and the cGAS/Sting pathway is important for DC activation (75). To investigate if the expansion of DC in the *Fcgr2b$^{-/-}$* mice is directly mediated by Sting signaling, the bone-marrow derived dendritic cells (BMDC) were differentiated into immature DC and subsequently stimulated with Sting ligands (DMXAA), DMSO, and LPS (as a control) to assess if Sting played a role in DC maturation. The LPS control induced the immature DC to increase the expression of MHC-II (IA-b) and CD80, which suggested the phenotypes of mature DC, from both *Sting*-sufficient and *Sting*-deficient mice (Figure 21A and 21C). While the immature DC from wild-type and *Fcgr2b$^{-/-}$* mice also showed the increasing percentage of IA-b$^+$ and CD80$^+$ DC cells after DMXAA stimulation, but the *Sting*-deficient mice did not develop these mature phenotypes (Figure 21B and 21D).
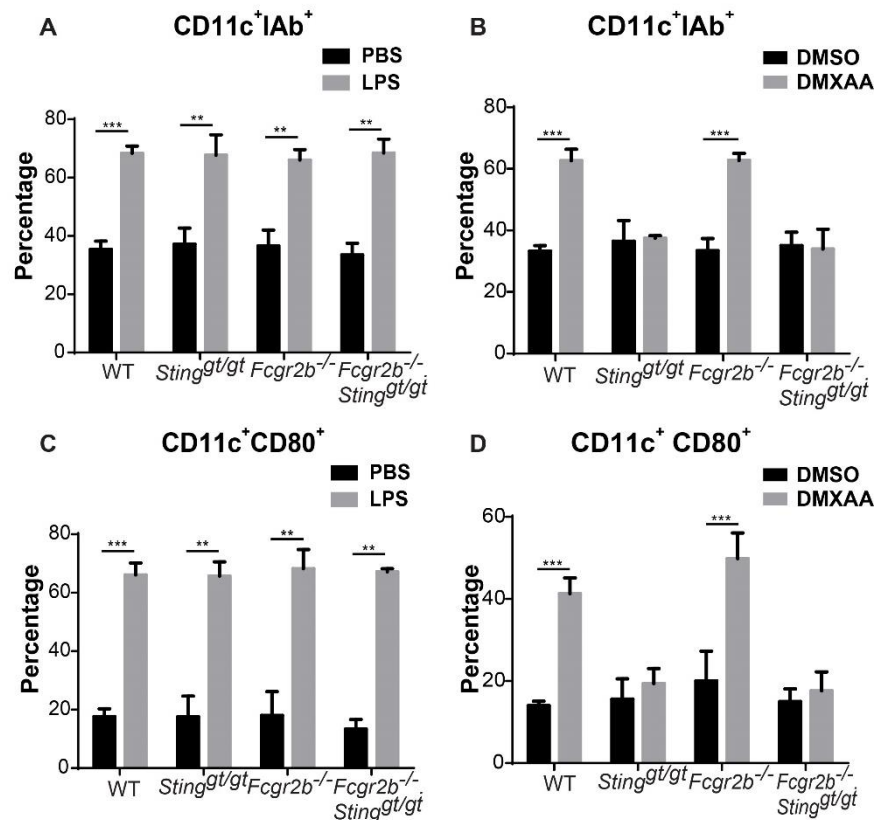
Figure 21 Sting activation increases the maturation of dendritic cells.
Bone marrows were isolated from wild-type, $Sting^{gt/gt}$, $Fcgr2b^{-/-}$ and $Fcgr2b^{-/-}$. $Sting^{gt/gt}$ mice at the age of 6-7 months. (A-D) IL-4 and GM-CSF differentiated bone marrow-derived dendritic cells (BMDC) for five days then immature BMDC were stimulated with LPS or DMXAA for 24 hours. Flow cytometry analysis shows the percentage of (A-B) CD11c$^+$ IAb$^+$ cells and (C-D) CD11c$^+$ CD80$^+$ cells. Data show as mean ± SEM (N=3–5; *p < 0.05, **p<0.01 and ***p<0.001).

Furthermore, the supernatant from BMDC culture with DMXAA stimulation showed the increase in the concentration of IL-1α, IL-6, TNF-α, and MCP-1 in the wild-type and *Fcgr2b*$^{-/-}$ mice but not in Sting-deficient mice and double-deficient mice (Figure 22A-22D). These data suggested that Sting signaling pathway mediated DC maturation, activation stage, and cytokine production.

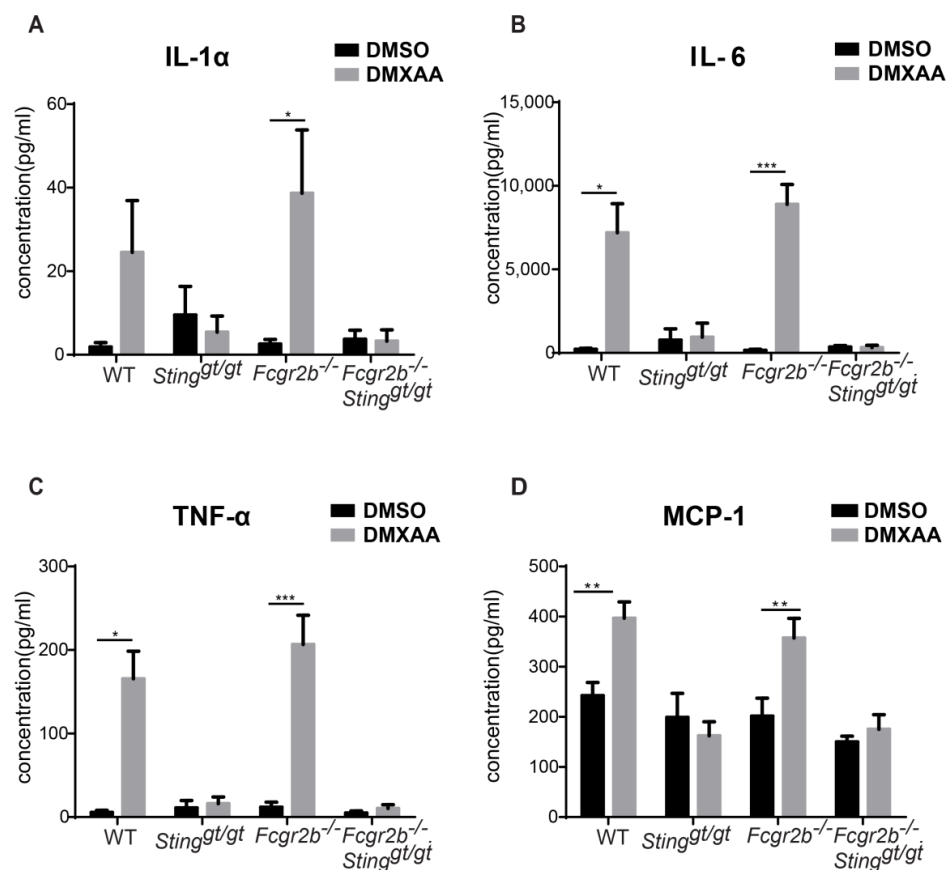Figure 22 Sting-mediated signaling promotes cytokine production in DC. (A-D) Supernatants were collected and analyzed after DMXAA stimulation for 24 hours. Cytometric bead array shows the levels of (A) IL-1α, (B) IL-6, (C) TNF-α and (D) MCP-1. Data show as mean ± SEM (N=3–5; *p < 0.05, **p<0.01 and ***p<0.001).

Sting signaling promotes the differentiation of plasmacytoid dendritic cells (pDC)

To better understand the function of Sting in DC, the quantitative proteomic analysis of Sting activated BMDC in the *Fcgr2b*$^{-/-}$ mice compared to the double-deficient mice were performed using a dimethyl labeling method. The Volcano plot showed the protein that highly expressed were interferon-regulated proteins (Figure 23). This finding may result from the increase of IFN-I production in the culture medium, which could upregulate the interferon-regulated proteins.
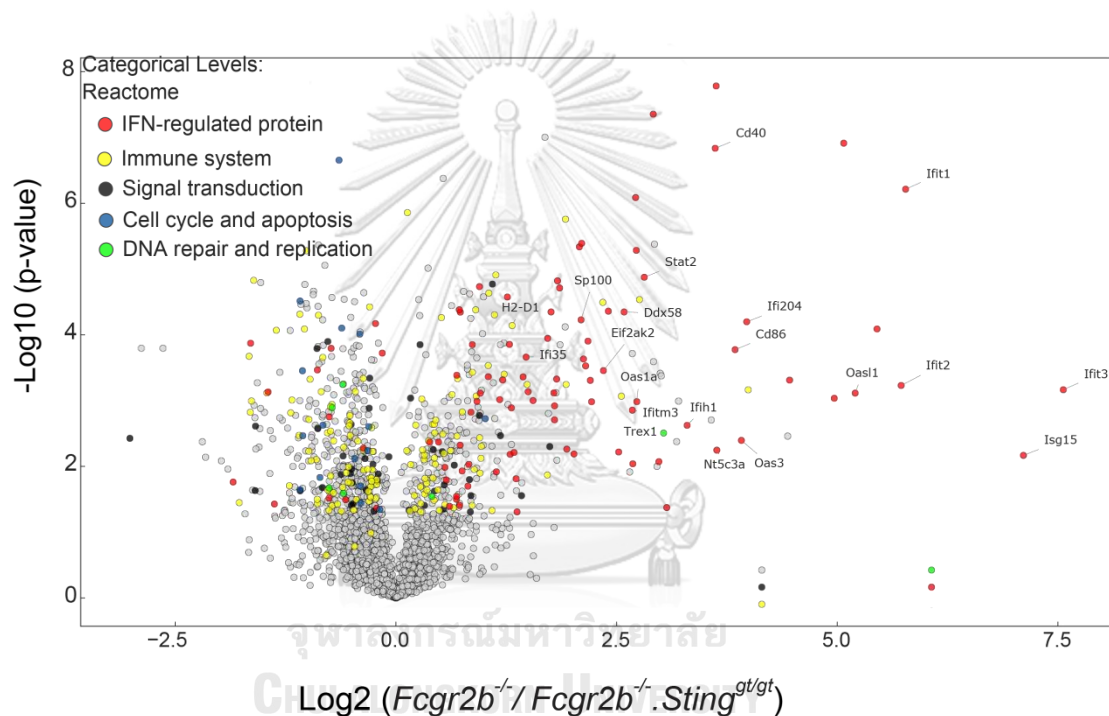

Figure 23 *Fcgr2b*$^{-/-}$ increase the expression of interferon-regulated proteins.
Volcano plot of protein expressions from proteomic analysis of DMXAA activated BMDC of *Fcgr2b*$^{-/-}$ and *Fcgr2b*$^{-/-}$. *Sting*$^{gt/gt}$ mice at the age of 6-7 months (N=4 per group).

The hypothesis of this study is Sting might promote the differentiation of pDC (the major producer of IFN-I). To confirm this hypothesis, the in vitro culture of BMDC with DMXAA and LPS (as a control) showed a significant increase in pDC and IFN-β production with DMXAA but not with LPS stimulation (Figure 24A-24D). Also, the results show the morphology of these cells by the imaging flow cytometry and found the pDC expressed CD80 and IA-b as well (Figure 24E -24F).
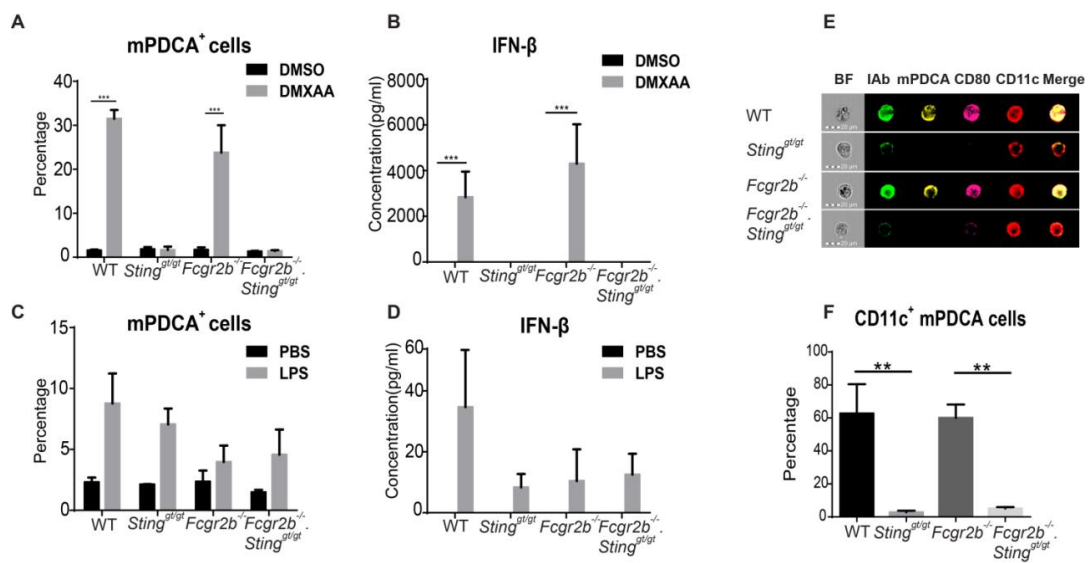
Figure 24 Sting activation promotes differentiation of plasmacytoid dendritic cells (pDC).

The percentage of pDC (PDCA+ cells) after (A) DMXAA activation and (C) LPS activation for 24 hours (N = 3–4 per group). (B and D) The level of IFN-β from the culture supernatant of activated BMDC with (B) DMXAA and (C) LPS (N = 5 per group). (E and F) Imaging flow cytometry of DMXAA activated BMDC shows (E) the representative staining of IA-b (green), mPDCA (yellow), CD80 (pink), and CD11c (red) and (F) the percentage of CD11c+mPDCA+ cells (N= 3 mice per group). A representative of 3 experiments. Data show as mean± SEM (**p<0.01 and ***p<0.001).

Sting signaling increases the interaction with Lyn kinase

Moreover, to better understand the STING interacting protein, the immunoprecipitation of the Sting using the Sting antibody targeted N-terminal were performed. After BMDC were activated with DMXAA for 3 hours, the cells were collected and analyzed by mass spectrometry to identify the Sting-interacting molecules. Among the proteins detected, Lyn, a member of Src family kinases, has been shown the function in the maturation of DC and pDC response (76, 77). To determine this interaction, western blot was performed. The immunoprecipitation confirmed that Lyn interacted with Sting after DMXAA stimulation in WT BMDC while Lyn constitutively interacted with Sting in the *Fcgr2b*-deficient BMDC (Figure 25A). This interaction could result from the intrinsic activation of Sting in the *Fcgr2b*$^{-/-}$ mice. This activation did not change the protein abundance of Lyn and Sting in total cell lysate (Figure 25B).
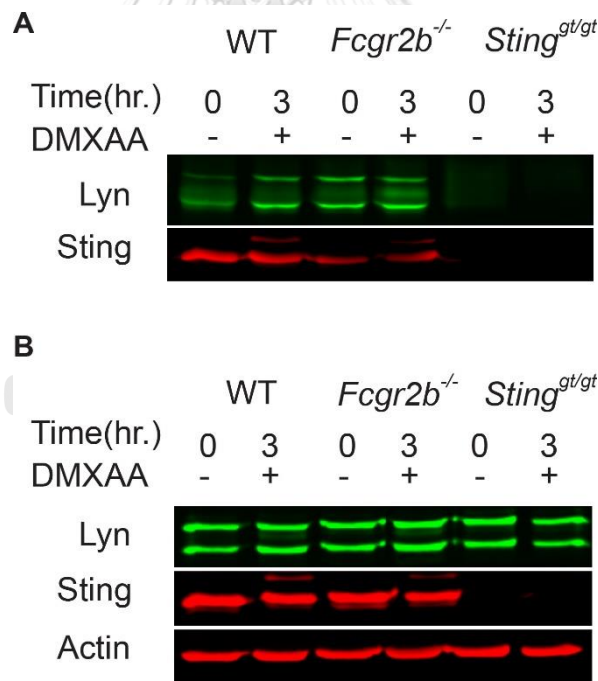
Figure 25 Sting activation recruited Lyn kinase.

(A and B) Fluorescent western blot shows (A) the immunoprecipitation with Sting (red) and blots with Lyn (green) and (B) cell lysate of activated BMDC with DMXAA at 0 and 3 hr. A representative of 4 experiments.

Interestingly, the IP‑Sting showed another band of protein which identified by mass spectrometry as the phosphorylation of Sting at Serine 357 (Ser357) (Figure 26A and 26B).
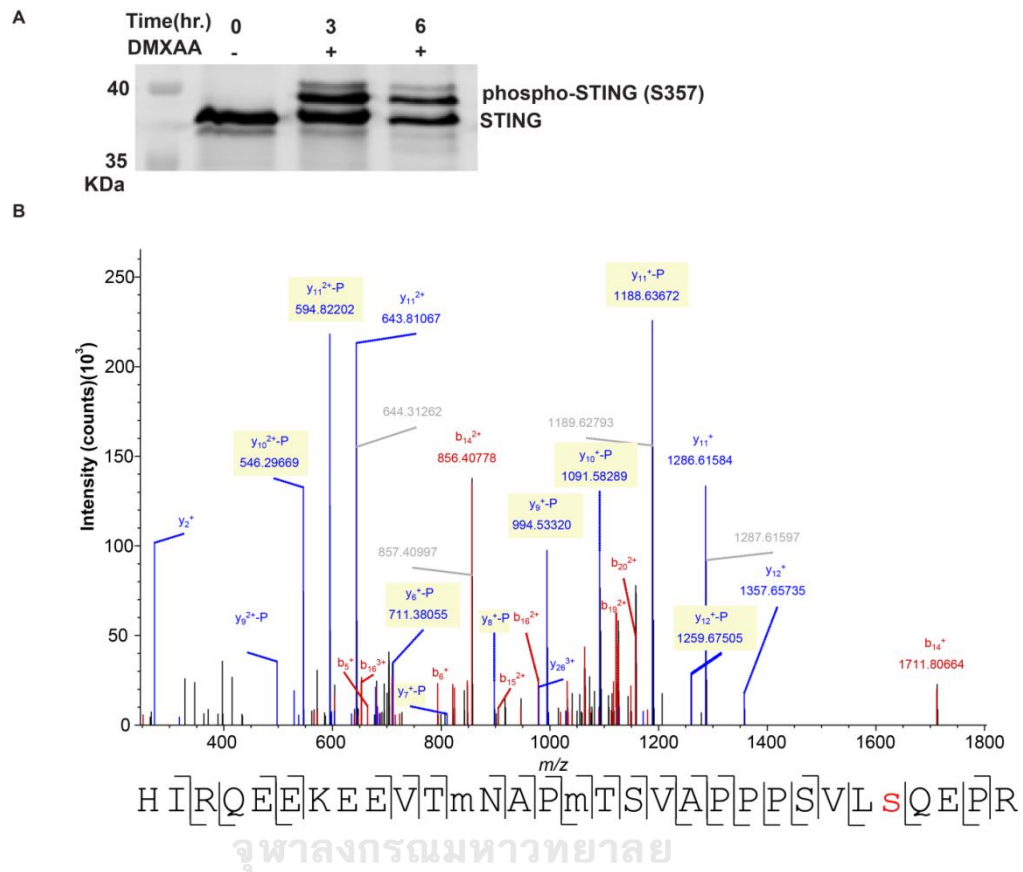
Figure 26 Phosphorylation of Sting after stimulated with DMXAA.

(A) A representative of western blot analysis from immunoprecipitation with Sting of *Fcgr2b*$^{-/-}$ mice (N= 4). The band was shown in STING protein of activated BMDC with DMXAA at 0, 3 and 6 hr. and phosphorylation of STING at Ser357. (B) Mass spectra of phosphorylation of STING at Ser357 of activated BMDC from *Fcgr2b*$^{-/-}$ mice after stimulated with DMXAA for 3 hours and followed by immunoprecipitation with Sting.

Sting mediated DC maturation and differentiation via Lyn signaling pathway

Lyn kinase regulates DC maturation, and genetic deletion of Lyn ablates pDC (77, 78). This study hypothesized that Sting promoted DC maturation and pDC differentiation through Lyn signaling pathway. WT-BMDC was treated with Lyn inhibitors PP2 followed by DMXAA stimulation and determined the maturation in the CD11c$^+$ population. The result shows pan SFK inhibitor PP2 decreased Sting-mediated the percentage of CD80, I-Ab, and mean fluorescent of I-Ab on conventional DC as shown in Figure 27A-27C and the differentiation of pDC (Figure 27D).
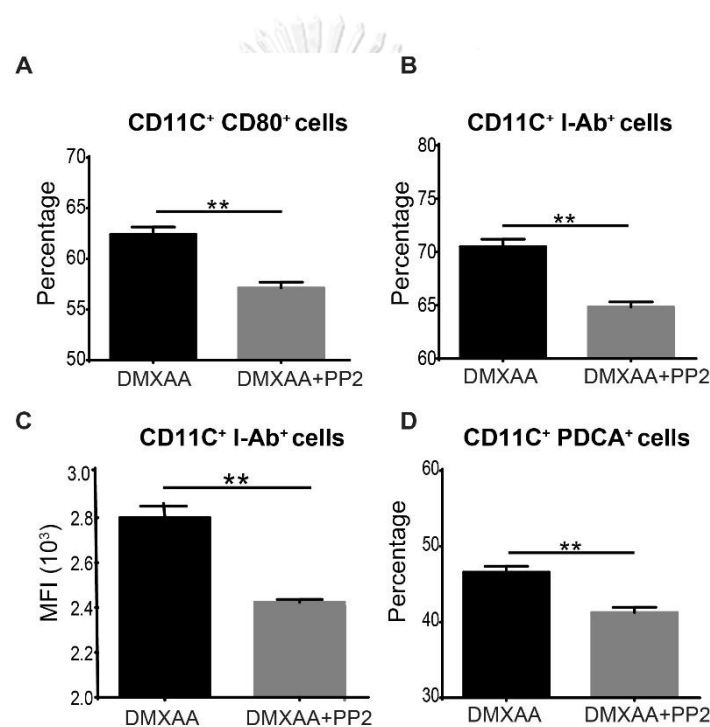
Figure 27 Lyn inhibition decreases the maturation of activated WT-BMDC. (A-B) Flow cytometry analysis of BMDC from wild-type mice at the age of 6-7 months. Data shown in the percentage of (A) CD11c$^+$ CD80$^+$ cells, (B) CD11c$^+$ I-Ab$^+$ cells, (C) mean fluorescence intensity (MFI) of I-Ab expressing DC and (D) PDCA$^+$CD11c$^+$ cells (N = 3 mice per group). Data show as mean± SEM (**p<0.01).

In addition, to determine whether Sting signaling mediated downstream through a LYN-PI3K-Akt pathway to promote DC maturation, the western blots of WT-BMDC were tested. The result showed that the activation of Sting increased the

phosphorylation of LYN (Tyr507) and AKT (Ser473), which were inhibited by PP2 (Figure 28). In contrast, this treatment did not change the expression of total LYN and AKT (Figure 28).
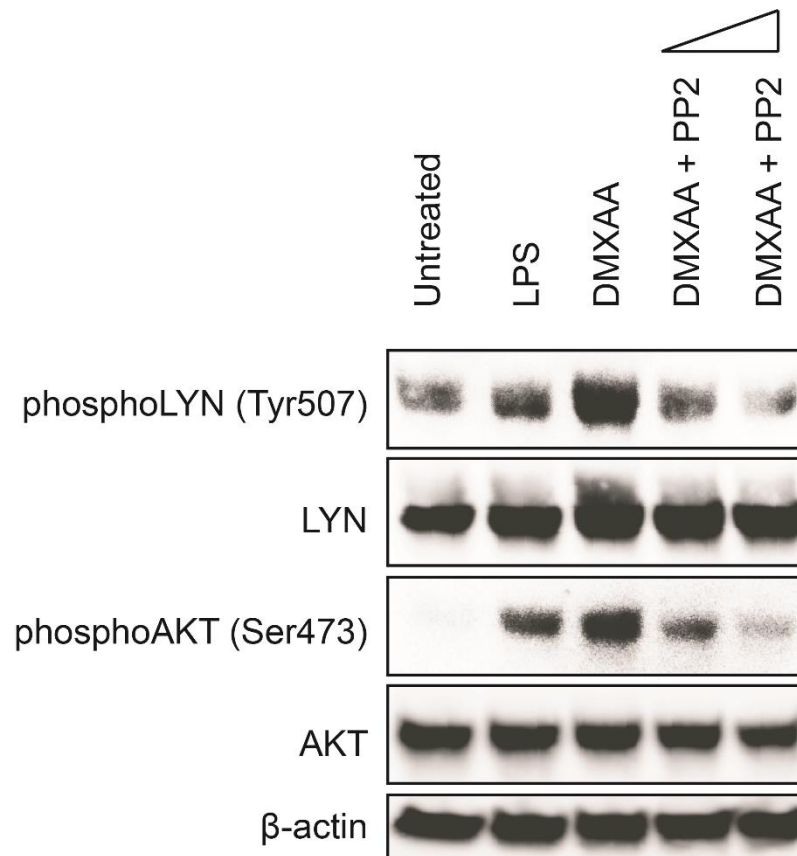
Figure 28 Sting signaling promote LYN-PI3K-AKT pathway.

A representative of western blot analysis from WT-BMDC after treated with PP2 followed by DMXAA stimulation (N= 3). The band was shown pLYN, and pAKT.

Additionally, the co-localization of Sting and Lyn by confocal microscopy in the BMDC derived from WT and the *Fcgr2b*$^{-/-}$ mice were identified (Figure 29A and 29B). The results found that LYN interacts with Sting in immature BMDC of the *Fcgr2b*-deficiency mice and increase after activating with DMXAA. The previous studies show that genetic deletion of *Lyn* ablates pDC (77). The *Fcgr2b*-deficient BMDC constitutively showed a certain degree of the co-localization between Sting and LYN, and the activation promoted the interaction between Sting and LYN (Figure 29B). The data

suggested that Sting mediated maturation and differentiation of DCs and pDCs, respectively, is dependent on an LYN signaling pathway.

Figure 29 Co-localization of Sting and Lyn in activated BMDC of WT and

Fcgr2b^{-/-} mice.

 (A and B) Confocal microscope of DMXAA activated BMDC for 6 hours. Staining BMDC shows Lyn (green), Sting (red), and DAPI (blue). A representative of 3 experiments.

However, Src family kinases, Fyn, and Lyn have been shown the function in the maturation of DC and pDC response (77). The co-localization of Sting and Fyn by confocal microscopy in the BMDC derived from WT, and the *Fcgr2b*^{-/-} mice were

identified. The result indicates that Lyn, but not Fyn, showed the co-localization with Sting upon Sting activation as shown in Figure 30.
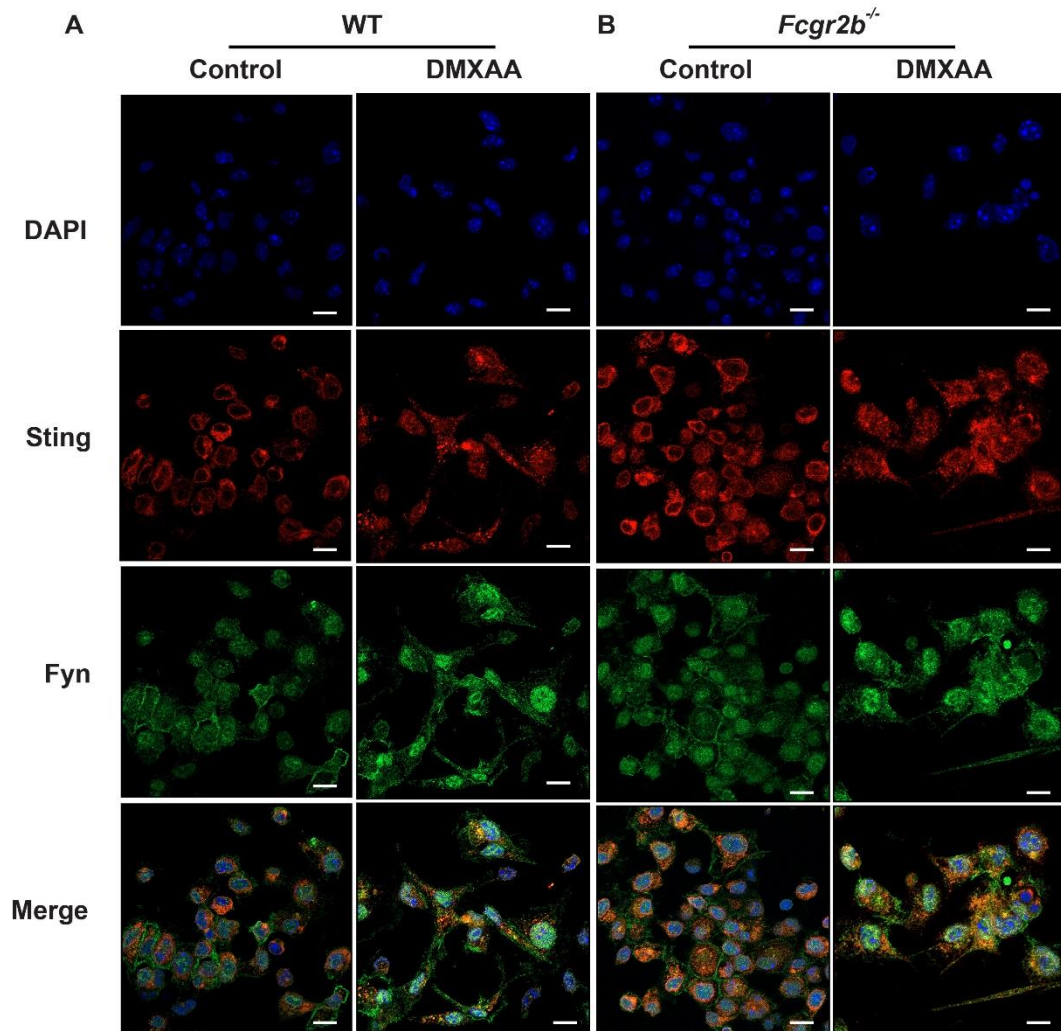
Figure 30 Co-localization of Sting and Fyn in activated BMDC of WT and *Fcgr2b*$^{-/-}$ mice.

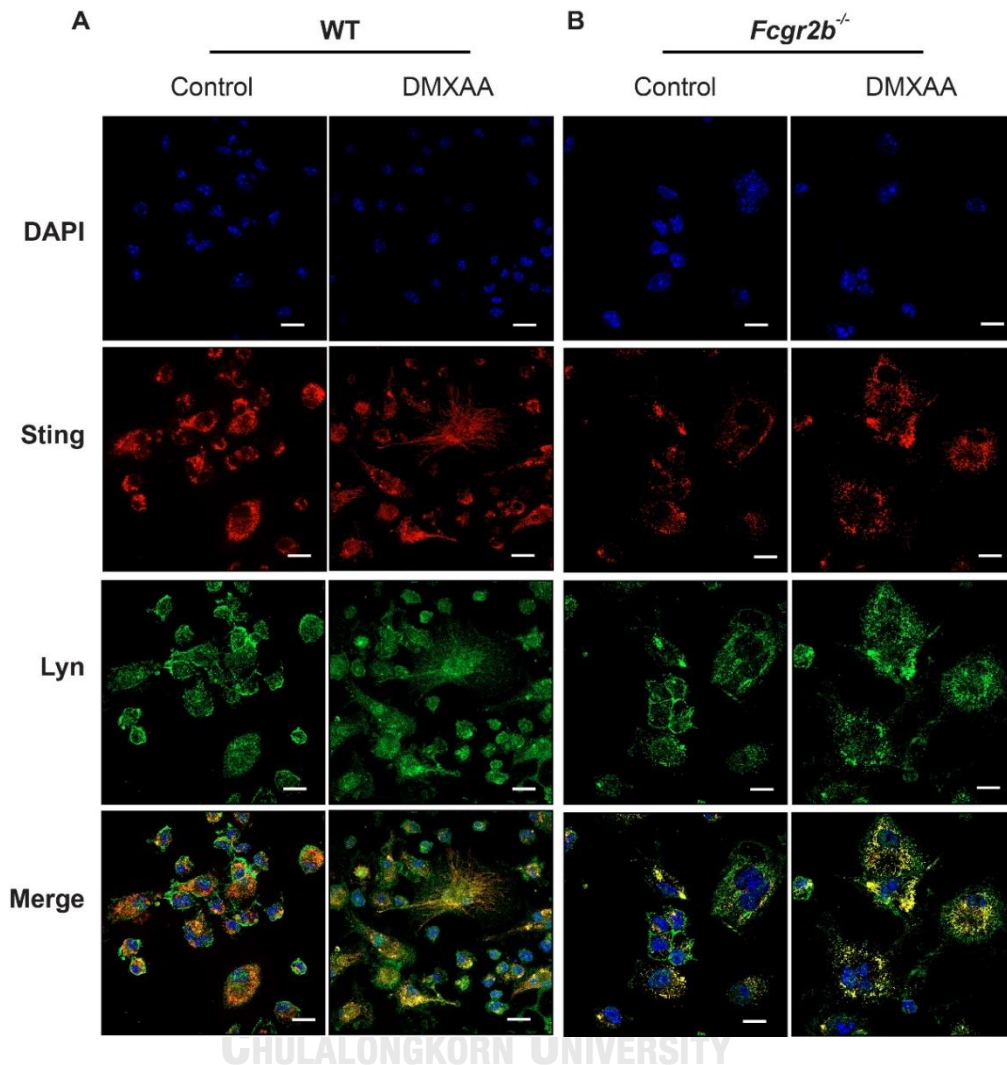 (A and B) Confocal microscope of DMXAA activated BMDC for 6 hours. Staining BMDC shows Fyn (green), Sting (red), and DAPI (blue). A representative of 3 experiments.

Adoptive transfer of Sting expressing BMDC from *Fcgr2b$^{-/-}$ mice* increases autoantibodies in the wild-type mice

To determine if Sting contributes lupus pathogenesis in wild-type mice, the adoptive transfer of Sting-activated BMDC from *Fcgr2b$^{-/-}$* mice to wild-type mice were performed. The results show that the anti-dsDNA significantly increased in the wild-type mice who received *Sting-* sufficient BMDC compared to the wild-type (non-recipient) controls (Figure 31). The results suggest that the BMDC derived from the *Fcgr2b$^{-/-}$* mice induced the recipients to produce a higher level of anti-dsDNA than normal mice.
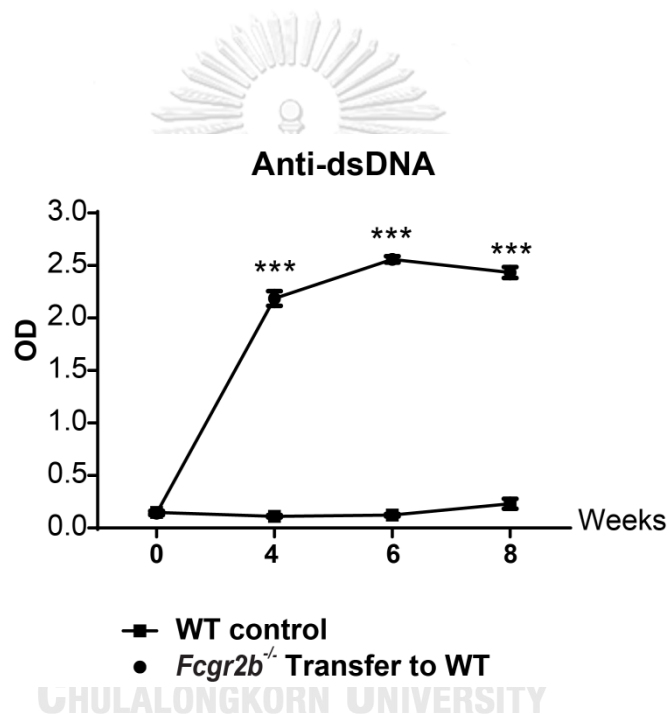
Figure 31 Adoptive transfer of Sting expressing BMDC increase anti-dsDNA in wild-type mice.

DMXAA activated BMDC from *Fcgr2b$^{-/-}$* were transferred into the recipient mice (wild-type). (A) The level of anti-dsDNA from the sera (1:100) measured by ELISA (N=4-5 per group).

Additionally, to investigate the immune-phenotypes in wild type that received the Sting-activated BMDC compared to the control, the flow cytometry analysis of spleens from all WT-recipient mice were performed. The results showed that the increased percentage of T effector memory (CD4+CD44hiCD62Llo), CD4+ICOS+cells, plasma cells (CD138+ cells) and germinal center B cells (B220+GL7+ cells) compared with the wild-type (non-recipient) controls (Figure 32).
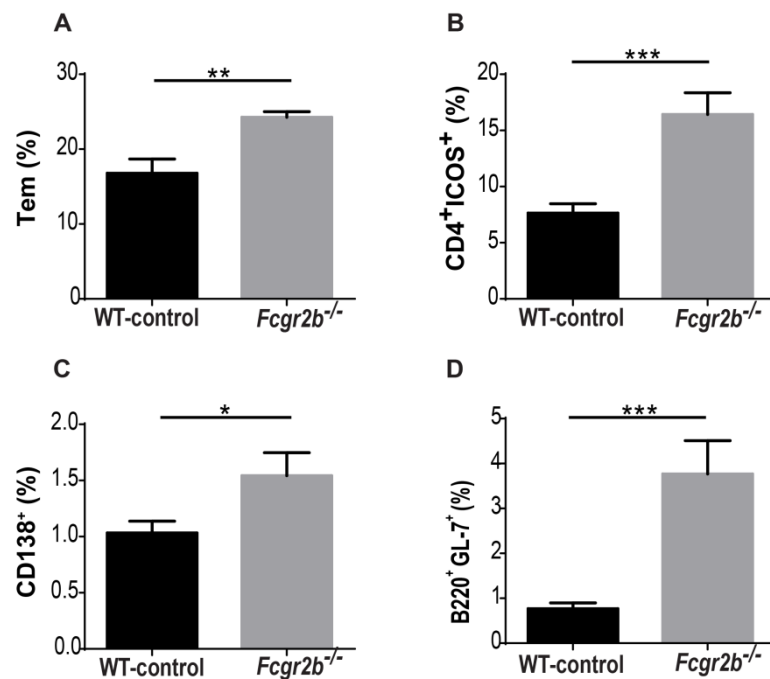
Figure 32 Sting-activated BMDC increase the activated immune cells in recipient wild type mice.

Flow cytometry analysis of recipient splenocytes after BMDC transferred every 2 weeks for 4 times show the percentage of (A) effector T cells (CD4+CD44hiCD62Llo), (B) CD4+ICOS+ cells, (C) CD138+ cells and (D) B220+GL7+ cells (N=4-7 per group). Data show as mean ± SEM (*p < 0.05, **p<0.01 and ***p<0.001).

Also, the immunofluorescences staining at the kidney of the wild type recipient mice were determined. These results found that increase of IgG deposition and CD45⁺ cell infiltration in wild type that received Sting-sufficient BMDC while did not show in the wild type control (Figure 33).
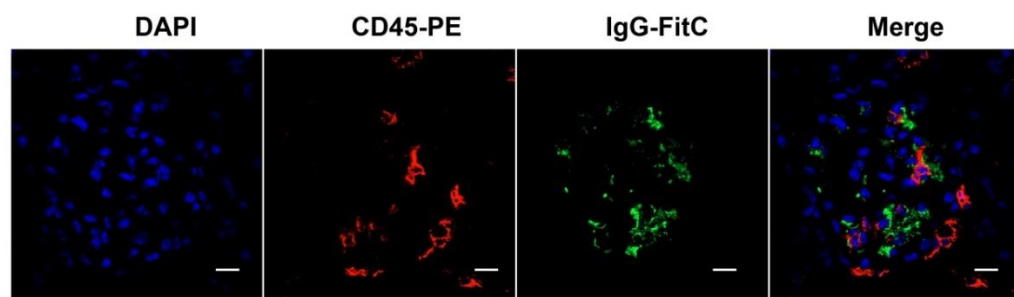
Figure 33 Sting-activated BMDC induce immune complex deposition in the kidney of WT-recipient mice.

(A and B) Immunofluorescence staining of the kidneys from recipient wild-type mice show in green (IgG), red (CD45), and blue (DAPI). Data are representative of 4 mice per group (scale bar=10 μm).

**Adoptive transfer of Sting expressing BMDC induce lupus development in the
$Fcgr2b^{-/-}.Sting^{gt/gt}$ mice**

The Sting signaling pathway activated the immature BMDC to differentiate into the mature DC and pDC which are capable of promoting T cell proliferation and producing the inflammatory cytokines (Figure 18B, 18D, 22A, 22B, 24A, and 24B). The proposed of this study is that Sting may induce the lupus disease by initially acting through the DC activation. To confirm this hypothesis, the adoptive transfers of Sting-activated BMDC into the double-deficient mice were performed. The anti-dsDNA significantly increased in the recipient mice who received $Sting$-sufficient BMDC compared to the non-recipient controls (Figure 34). The BMDC derived from Sting-sufficient mice (both WT and $Fcgr2b^{-/-}$) induced the recipients to produce a higher titer of anti-dsDNA than the ones from the double-deficient mice   (Figure 34).
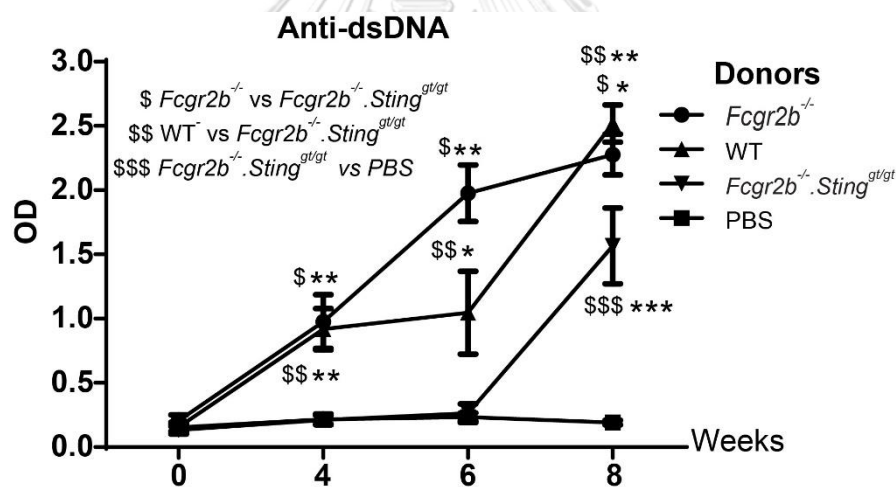
Figure 34 Increase of anti-dsDNA in the recipient of double-deficient mice.
DMXAA activated BMDC from $Fcgr2b^{-/-}$, WT, and $Fcgr2b^{-/-}.Sting^{gt/gt}$ were transferred into the recipient mice ($Fcgr2b^{-/-}. Sting^{gt/gt}$). (A) The level of anti-dsDNA from the sera (1:100) measured by ELISA (N=5-10 per group). Data show as mean ± SEM (*p < 0.05, **p<0.01, and ***p<0.001).

In addition, the flow cytometry analysis of spleens from all groups of recipient mice showed the increase in the percentage of T effector memory (T_{em}), $CD4^+ICOS^+$, and germinal center B cells when compared with PBS injection group (Figure 35A-35C). However, the transfer of Sting-activated BMDC from the $Fcgr2b^{-/-}$ mice significantly induced the T effector memory (T_{em}), $CD4^+ICOS^+$, and germinal center B cells, but did not increase $CD138^+$ cells, $B220^+IAb^+$ cells (Figure 32D).
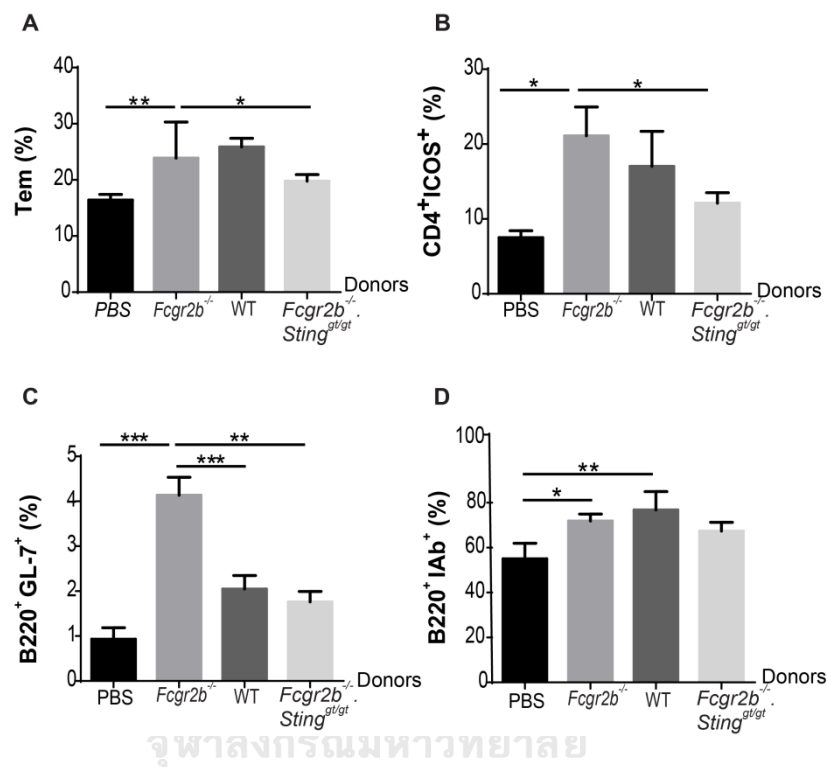
Figure 35 Increase of activated immune cells in recipient of double-deficient mice.
(A-E) Flow cytometry analysis of recipient splenocytes after BMDC transferred every 2 weeks for 4 times show the percentage of (A) effector T cells ($CD4^+CD44^{hi}CD62L^{lo}$), (B) $CD4^+ICOS^+$ cells, (C) $B220^+GL7^+$ cells and (D) $B220^+IAb^+$ cells (N=5-10 per group). Data show as mean ± SEM (*p < 0.05, **p<0.01, and ***p<0.001).

Next, the immunofluorescences staining at the kidney of the recipient mice were performed. The recipient of Sting-sufficient BMDC showed the increase of IgG deposition and $CD45^+$ cell infiltration while Sting-deficient BMDC did not (Figure 36A-D). Nevertheless, the $Fcgr2b^{-/-}$ BMDC induced more immune complex and $CD45^+$ cells

in the kidneys (Figure 33B and 33C). The results suggested that the restoration of Sting signaling pathway in dendritic cells is essential for lupus development in the $Fcgr2b^{-/-}.Sting^{gt/gt}$ mice.
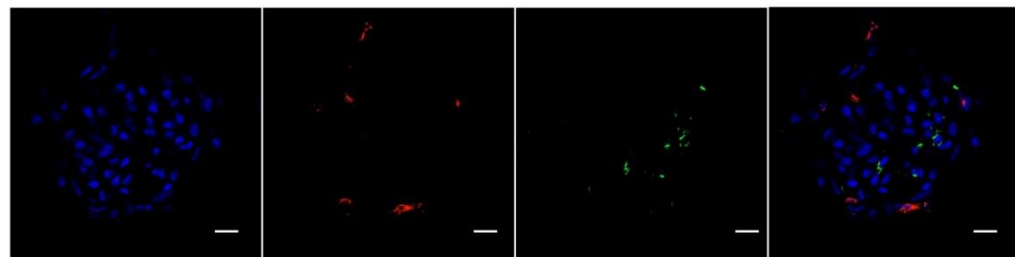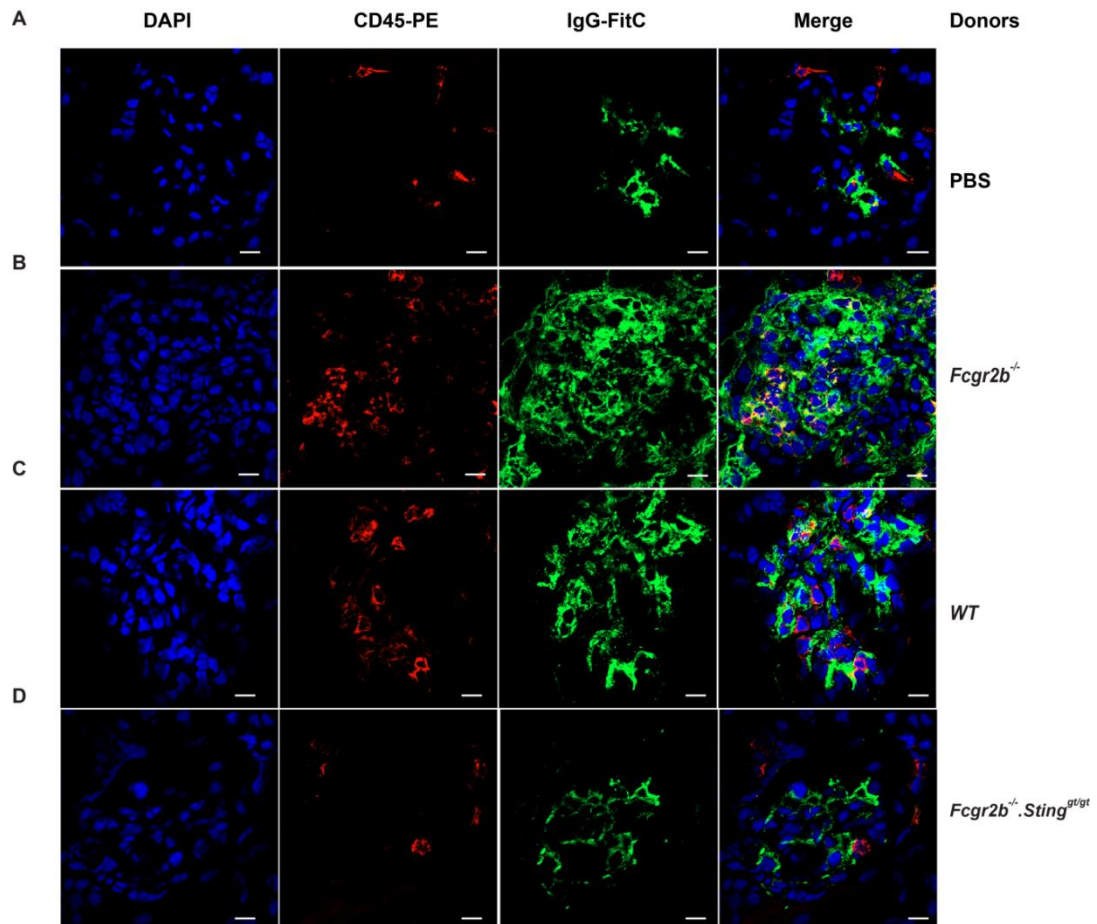

Figure 36 Sting-activated BMDC induce immune complex deposition in the kidney double-deficient mice.

(A-D) Immunofluorescence staining of the kidney from the $Fcgr2b^{-/-}. Sting^{gt/gt}$ recipient mice after the transfer with (F) PBS control, DMXAA activated BMDC from (G) $Fcgr2b^{-/-}$, (H) WT and (I) $Fcgr2b^{-/-}. Sting^{gt/gt}$. The confocal microscope shows DAPI (blue), CD45 (red) and IgG (green). The representative of 3 experiments (scale bar=10 um).

CHAPTER VI

DISCUSSION

The 129/B6.*Fcgr2b*$^{-/-}$ mice carrying Nba2 region, a locus on a spontaneous lupus mouse model that important for SLE pathogenesis, expressed constitutively the IFN-activated gene 202 (Ifi202). The Ifi202 is a lupus-susceptibility gene that increased the progression of glomerulonephritis in lupus mouse models (79). The CD19$^+$ cells from B6.Nba2 show the increase of Ifi202 and the decreases of Sting expression (80). However, the overexpression of Ifi202 can activate Sting-dependent IFN-I response and the 129/B6.*Fcgr2b*$^{-/-}$ mice increase the expression of IFN-β (81, 82). Here, these studies show the high expression of Ifi202, Sting, IFN-β, and interferon-inducible genes including Irf7, Ifn-γ, Mx1, and Cxcl10 from the spleen of the 129/B6.*Fcgr2b*$^{-/-}$ mice. Although Sting functions as a negative regulator in the Mrl/*lpr* lupus mice (25), this data shows that Sting is required for the lupus development in the 129/B6.*Fcgr2b*$^{-/-}$ mice. It is possible that Sting will also play a crucial role in other lupus mouse models which contained Nba2 region.

The survival of the 129/B6.*Fcgr2b*$^{-/-}$ mice depends on the autoantibody production and glomerulonephritis (55, 83) and the data from the previous study indicated that 6 months old of Fcgr2b$^{-/-}$ generated in 129 background mice showed the full lupus phenotypes (28). Moreover, it is found that Sting is required for the antibody production induced by cyclic-di-GMP in vitro (84). This study suggested that Sting facilitated the autoantibody production, inflammatory cell infiltration, and glomerulonephritis in the 129/B6.*Fcgr2b*$^{-/-}$ mice. Therefore, in the absent of Sting, resulting in improved the survival rate of 129/B6.*Fcgr2b*$^{-/-}$ mice.

Investigations by several studies conclude that the expression of interferon-inducible genes associated with SLE disease activity (85). This study detected the very high expression of a hundred of IFN inducible genes in the kidneys of 129/B6.*Fcgr2b*$^{-/-}$ mice by microarray that showed more severe pathology. The absence of Sting signaling in the *Fcgr2b*$^{-/-}$ mice partly decreased the expression of interferon-inducible genes in

the kidney. This data suggested that other nucleic acid sensors may promote the type I interferon production or signaling leads to destructive of kidneys in the *Fcgr2b*$^{-/-}$ mice as well. The Sting-dependent lupus phenotypes do not mediate only through type-I interferon pathway.

Sting expresses and functions differentially depended on the cell types. The previous study reported that STING was a low expression in B cell from SLE patients and MRL/lpr mice. These finding may contribute to the pathogenesis of SLE by increasing the activation of the JAK1-STAT1 signaling indirectly by STING (86). Whereas, Sting signals coordinately with B cell receptor (BCR) signaling to promote antibody response (87). The results showed that the spontaneous germinal center B cells and MHC-II expression in the *Fcgr2b*$^{-/-}$ mice were *Sting*-dependent. However, plasma cell expansion was *Sting*-independent. This data suggested Sting may contribute to the autoantibody production through memory B cells.

Sting also activates T cells by treatment with Sting ligand (DMXAA) induced not only *Sting*-dependent expression of ISGs and type I IFN production but also mediated cell stress and death (88). Nevertheless, this study found that the increase of T effector memory (T$_{em}$) in the *Fcgr2b*$^{-/-}$ mice was Sting-dependent. The expansion of T$_{em}$ may directly mediate through the interaction with antigen presenting cells, not directly via Sting signaling in T cells.

Sting agonist (DMXAA) treated mice show the increased expression of CD80, CD86, and MHC-II on DC and IFN-β production suggesting promotes the mature phenotypes of DC as the antigen-presenting cells (APC) which increase the expansion of T cells (89). This observation found the reduction of DC expansion in the *Fcgr2b*$^{-/-}$ mice, which depended on Sting signaling.

To confirm if Sting was required for DC maturation and cytokine production, co-culture of activated DC with T cells were performed. These DC became professional APC and could promote T cell differentiation. The IFN-γ producing CD4^{+} cells in the spleen and lymph nodes of the *Fcgr2b*$^{-/-}$ mice were reduced in the absence of Sting. The Sting-expressing DC derived from WT and *Fcgr2b*$^{-/-}$ mice stimulated naïve T cells to proliferate, but the ability of T cell to differentiate and produce IFN-γ did not

depend on intrinsic Sting expression on T cells. Interestingly, only DC from the *Fcgr2b*$^{-/-}$ mice can increase the IFN-γ production in CD4+ T cells. Furthermore, the previous data found that Sting-deficient mice fail to prime CD8$^+$ T cell leading to nonproductive T cell activation *in vivo* (90). Thus, this data suggested the DC from the *Fcgr2b*$^{-/-}$ mice have the intrinsic property that promotes the generation of Tem or autoreactive T cells.

The cGAS-STING signaling can activate human pDCs to produce IFN-I and knockdown of Sting using siRNA in CAL-1 cells can cause the reduction of IFN response (69). The proteomic data showed the upregulation of interferon-regulated protein after Sting-activation with DMXAA, which implied that the culture environment should enrich with type-I IFN. Sting activation with DMXAA led to phosphorylation of Ser357 of mouse Sting (homolog Ser358 in human Sting), and this site is phosphorylated by TBK1 which subsequently promoting type I IFN production (91, 92). The identification of pDC, a major producer of type-I IFN, after Sting activation, uncovered the role of Sting in the differentiation of pDC. These data revealed that Sting was essential for the generation of pDCs. Besides, this study identified several Sting-interacting proteins by mass spectrometry. Lyn kinase has been shown the role in the differentiation of pDC (77).

The recruitment of Lyn kinase to Sting after DMXAA stimulation suggested Sting mediated signaling through Lyn kinase. Also, the proteomics data of Sting-activated BMDC showed a significant increase of phosphoinositide 3-kinase adapter protein 1 (Pik3ap1) and receptor of activated protein C kinase 1 (Rack1). Pik3ap1 is an adaptor that signals to the phosphoinositide 3-kinase (PI3K) (93). Lyn and RACK1 are co-immunoprecipitated in membrane complexes (94). RACK1 silencing effected on the phosphorylation of AKT (95). This data suggest that the downstream of Sting-Lyn signaling may mediate through the PI3K-AKT pathway. The inhibition of LYN kinase during Sting activation abolished DC maturation and pDC differentiation. The data suggested Sting mediated differentiation of BMDC through the LYN signaling pathway.

Depletion of pDC ameliorates the autoimmune phenotypes in BXSB lupus-prone mice and B6.Nba2 mice (96, 97). These data strongly suggested Sting involving in DC function both DC maturation and pDC differentiation. The adoptive transfer of *Sting* sufficient BMDC can induce autoantibody production regardless of *Fcgr2b* status.

However, the absence of *Fcg2b* in the BMDC can accelerate the autoimmune phenotypes, including the immune complex deposition and inflammatory cell infiltration in the double-deficient recipient mice. Additionally, the adoptive transfers of *Sting sufficient* BMDC derived from Fcg2-/- mice increase the antibody production and activated immune cells but did not change the kidney pathology in wild type recipients.

Nevertheless, wild type recipient mice do not develop glomerulonephritis. The data implied that these wild type mice require lupus-susceptibility gene to progress of the disease (79). In summary, these data elaborated the vital function of Sting in the autoimmune *Fcgr2b*$^{-/-}$ lupus mouse model. The inhibition of STING signaling is a promising therapeutic target for SLE patients.

CHAPTER VII

CONCLUSION

129/B6.*Fcgr2b*⁻/⁻ mice present the strong lupus phenotype

First, the results show the increase of *Ifi202* and *Sting* expression in the 129/B6.*Fcgr2b*⁻/⁻ mice. Moreover, it is found that the interferon-inducible genes, including Ifn-β, *Irf3*, *Irf5*, Ifn-γ, *Cxcl10*, and *Mx1*, were also increased in the spleen of 129/B6.*Fcgr2b*⁻/⁻ mice.

The *Fcgr2b*-deficient mice start to die at the age of 6 months, and the survival rates drop to 22.2 % by 12 months old, while the survival rates of double-deficient mice are   77.7 %. The effect of one allele of Sting to survival rates of Fcgr2b-deficient mice does not show a significant difference. This finding concludes that Sting increases survival rates and improves the lupus phenotypes in 129/B6.*Fcgr2b*⁻/⁻ lupus mice model.

The activation of Sting pathway involved in the pathogenesis of SLE in lupus mice

In the absence of Sting, the lupus phenotypes of 129/B6.*Fcgr2b*-deficient mice were improved, including:

1. The kidney staining of Fcgr2b-deficient mice shows inflammatory cell infiltrations, enlarged glomeruli, and crescentic glomeruli, but double-deficient mice do not develop glomerulonephritis.

2. Antinuclear antibody (ANA) and anti-dsDNA production in the serum were decreases in the double-deficient mice. The results suggest that the high levels of autoantibodies are from the Sting-dependent.

3. Sting-mediated signaling induces type I interferon production and leads to the increase of interferon-inducible gene expression while the interferon signature genes in the kidneys were diminished in the double-deficient mice.

4. In order to understand the immunological importance of Sting in lupus *Fcgr2b*-deficient mice, the flow cytometry were characterized by the subsets of splenocytes from affected mice and their controls. The activated immune cells

decrease in the percentage and numbers in the double-deficient mice, especially CD11c⁺cells, plasmacytoid dendritic cells, and effector T cells. Also, B cells in the germinal center reduced in the double-deficient mice but not plasma cells.

The Sting-mediated pathway promotes maturation of dendritic cells and plasmacytoid dendritic cells differentiation via Lyn kinase pathway

1. The in vitro culture of bone-marrow derived dendritic cells with Sting ligands were performed and tested for the differentiation, activation stage, and cytokine production. Sting activation using DMXAA promoted the differentiation of immature DC to become pDC in the wild type and *Fcgr2b⁻/⁻* mice. In the absence of Sting, the immature DC cannot differentiate into pDC or get activated to express MHC class II (IAb⁺) and become professional antigen-presenting.

2. The proteomic analysis of activated BMDCs was performed and found the interferon-regulated proteins increase in *Sting-sufficient* BMDC.

3. To discover the new unbiased Sting-signaling pathway by immunoprecipitation assay, After Sting activation, Sting was phosphorylated, and Lyn was recruited to interact with Sting.

4. Regarding the observation of PI3K adaptor proteins associate with Sting after agonist treatment. The association of Sting and Lyn-PI3K-Akt pathway suggested Sting mediated maturation and differentiation of BMDC through the Lyn signaling pathway

The Sting-mediated pathway contribute to SLE via DNA sensor-mediated signaling in antigen presenting cells

The adoptive transfer of Sting‑activated bone marrow‑derived dendritic cells (BMDC) into the *Sting*-deficiency 129/B6.*Fcgr2b⁻/⁻* mice restored the lupus phenotypes. These data suggested that Sting signaling expressed in the dendritic cells induced the autoimmune development in the 129/B6.*Fcgr2b⁻/⁻* mice.

This study concludes that the signaling through stimulator of interferon genes (Sting) leads to type I interferon production and lupus pathogenesis (Figure 37). These

findings provide the proof of concept that inhibition of STING signaling is a promising therapeutic target for SLE patients. Sting is a new molecule which promising therapeutic target for lupus disease.
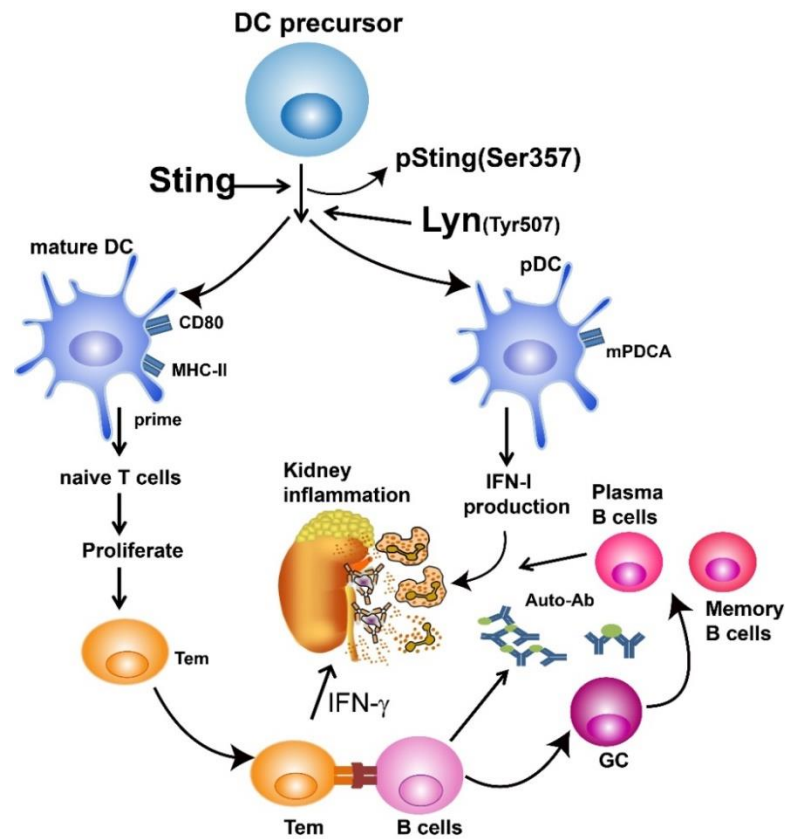

Figure 37 Activation of Sting induces lupus development by promoting dendritic cell maturation and plasmacytoid dendritic cell differentiation via Lyn kinase.

In summary, this study confirmed the essential function of Sting in the autoimmune $Fcgr2b^{-/-}$ lupus mouse model. Inhibition of STING signaling represents a promising therapeutic target for SLE patients.

REFERENCES

1.   Muskardin TLW, Niewold TB. Type I interferon in rheumatic diseases. Nature Reviews Rheumatology. 2018;14(4):214.

2.   Baechler EC, Batliwalla FM, Karypis G, Gaffney PM, Ortmann WA, Espe KJ, et al. Interferon-inducible gene expression signature in peripheral blood cells of patients with severe lupus. Proceedings of the National Academy of Sciences. 2003;100(5):2610-5.

3.   Niewold TB, Clark DN, Salloum R, Poole BD. Interferon Alpha in Systemic Lupus Erythematosus. Journal of Biomedicine and Biotechnology. 2010;2010:8.

4.   Lauwerys BR, Ducreux J, Houssiau FA. Type I interferon blockade in systemic lupus erythematosus: where do we stand? Rheumatology. 2013;53(8):1369-76.

5.   Keating SE, Baran M, Bowie AG. Cytosolic DNA sensors regulating type I interferon induction. Trends in immunology. 2011;32(12):574-81.

6.   Asselin-Paturel C, Brizard G, Chemin K, Boonstra A, O'Garra A, Vicari A, et al. Type I interferon dependence of plasmacytoid dendritic cell activation and migration. Journal of Experimental Medicine. 2005;201(7):1157-67.

7.   Pisitkun P, Deane JA, Difilippantonio MJ, Tarasenko T, Satterthwaite AB, Bolland S. Autoreactive B cell responses to RNA-related antigens due to TLR7 gene duplication. Science. 2006;312(5780):1669-72.

8.   Christensen SR, Shupe J, Nickerson K, Kashgarian M, Flavell RA, Shlomchik MJ. Toll-like receptor 7 and TLR9 dictate autoantibody specificity and have opposing inflammatory and regulatory roles in a murine model of lupus. Immunity. 2006;25(3):417-28.

9.   Deane JA, Pisitkun P, Barrett RS, Feigenbaum L, Town T, Ward JM, et al. Control of toll-like receptor 7 expression is essential to restrict autoimmunity and dendritic cell proliferation. Immunity. 2007;27(5):801-10.

10.   Sacre K, Criswell LA, McCune JM. Hydroxychloroquine is associated with impaired interferon-alpha and tumor necrosis factor-alpha production by plasmacytoid dendritic cells in systemic lupus erythematosus. Arthritis research & therapy. 2012;14(3):R155.

11.   Yan N. Immune Diseases Associated with TREX1 and STING Dysfunction. Journal of Interferon & Cytokine Research. 2017;37(5):198-206.

12.   Crow YJ, Hayward BE, Parmar R, Robins P, Leitch A, Ali M, et al. Mutations in the gene encoding the 3′-5′ DNA exonuclease TREX1 cause Aicardi-Goutieres syndrome at the AGS1 locus. Nature genetics. 2006;38(8):917.

13.   Peschke K, Friebe F, Zimmermann N, Wahlicht T, Schumann T, Achleitner M, et al. Deregulated type I IFN response in TREX1-associated familial chilblain lupus. The Journal of investigative dermatology. 2014;134(5):1456.

14.   Morita M, Stamp G, Robins P, Dulic A, Rosewell I, Hrivnak G, et al. Gene-targeted mice lacking the Trex1 (DNase III) 3′⟶ 5′ DNA exonuclease develop inflammatory myocarditis. Molecular and cellular biology. 2004;24(15):6719-27.

15.   Stetson DB, Ko JS, Heidmann T, Medzhitov R. Trex1 prevents cell-intrinsic initiation of autoimmunity. Cell. 2008;134(4):587-98.

16.   Ahn J, Gutman D, Saijo S, Barber GN. STING manifests self DNA-dependent inflammatory disease. Proceedings of the National Academy of Sciences. 2012;109(47):19386-91.

17.   Burdette DL, Vance RE. STING and the innate immune response to nucleic acids in the cytosol. Nature immunology. 2013;14(1):19.

18.   Cai X, Chiu Y-H, Chen ZJ. The cGAS-cGAMP-STING pathway of cytosolic DNA sensing and signaling. Molecular cell. 2014;54(2):289-96.

19.   Ablasser A, Goldeck M, Cavlar T, Deimling T, Witte G, Röhl I, et al. cGAS produces a 2′-5′-linked cyclic dinucleotide second messenger that activates STING. Nature. 2013;498(7454):380.

20.   Wu J, Sun L, Chen X, Du F, Shi H, Chen C, et al. Cyclic GMP-AMP is an endogenous second messenger in innate immune signaling by cytosolic DNA. Science. 2013;339(6121):826-30.

21.   Gall A, Treuting P, Elkon KB, Loo Y-M, Gale M, Jr., Barber GN, et al. Autoimmunity initiates in nonhematopoietic cells and progresses via lymphocytes in an interferon-dependent autoimmune disease. Immunity. 2012;36(1):120-31.

22.   Perry D, Sang A, Yin Y, Zheng Y-Y, Morel L. Murine Models of Systemic Lupus Erythematosus. Journal of Biomedicine and Biotechnology. 2011;2011.

23.   Murphy ED, Roths JB. A y chromosome associated factor in strain bxsb producing accelerated autoimmunity and lymphoproliferation. Arthritis & Rheumatism. 1979;22(11):1188-94.

24.   Nickerson KM, Christensen SR, Shupe J, Kashgarian M, Kim D, Elkon K, et al. TLR9 Regulates TLR7- and MyD88-Dependent Autoantibody Production and Disease in a Murine Model of Lupus. The Journal of Immunology. 2010;184(4):1840.

25.   Sharma S, Campbell AM, Chan J, Schattgen SA, Orlowski GM, Nayar R, et al. Suppression of systemic autoimmunity by the innate immune adaptor STING. Proceedings of the National Academy of Sciences. 2015;112(7):E710.

26.   Hron JD, Peng SL. Type I IFN Protects Against Murine Lupus. The Journal of Immunology. 2004;173(3):2134.

27.   Bolland S, Ravetch JV. Spontaneous Autoimmune Disease in FcγRIIB-Deficient Mice Results from Strain-Specific Epistasis. Immunity. 2000;13(2):277-85.

28.   Boross P, Arandhara VL, Martin-Ramirez J, Santiago-Raber M-L, Carlucci F, Flierman R, et al. The Inhibiting Fc Receptor for IgG, FcγRIIB, Is a Modifier of Autoimmune Susceptibility. The Journal of Immunology. 2011;187(3):1304.

29.   Choubey D. Interferon-inducible Ifi200-family genes as modifiers of lupus susceptibility. Immunology Letters. 2012;147(1):10-7.

30.   Sato-Hayashizaki A, Ohtsuji M, Lin Q, Hou R, Ohtsuji N, Nishikawa K, et al. Presumptive role of 129 strain–derived Sle16 locus in rheumatoid arthritis in a new mouse model with Fcγ receptor type IIb–deficient C57BL/6 genetic background. Arthritis & Rheumatism. 2011;63(10):2930-8.

31.   Rozzo SJ, Allard JD, Choubey D, Vyse TJ, Izui S, Peltz G, et al. Evidence for an Interferon-Inducible Gene, Ifi202, in the Susceptibility to Systemic Lupus. Immunity. 2001;15(3):435-43.

32.   Almine JF, O'Hare CAJ, Dunphy G, Haga IR, Naik RJ, Atrih A, et al. IFI16 and cGAS cooperate in the activation of STING during DNA sensing in human keratinocytes. Nature Communications. 2017;8:14392.

33.   Crispin JC, Hedrich CM, Tsokos GC. Gene-function studies in systemic lupus erythematosus. Nat Rev Rheumatol. 2013;9(8):476-84.

34.   Bolland S, Yim Y-S, Tus K, Wakeland EK, Ravetch JV. Genetic Modifiers of Systemic Lupus Erythematosus in Fcγ̯RIIB<sup>−/−</sup> Mice. The Journal of Experimental Medicine. 2002;195(9):1167.

35.   Kyogoku C, Dijstelbloem HM, Tsuchiya N, Hatta Y, Kato H, Yamaguchi A, et al. Fcγ receptor gene polymorphisms in Japanese patients with systemic lupus erythematosus: Contribution of FCGR2B to genetic susceptibility. Arthritis & Rheumatism. 2002;46(5):1242-54.

36.   Szczerba BM, Rybakowska PD, Dey P, Payerhin KM, Peck AB, Bagavant H, et al. Type I Interferon Receptor Deficiency Prevents Murine Sjögren's Syndrome. Journal of Dental Research. 2013;92(5):444-9.

37.   Perl A. Pathogenic mechanisms in systemic lupus erythematosus. Autoimmunity. 2010;43(1):1-6.

38.   Autoimmune Disease: Mechanisms. eLS.

39.   Smyk D, Rigopoulou EI, Baum H, Burroughs AK, Vergani D, Bogdanos DP. Autoimmunity and Environment: Am I at risk? Clinical Reviews in Allergy & Immunology. 2012;42(2):199-212.

40.   Crampton SP, Morawski PA, Bolland S. Linking susceptibility genes and pathogenesis mechanisms using mouse models of systemic lupus erythematosus. Disease Models &amp; Mechanisms. 2014;7(9):1033.

41.   Jakes RW, Bae S-C, Louthrenoo W, Mok C-C, Navarra SV, Kwon N. Systematic review of the epidemiology of systemic lupus erythematosus in the Asia-Pacific region: Prevalence, incidence, clinical features, and mortality. Arthritis Care & Research. 2012;64(2):159-68.

42.   Tsuchiya N, Kyogoku C. Role of Fcγ receptor IIb polymorphism in the genetic background of systemic lupus erythematosus: Insights from Asia. Autoimmunity. 2005;38(5):347-52.

43.   Krishnamurthy S, Mahadevan S. Systemic Lupus Erythematosus: Recent Concepts in Genomics, Pathogenetic Mechanisms, and Therapies. ISRN Immunology. 2011;2011:7.

44.   Ohl K, Tenbrock K. Inflammatory cytokines in systemic lupus erythematosus. Journal of Biomedicine and Biotechnology. 2011;2011.

45.   Kim J-M, Park S-H, Kim H-Y, Kwok S-K. A Plasmacytoid Dendritic Cells-Type I Interferon Axis Is Critically Implicated in the Pathogenesis of Systemic Lupus Erythematosus. International Journal of Molecular Sciences. 2015;16(6):14158-70.

46.   Niewold TB. Interferon alpha as a primary pathogenic factor in human lupus. Journal of interferon & cytokine research : the official journal of the International Society for Interferon and Cytokine Research. 2011;31(12):887-92.

47.   Joo H, Coquery C, Xue Y, Gayet I, Dillon SR, Punaro M, et al. Serum from patients with SLE instructs monocytes to promote IgG and IgA plasmablast differentiation. The Journal of Experimental Medicine. 2012;209(7):1335-48.

48.   Banchereau J, Pascual V. Type I Interferon in Systemic Lupus Erythematosus and Other Autoimmune Diseases. Immunity. 2006;25(3):383-92.

49.   Nacionales DC, Kelly-Scumpia KM, Lee PY, Weinstein JS, Lyons R, Sobel E, et al. DEFICIENCY OF THE TYPE I INTERFERON RECEPTOR PROTECTS MICE FROM EXPERIMENTAL LUPUS. Arthritis and rheumatism. 2007;56(11):3770-83.

50.   Obermoser G, Pascual V. The interferon-α signature of systemic lupus erythematosus. Lupus. 2010;19(9):1012-9.

51.   Baechler EC, Batliwalla FM, Karypis G, Gaffney PM, Ortmann WA, Espe KJ, et al. Interferon-inducible gene expression signature in peripheral blood cells of patients with severe lupus. Proceedings of the National Academy of Sciences. 2003;100(5):2610-5.

52.   Ronnblom L, Elkon KB. Cytokines as therapeutic targets in SLE. Nat Rev Rheumatol. 2010;6(6):339-47.

53.   Crampton SP, Morawski PA, Bolland S. Linking susceptibility genes and pathogenesis mechanisms using mouse models of systemic lupus erythematosus. Disease Models & Mechanisms. 2014;7(9):1033-46.

54.   Kirou KA, Gkrouzman E. Anti-interferon alpha treatment in SLE. Clinical Immunology. 2013;148(3):303-12.

55.   Bolland S, Yim Y-S, Tus K, Wakeland EK, Ravetch JV. Genetic Modifiers of Systemic Lupus Erythematosus in FcγRIIB(−/−) Mice. The Journal of Experimental Medicine. 2002;195(9):1167-74.

56.   Park H, Sheen DH, Lim MK, Shim SC. Animal Models in Systemic Lupus Erythematosus. J Rheum Dis. 2012;19(4):173-88.

57.   Bygrave AE, Rose KL, Cortes-Hernandez J, Warren J, Rigby RJ, Cook HT, et al. Spontaneous Autoimmunity in 129 and C57BL/6 Mice—Implications for Autoimmunity Described in Gene-Targeted Mice. PLOS Biology. 2004;2(8):e243.

58.   Smith KGC, Clatworthy MR. FcgammaRIIB in autoimmunity and infection: evolutionary and therapeutic implications. Nature reviews Immunology. 2010;10(5):328-43.

59.   Niederer HA, Clatworthy MR, Willcocks LC, Smith KGC. FcγRIIB, FcγRIIIB, and systemic lupus erythematosus. Annals of the New York Academy of Sciences. 2010;1183(1):69-88.

60.   Nimmerjahn F, Ravetch JV. Fcγ Receptors: Old Friends and New Family Members. Immunity. 2006;24(1):19-28.

61.   Takai T. Roles of Fc receptors in autoimmunity. Nature Reviews Immunology. 2002;2(8):580-92.

62.   Malbec O, Fong DC, Turner M, Tybulewicz VLJ, Cambier JC, Fridman WH, et al. Fcε Receptor I-Associated lyn-Dependent Phosphorylation of Fcγ Receptor IIB During Negative Regulation of Mast Cell Activation. The Journal of Immunology. 1998;160(4):1647.

63.   Leiss H, Niederreiter B, Bandur T, Schwarzecker B, Blüml S, Steiner G, et al. Pristane-induced lupus as a model of human lupus arthritis: evolvement of autoantibodies, internal organ and joint inflammation. Lupus. 2013;22(8):778-92.

64.   Reeves WH, Lee PY, Weinstein JS, Satoh M, Lu L. Induction of autoimmunity by pristane and other naturally occurring hydrocarbons. Trends in Immunology. 2009;30(9):455-64.

65.   Zhuang H, Szeto C, Han S, Yang L, Reeves WH. Animal Models of Interferon Signature Positive Lupus. Frontiers in Immunology. 2015;6(291).

66.   Barrat FJ, Elkon KB, Fitzgerald KA. Importance of Nucleic Acid Recognition in Inflammation and Autoimmunity. Annual Review of Medicine. 2016;67(1):323-36.

67.   Härtlova A, Erttmann SF, Raffi FAM, Schmalz AM, Resch U, Anugula S, et al. DNA Damage Primes the Type I Interferon System via the Cytosolic DNA Sensor STING to Promote Anti-Microbial Innate Immunity. Immunity. 2015;42(2):332-43.

68.   Ishikawa H, Ma Z, Barber GN. STING regulates intracellular DNA-mediated, type I interferon-dependent innate immunity. Nature. 2009;461(7265):788-92.

69.   Bode C, Fox M, Tewary P, Steinhagen A, Ellerkmann RK, Klinman D, et al. Human plasmacytoid dendritic cells elicit a Type I Interferon response by sensing DNA via the cGAS-STING signaling pathway. European Journal of Immunology. 2016;46(7):1615-21.

70.   Jeremiah N, Neven B, Gentili M, Callebaut I, Maschalidi S, Stolzenberg M-C, et al. Inherited STING-activating mutation underlies a familial inflammatory syndrome with lupus-like manifestations. The Journal of Clinical Investigation. 2014;124(12):5516-20.

71.   Liu Y, Jesus AA, Marrero B, Yang D, Ramsey SE, Montealegre Sanchez GA, et al. Activated STING in a Vascular and Pulmonary Syndrome. New England Journal of Medicine. 2014;371(6):507-18.

72.   Chan O, Madaio MP, Shlomchik MJ. The Roles of B Cells in MRL/lpr Murine Lupus. Annals of the New York Academy of Sciences. 1997;815(1):75-82.

73.   Makjaroen J, Somparn P, Hodge K, Poomipak W, Hirankarn N, Pisitkun T. Comprehensive Proteomics Identification of IFN-λ3-regulated Antiviral Proteins in HBV-transfected Cells. Molecular &amp; Cellular Proteomics. 2018;17(11):2197.

74.   Sauer J-D, Sotelo-Troha K, von Moltke J, Monroe KM, Rae CS, Brubaker SW, et al. The N-ethyl-N-nitrosourea-induced Goldenticket mouse mutant reveals an essential function of Sting in the in vivo interferon response to Listeria monocytogenes and cyclic dinucleotides. Infection and immunity. 2011;79(2):688-94.

75.   Marinho FV, Benmerzoug S, Rose S, Campos PC, Marques JT, Bafica A, et al. The cGAS/STING Pathway Is Important for Dendritic Cell Activation but Is Not Essential to

Induce Protective Immunity against Mycobacterium tuberculosis Infection. J Innate Immun. 2018;10(3):239-52.

76.   Chu CL, Lowell CA. The Lyn tyrosine kinase differentially regulates dendritic cell generation and maturation. J Immunol. 2005;175(5):2880-9.

77.   Dallari S, Macal M, Loureiro ME, Jo Y, Swanson L, Hesser C, et al. Src family kinases Fyn and Lyn are constitutively activated and mediate plasmacytoid dendritic cell responses. Nature Communications. 2017;8:14830.

78.   Chu C-L, Lowell CA. The Lyn Tyrosine Kinase Differentially Regulates Dendritic Cell Generation and Maturation. The Journal of Immunology. 2005;175(5):2880.

79.   Ichii O, Kamikawa A, Otsuka S, Hashimoto Y, Sasaki N, Endoh D, et al. Overexpression of interferon-activated gene 202 (Ifi202) correlates with the progression of autoimmune glomerulonephritis associated with the MRL chromosome 1. Lupus. 2010;19(8):897-905.

80.   Panchanathan R, Liu H, Xin D, Choubey D. Identification of a negative feedback loop between cyclic di-GMP-induced levels of IFI16 and p202 cytosolic DNA sensors and STING. Innate Immunity. 2013;20(7):751-9.

81.   Burdette DL, Vance RE. STING and the innate immune response to nucleic acids in the cytosol. Nature Immunology. 2012;14:19.

82.   Panchanathan R, Shen H, Duan X, Rathinam VAK, Erickson LD, Fitzgerald KA, et al. Aim2 Deficiency in Mice Suppresses the Expression of the Inhibitory Fcγ Receptor (FcγRIIB) through the Induction of the IFN-Inducible p202, a Lupus Susceptibility Protein. The Journal of Immunology. 2011;186(12):6762.

83.   Pisitkun P, Ha H-L, Wang H, Claudio E, Tivy Caitlyn C, Zhou H, et al. Interleukin-17 Cytokines Are Critical in Development of Fatal Lupus Glomerulonephritis. Immunity. 2012;37(6):1104-15.

84.   Walker MM, Crute BW, Cambier JC, Getahun A. B Cell–Intrinsic STING Signaling Triggers Cell Activation, Synergizes with B Cell Receptor Signals, and Promotes Antibody Responses. The Journal of Immunology. 2018;201(9):2641.

85.   Feng X, Wu H, Grossman JM, Hanvivadhanakul P, FitzGerald JD, Park GS, et al. Association of increased interferon-inducible gene expression with disease activity and

lupus nephritis in patients with systemic lupus erythematosus. Arthritis & Rheumatism. 2006;54(9):2951-62.

86.   Dong G, You M, Ding L, Fan H, Liu F, Ren D, et al. STING negatively regulates double-stranded DNA-activated JAK1-STAT1 signaling via SHP-1/2 in B cells2015.

87.   Walker MM, Crute BW, Cambier JC, Getahun A. B Cell–Intrinsic STING Signaling Triggers Cell Activation, Synergizes with B Cell Receptor Signals, and Promotes Antibody Responses. The Journal of Immunology. 2018:ji1701405.

88.   Larkin B, Ilyukha V, Sorokin M, Buzdin A, Vannier E, Poltorak A. Cutting Edge: Activation of STING in T Cells Induces Type I IFN Responses and Cell Death. Journal of immunology (Baltimore, Md : 1950). 2017;199(2):397-402.

89.   Curran E, Chen X, Corrales L, Kline DE, Dubensky TW, Jr., Duttagupta P, et al. STING Pathway Activation Stimulates Potent Immunity against Acute Myeloid Leukemia. Cell reports. 2016;15(11):2357-66.

90.   Woo S-R, Fuertes MB, Corrales L, Spranger S, Furdyna MJ, Leung MYK, et al. STING-dependent cytosolic DNA sensing mediates innate immune recognition of immunogenic tumors. Immunity. 2014;41(5):830-42.

91.   Tanaka Y, Chen ZJ. STING Specifies IRF3 Phosphorylation by TBK1 in the Cytosolic DNA Signaling Pathway. Science Signaling. 2012;5(214):ra20.

92.   Zhong B, Yang Y, Li S, Wang Y-Y, Li Y, Diao F, et al. The Adaptor Protein MITA Links Virus-Sensing Receptors to IRF3 Transcription Factor Activation. Immunity. 2008;29(4):538-50.

93.   Aiba Y, Kameyama M, Yamazaki T, Tedder TF, Kurosaki T. Regulation of B-cell development by BCAP and CD19 through their binding to phosphoinositide 3-kinase. Blood. 2008;111(3):1497-503.

94.   Sutton P, Borgia JA, Bonomi P, Plate JM. Lyn, a Src family kinase, regulates activation of epidermal growth factor receptors in lung adenocarcinoma cells. Mol Cancer. 2013;12:76.

95.   Liu B, Wang C, Chen P, Wang L, Cheng Y. RACK1 promotes radiation resistance in esophageal cancer via regulating AKT pathway and Bcl-2 expression. Biochem Biophys Res Commun. 2017;491(3):622-8.

96.   Davison LM, Jørgensen TN. Sialic Acid–Binding Immunoglobulin-Type Lectin H–Positive Plasmacytoid Dendritic Cells Drive Spontaneous Lupus-like Disease Development in B6.Nba2 Mice. Arthritis & Rheumatology. 2015;67(4):1012-22.

97.   Rowland SL, Riggs JM, Gilfillan S, Bugatti M, Vermi W, Kolbeck R, et al. Early, transient depletion of plasmacytoid dendritic cells ameliorates autoimmunity in a lupus model. The Journal of Experimental Medicine. 2014;211(10):1977.

APPENDIX

Decrease spleen weight of *Fcgr2b$^{-/-}$. Sting$^{gt/gt}$* mice

The data from previous study indicated that 6 months old of *Fcgr2b$^{-/-}$* generated in 129 background mice showed the full lupus phenotypes (28). This results confirmed that the spleen weight of Fcgr2b$^{-/-}$ mice at the age of 6 months which bigger than WT, *Sting$^{gt/gt}$* and *Fcgr2b$^{-/-}$. Sting$^{gt/gt}$* mice (Figure 38)
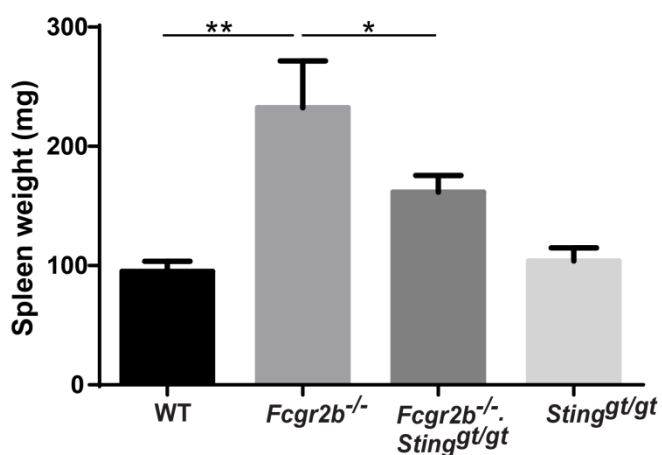
Figure 38 Spleen weights of all experimented mice.

All mice were sacrificed at the age of 6 months to investigate the spleen weight (mg).

Decrease the total number of activated immune cells in the double-deficient mice

The activated immune cells including total dendritic cells (CD11c+ cells), plasmacytoid dendritic cells, effector T cells and germinal center B cells reduce in numbers or function in the double-deficient mice to Fcgr2b-deficient mice (Figure 39).
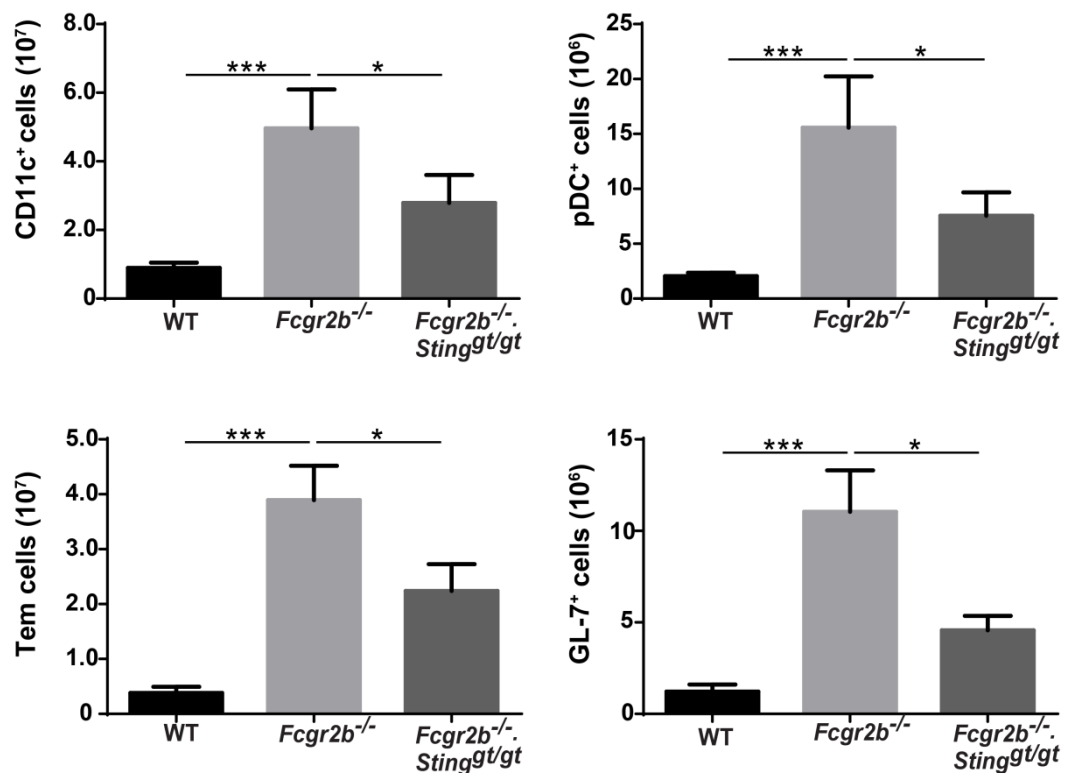
Figure 39 Decrease total numbers of activated immune cells in the double deficient mice.

The splenocytes of the mice were collected at the age of 6 months to investigate the activated immune cells.

Sting activation promotes differentiation of plasmacytoid dendritic cells (pDC)

Sting activation using DMXAA promoted the differentiation of immature DC to become pDC in the wild type and Fcgr2b$^{-/-}$ mice. In the absence of Sting the immature DC cannot differentiate into pDC (Figure 40)
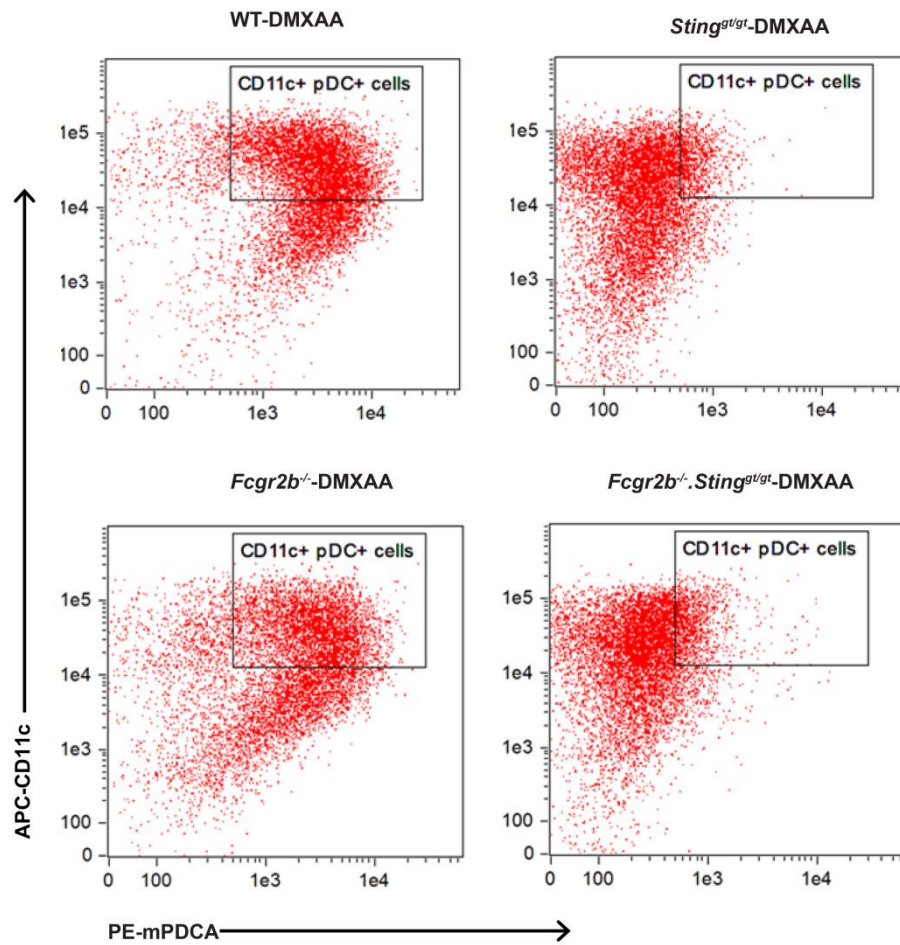
Figure 40 The differentiation of immature DC after Sting activation

Immature BMDC become plasmacytoid dendritic cells BMDC were detected by flow cytometry. Representative of flow cytometric analysis of CD11c$^+$PDCA$^+$ cells.
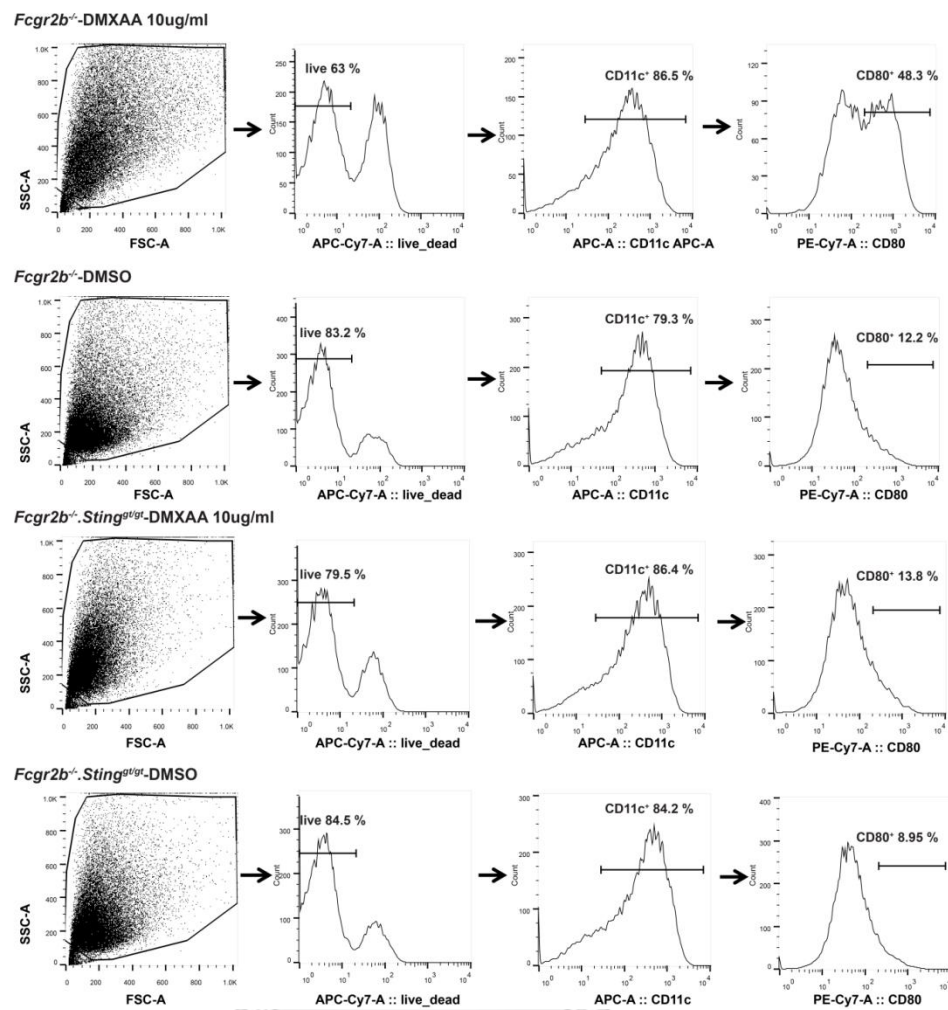
Figure 41 Flow cytometry representative of immature DC after Sting activation.
BMDC were detected by flow cytometry. Representative of flow cytometry of live
cells, CD11c$^+$ cells and CD80$^+$ cells

Purification of CD4 T cells from lymph nodes and spleen

      To determine the function of Sting in T cells, the naïve T cells and CD4 T cells
were isolated from lymph nodes and spleen of all mice using naïve T cells isolation
kit and anti-CD4 antibody-conjugated microbeads. The cells viability and purity of
isolated T cells were examined by flow cytometry. The results show that the naïve T
cells and CD4 T cells viability and purity were greater than 90% and 95%, respectively.
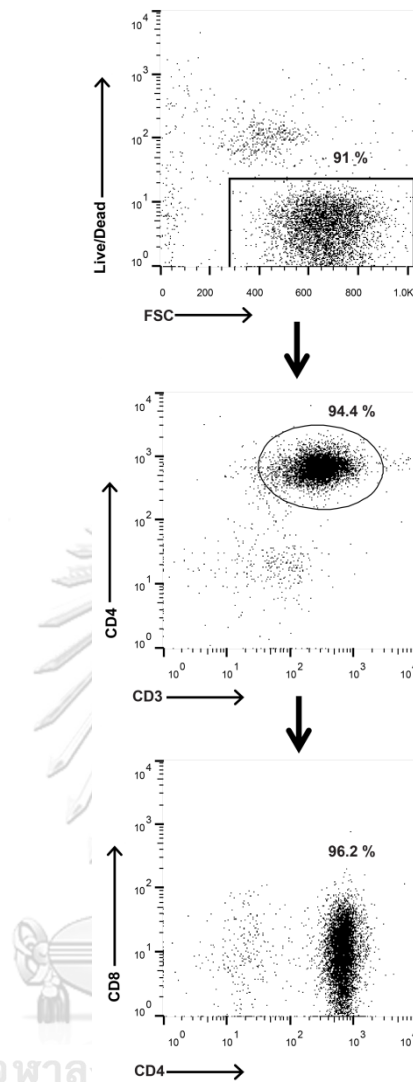
Figure 42 Representative of cell viability and purity of isolated naïve T cells and CD4+
T cells.

Mouse T cells were isolated from lymph nodes and spleen and stained with APC-
Cy7-Viability dye, APC-CD3, FitC-CD4 and PE-CD8 antibodies, and analyzed by flow
cytometry.

Genotyping

DNA extraction

Reagents

1. DNA lysis solution including 40mM Tris-HCl pH 8. 0, 20mM EDTA, 0.5% SDS 20mM NaCl, and 0.5% Beta-mercaptone

2. Saturated NaCl (approximately 6 M)

Protocol

Mouse tails were lysed in 500 µl of DNA lysis buffer and added 20 µl of proteinase K (20mg/ml). Incubate at 55°C. for overnight. After that, add 250 µl of 6 M NaCl shake well for 15 secs and let it stand for 15 minutes on ice. The mixture was centrifuged 15 minutes at 13,000 rpm for 4°C and transferred the clear supernatant (DNA solution) into a new tube and then precipitate the DNA with 750 µl of ice cold of absolute ethanol. Pellet gently by spinning at 13,000 rpm, 4°C for 15 min. Wash the DNA precipitate with 70% ethanol and air dry. Dissolve DNA with appropriate nuclease water

2. PCR for FcɣRIIb-/- genotyping

   2.1 Primer: FcREC1-Forward: 5'-AAGGCTGTGGTCAAACTCGAGCC-3'

        OL4143: 5'-CTCGTGCTTTACGGTATCGCC -3'

        OL4080: 5'-TTGACTGTGGCCTTAAACGTGTAG -3'

2.2 PCR condition: 1 cycle of 94°C for 3 minutes followed by 35 cycles of 94°C for 45 seconds, 60°C for 1 minute, 72°C for 1 minute and 72°C for 5 minute

3. Gel electrophoresis

   The PCR products were run on 2 % agarose gel.

   The Fcgr2b+/+ should give 173 bp only and +/- should give 173 bp + 232 bp products. However, Fcgr2b -/- or knockout mice should give only 232 bp as show in Figure 42.
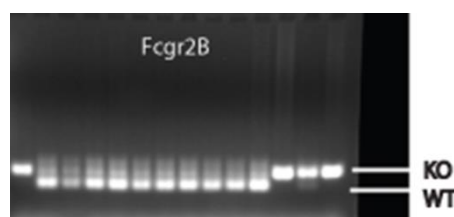
Figure 43 PCR products size of *Fcgr2b^{+/+}, Fcgr2b^{+/-} and Fcgr2b ^{-/-}*.

4. Mastermix for genotyping using Sting probe (1 reaction)

Sting sequence, exon 6

GGCTCCAGGCCCGGATCCGAATGTTCAATCAGCTACATAACAACATGCTCAGTGGTGCAGGGAG
CCGAAGACTGTACA[T/A]CCTCTTTCCATTGGACTGTGGGGTGCCTGACAACCTGAGTGTAGTT
GACCCCAACATTCGATTCCGAGATATGCTGCCCCAGCAAAACATCGACCGTGCTGGCATCAAGA
ATCGGGTTTATTCCAACAGCGTCTACGAGATTCTGGAGAACGGACAGCCA

Forward Sting for genotyping: GCCCGGATCCGAATGTTCAATCA

Reverse Sting for genotyping: GGCAGCATATCTCGGAATCGAATGT

Reporter-VIC -Sting-WT: GACTGTACATCCTCTTTCCA (Sting-T596-WT)

Reporter-FAM-Sting-mutant: GACTGTACAACCTCTTTCCA (Sting-A596-mut)

Master mixes

TaqMan Universal PCR Master Mix	5	µl
10X Sting-GT probe	1	µl
50 ng/µl of DNA	2	µl
Nuclease-free	2	µl
Total	10	µl

3. Materials for gene expression

Mastermix of iScript™ cDNA Synthesis (1 reaction)

5x iScript Reaction Mix	4	µl
iScript Reverse Transcriptase	1	µl
Nuclease-free water	Variable	
RNA template (1 µg total RNA)*	Variable	
Total	20	µl

Mastermix for real time PCR using SYBR green (1 reaction)

SsoAdvanced universal SYBR® Green supermix (2x)	5	µl
10 µM Forward primer	0.5	µl
10 µM Reverse primer	0.5	µl
5 ng/µl cDNA	2	µl
Nuclease-free	2	µl
Total	10	µl

Cell culture

Complete RPMI 1640 (100 ml) (Store at 4°C)

Incomplete RPMI 1640	85	ml
FBS	10	ml
10000 U/ml Penicillin/Streptomycin	1	ml
100X MEM-NEAA	1	ml
100X Na pyruvate	1	ml
100X L-glutamine	1	ml
100X Hepes buffer	1	ml

Buffer for T cells isolation (100 ml) (Store at 4°C)

1X PBS, pH 7.2	100	ml
BSA (final concentration 0.5 %)	0.5	g
EDTA (final concentration 2 mM)	0.074	g

CFSE (formally known as 5-(and 6)-Carboxyfluorescein diacetate succinimidyl ester of CFDA SE)

Stock CFSE 100 µg/vial was reconstituted with 36 µl of DMSO to yield a concentration of 5 mM. Prepare a working solution 50 µM

5 Mm CFSE	1	µl
1X PBS, pH 7.2	99	µl
Final concentration of CFSE	0.5 µM/ 1.5 * 10^6 cells	

Phorbol 12-myristate 13-acetate (PMA)

Stock PMA 5 mg/vial was reconstituted with 1 ml of DMSO to yield a concentration of 5 mg/ml. Prepare a working solution 5 mg/ml

5 mg/ml PMA	1	µl
Complete media RPMI 1640	9999	µl
Final concentration of PMA	25	ng/ml

Ionomycin from Streptomyces conglobatus

Stock Ionomycin 1 mg/vial was reconstituted with 1 ml of DMSO to yield a concentration of 5 mg/ml. Prepare a working solution 1 mg/ml

1 mglml Ionomycin	1	µl

Complete media RPMI 1640	9	µl
Final concentration of Ionomycin	1	µg/ml

DMXAA or Murine STING ligand (5,6-dimethylxanthenone-4-acetic acid)

    Stock DMXAA 5 mg/vial was reconstituted with 500 µl of DMSO to yield a concentration of 5 mg/0.5 ml.

Final concentration of DMXAA	10	µg/ml

Materials for proteomics analysis

Reagents for SDS- polyacrylamide gel preparation

1.5 M Tris-HCl pH 8.8

Tris base	181.7	g
Type I water	700	ml

Adjusted pH to 8.8 by conc. HCl and then the final volume of this solution was adjusted with type I water to 1,000 ml.

1 M Tris-HCl pH 6.8

Tris base	121.1	g
Type I water	700	ml

Adjusted pH to 6.8 by conc. HCl and then the final volume of this solution was adjusted with type I water to 1,000 ml.

10% SDS, 1 mM NaN3

SDS	20 g
100 mM NaN3	2 ml
Add dd-H_2O to 200 ml	

10% Ammonium persulphate (APS)

Ammonium persulfate	0.1	g
Milli Q	1	ml

Electrophoresis

10X Tris/Glycine/SDS

10X Tris/Glycine:

ultrapure Tris	30.3 g
glycine	144.1 g
Add dd-H_2O, to 1 L filter and store at RT	

1X Tris/Glycine:

10X Tris/Glycine	100 ml	
Milli Q H$_2$O	900 ml	

10 % SDS-PAGE (2 gel)

Milli Q	4,175	µl
40% Acrylamide gel	3,125	µl
1.5 M Tris-HCl pH 8.8	2.5	ml
10% SDS	100	µl
10% APS	100	µl
TEMED	5	µl

4% stacking gel (2 gel)

Milli Q	3,650	µl
40% Acrylamide gel	625	µl
1 M Tris-HCl pH 6.8	625	µl
10% SDS	50	µl
10% APS	50	µl
TEMED	5	µl

Procedure

1) Prepare 500 ml of 1X Tris/Glycine/SDS per gel (running buffer)

2) Remove samples from -80 ^{0}C freezer. Remove MW markers from freezer (choose from low, high and full range MW). Place in heating block at 37 ^{0}C.

3) Cast resolving gel a night before and keep at 4 ^{0}C, cast stacking gel just before running SDS-PAGE

4) Put gels in a tank then add running buffer in both upper and lower chamber.

5) Remove combs in wells.

6) Vortex samples before loading.

7) Preferably leave 1st and last well empty.

8) Carefully load wells with calculated amount of sample.

9) Put on cover lid and set at constant volts, 100-200 volts for 45min-90min (the lower the voltage the sharper the band/separation.

Transfer

Reagents and buffers in western blotting assay

1X Transfer buffer (1 membrane)

Trans-Blot Turbo 5X Transfer buffer	20	ml
Ethanol	20	ml
Type I water	60	ml

10X TBS

Tris base	60.5	g
NaCl	88.7	g

Add dd-H_2O, to 1 L filter and store at 4^0C

1X TBST

10X TBS	100	ml
Tween 20	1	ml

Add dd-H_2O, to 1 L filter and store at 4^0C

Procedure

1) Prepare transfer buffer: 65 ml fairbanks Tris buffer + 3.0 ml 10% SDS, 1mM Na N_3 (Optional) Fill to 1500 ml. (0.02% SDS final)

2) Take gels out of cassette.

3) Have filter paper ready (1-2 per side depending on thickness of sponge).

4) Put a piece of filter paper on top of one sponge.

5) Place gel on filter paper.

6) Place membrane on gel.

7) Place another filter paper on top of the nitrocellulose membrane, then press gently with roller

8) Place 2nd sponge on top of filter paper.

9) Put the sandwich in transfer cassette, gel side on black side.

10) Close transfer cassette and place in transfer holder with black towards the back (next to ice pack).

11) Place ice pack, stir bar, and transfer cassette in transfer tub.

12) Fill transfer tub with transfer buffer to the fill line.

13) Place transfer tub on a stirrer and start stirring.

14) Run at constant volts and set to 80-100 volts for 60 min (Mini gel system). These settings can be varying depended on your target proteins (bigger proteins require longer transfer time).

Protocol for Reversible Ponceau S Staining

Staining Solution: 0.1 % (w/v) Ponceau S in 1% (v/v) acetic acid

(1.31 mM Ponceau S // 0.175 M HOAc)

0.1 g	Ponceau S
99.0 mL	ultrapure H2O
1.0 mL	glacial acetic acid (99.5-99.8%)

Clearing Solution: 1.0 % (v/v) acetic acid (0.175 M HOAc) (for removing "background" stain from membrane, NOT for "destaining")

99.0 mL	ultrapure H2O
1.0 mL	glacial acetic acid (99.5-99.8%)

Isolation of femurs and tibias

1. Dendritic cells were obtained from mice' femur bone and tibia (at the age of 6-7 months)

2. Dissect the femur and tibia from surrounding muscles and remove excess tissue using sterile forceps and scissors, keeping the ends of the bone intact

3. Clean the intact bones in 70% ethanol in a sterile petridish (for disinfection)

4. After clean the intact bones with EtOH then soak the intact bones in sterile PBS or RPMI 1640 medium (for rinsing off ethanol.)

6. Trim both ends of femurs and tibia carefully using sterile, sharp scissors to expose the interior marrow shaft.

7. Insert the bones (2 femurs and 2 tibias/mouse) in inserted tube and centrifuge at 6000 rpm, 4^0C and collect the total BM in 1.5 ml tube

8. Resuspend cells in ACK lysis buffer. Normally use 4 ml for BM

9. Incubate cells in ACK for 5 min at RT and then Add 10 ml of PBS or medium to stop the lysis.

10. Spin 1200 rpm, 5 min, 4 ^{0}C and remove the supernatant

11. Resuspend cells in appropriate volume of complete medium and count it

Software and programs

Flow Jo v.10

GraphPad Prism 6.0

Adobe Illustrator CS3

Adobe Photoshop CS6

EndNote X8

VITA

NAME	Arthid Thim-uam
DATE OF BIRTH	02 May 1982
PLACE OF BIRTH	Tak, Thailand
INSTITUTIONS ATTENDED	B.SC. from Naresuan University
	M.SC. from Naresuan University
HOME ADDRESS	45/2 Moo 1 Tambol Maesalid
	Bantak, Tak
	Thailand
	63120

PUBLICATION

1. Issara-Amphorn J, Surawut S, Worasilchai N, Thim-uam A, Finkelman M, Chindamporn A, et al. The Synergy of Endotoxin and $(1{\longrightarrow}3)$-β-D-Glucan, from Gut Translocation, Worsens Sepsis Severity in a Lupus Model of Fc Gamma Receptor IIb-Deficient Mice. Journal of Innate Immunity. 2018;10(3):189-201.

2. Saiworn W, Thim-uam A, Visitchanakun P, Atjanasuppat K, Chantaraaumporn J, Mokdara J, et al. Cortical Bone Loss in a Spontaneous Murine Model of Systemic Lupus Erythematosus. Calcified Tissue International. 2018;103(6):686-97.

3. Surawut S, Panpetch W, Makjaroen J, Tangtanatakul P, Thim-Uam A, Wongphoom J, et al. Helicobacter pylori Infection Increased Anti-dsDNA and Enhanced Lupus Severity in Symptomatic FcγRIIb-Deficient Lupus Mice. Frontiers in Microbiology. 2018;9(1488).

4. Surawut S, Makjaroen J, Thim-uam A, Wongphoom J, Palaga T, Pisitkun P, et al. Increased susceptibility against

Cryptococcus neoformans of lupus mouse models (pristane-induction and FcGRIIb deficiency) is associated with activated macrophage, regardless of genetic background. Journal of Microbiology. 2019;57(1):45-53.

AWARD RECEIVED   Best oral presentation

- The 34th Annual Meeting The Allergy Asthma and Immunology Association of Thailand

Best poster presentation

- The 7th Federation of Immunological Societies of Asia-Oceania Congress (FIMSA 2018)